The University of
Nottingham

UNITED KINGDOM · CHINA · MALAYSIA

Access from the University of Nottingham repository:
http://eprints.nottingham.ac.uk/30315/1/jm-2015-005859.R2%20-%20JMC
%2058%2817%29%202015%206819.pdf

Discovery of a Novel Class of Negative Allosteric Modulator of the Dopamine D₂ Receptor Through Fragmentation of a Bitopic Ligand

Journal:	*Journal of Medicinal Chemistry*
Manuscript ID:	jm-2015-005859.R2
Manuscript Type:	Article
Date Submitted by the Author:	10-Aug-2015
Complete List of Authors:	Mistry, Shailesh; Monash University, Medicinal Chemistry Shonberg, Jeremy; Friedrich Alexander University, Pharmazeutische Chemie Draper-Joyce, Christopher; Monash Institute of Pharmaceutical Sciences, Drug Discovery Biology Klein Herenbrink, Carmen; Monash University, Monash Institute of Pharmaceutical Sciences, Drug Discovery Biology Michino, Mayako; National Institutes of Health, Computational Chemistry and Molecular Biophysics Unit, National Institute on Drug Abuse - Intramural Research Program Shi, Lei; Weill Medical College of Cornell University, Physiology and Biophysics Christopoulos, Arthur; Monash Institute of Pharmaceutical Sciences, Drug Discovery Biology Capuano, Ben; Monash University, Department of Medicinal Chemistry, Monash Institute of Pharmaceutical Sciences Scammells, Peter; Monash University, Medicinal Chemistry Lane, J. Robert; Monash Institute of Pharmaceutical Sciences, Drug Discovery Biology

SCHOLARONE™
Manuscripts

Discovery of a Novel Class of Negative Allosteric Modulator of the Dopamine D$_2$ Receptor Through Fragmentation of a Bitopic Ligand

Shailesh N. Mistry,[†,^] Jeremy Shonberg,[†,#] Christopher J. Draper-Joyce,[‡] Carmen Klein Herenbrink,[‡] Mayako Michino[§], Lei Shi,[§,‖,⊥] Arthur Christopoulos,[‡] Ben Capuano,[†] Peter J. Scammells[†,*] and J. Robert Lane[‡,*]

[†]Medicinal Chemistry, Monash Institute of Pharmaceutical Sciences, Monash University, Parkville 3052, Victoria, Australia.

[‡]Drug Discovery Biology, Monash Institute of Pharmaceutical Sciences, Monash University, Parkville 3052, Victoria, Australia.

[§]Computational Chemistry and Molecular Biophysics Unit, National Institute on Drug Abuse – Intramural Research Program, National Institutes of Health, Baltimore, MD, USA.

[‖]Department of Physiology and Biophysics, Weill Medical College of Cornell University, New York, NY, USA.

[⊥]Institute for Computational Biomedicine, Weill Medical College of Cornell University, New York, NY, USA
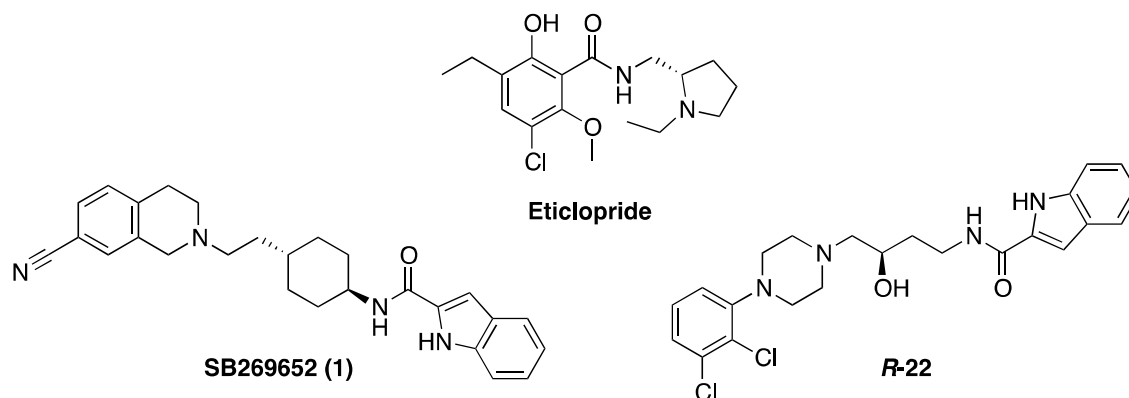
ABSTRACT

Recently, we have demonstrated that *N*-((*trans*)-4-(2-(7-cyano-3,4-dihydroisoquinolin-2(1*H*)-yl)ethyl)cyclohexyl)-1*H*-indole-2-carboxamide (SB269652) (**1**), adopts a bitopic pose at one protomer of a dopamine D_2 receptor (D_2R) dimer, to negatively modulate the binding of dopamine at the other protomer. The 1*H*-indole-2-carboxamide moiety of **1** extends into a secondary pocket between the extracellular ends of TM2 and TM7 within the D_2R protomer. To target this putative allosteric site, we generated and characterized fragments that include and extend from the 1*H*-indole-2-carboxamide moiety of **1**. *N*-Isopropyl-1*H*-indole-2-carboxamide (**3**) displayed allosteric pharmacology and sensitivity to mutations of the same residues at the top of TM2 as was observed for **1**. Using **3** as an 'allosteric lead', we designed and synthesised an extensive fragment library to generate novel SAR and identify *N*-butyl-1*H*-indole-2-carboxamide (**11d**), which displayed both increased negative cooperativity and affinity for the D_2R. These data illustrate that fragmentation of extended compounds can expose fragments with purely allosteric pharmacology.

INTRODUCTION

G protein-coupled receptors (GPCRs) are the largest superfamily of cell surface receptors and are targeted by approximately one third of current medicines.[1] There has been an increasing interest in targeting allosteric sites within these proteins (sites that are topographically distinct from the orthosteric binding site of the endogenous hormone or neurotransmitter) to achieve greater selectivity across receptor subtypes.[2] More recently, bitopic ligands, i.e. molecules in which orthosteric and allosteric pharmacophores have been linked together, have emerged as a new approach to develop selective GPCR ligands.[3,4] By concomitantly engaging both orthosteric and allosteric sites, bitopic ligands combine the advantages of selectivity that can result from engagement of an allosteric site, with the high affinity and well-defined structure-activity relationships associated with targeting an orthosteric binding pocket.[3,5] Such an approach has been successfully exploited to target GPCRs within the muscarinic acetylcholine receptor (mAChR) and adenosine receptor families.[6-9] In addition, recent studies have demonstrated that ligands that selectively target the M_1 and M_2 mAChRs may achieve their receptor-subtype-selectivity through a hitherto unappreciated bitopic mode of interaction.[10,11] One approach to explore the binding mode of bitopic ligands is to isolate both orthosteric and allosteric fragments from the parent structure.[10,11] This approach highlights the possibility that one may discover novel allosteric ligands for GPCRs by generating fragments of extended ligands that would be expected to solely interact with an allosteric pocket rather than the orthosteric pocket.

The dopamine D_1-D_5 receptors mediate the physiological functions of the catecholamine neurotransmitter, dopamine.[12] Many central nervous system diseases are treated with drugs that bind to the D_2-like dopamine receptors (i.e. the D_{2S}, $D_{2L,}$ D_3 and D_4 dopamine receptors). Drug discovery at these receptors has focused on targeting the orthosteric site with agonists used for the treatment of the motor symptoms of Parkinson's disease and antagonists or low efficacy partial agonists for the treatment of schizophrenia. However, allosteric targeting of these receptors may offer several

advantages, including maintenance of spatiotemporal patterns associated with endogenous neurohumoral signalling. However, despite such theoretical advantages this approach has yet to be exploited therapeutically in part due to the paucity of both allosteric scaffolds for this receptor and knowledge of the location of allosteric sites that can be targeted with small molecules.
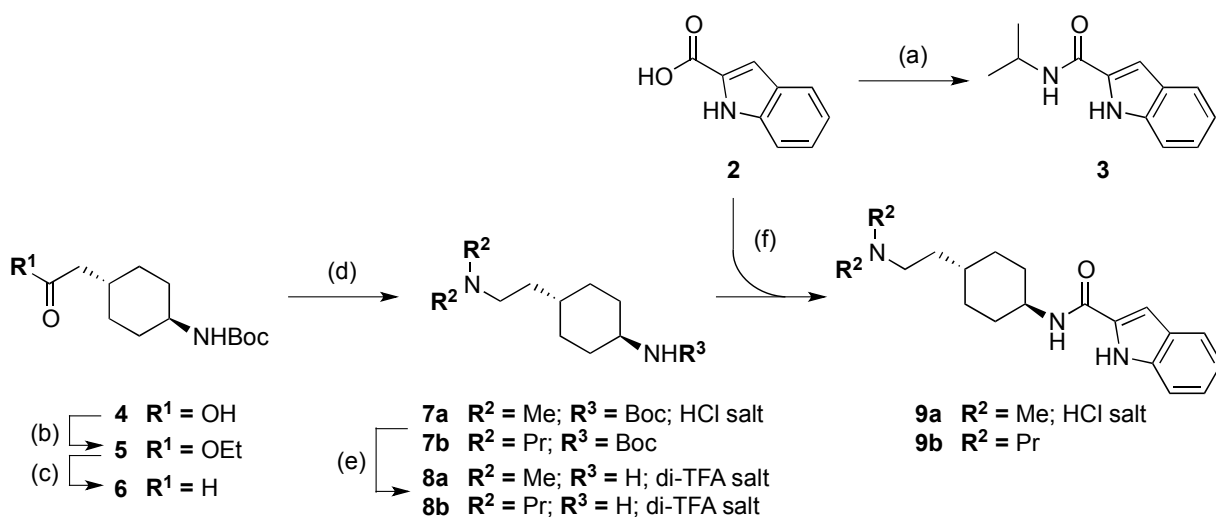

Figure 1. Structures of dopamine receptor ligands; **1** - negative allosteric modulator of the D_2R; Eticlopride – selective D_2R/D_3R antagonist; *R*-22 – selective D_3R antagonist.

Recently, we demonstrated that *N*-((*trans*)-4-(2-(7-cyano-3,4-dihydroisoquinolin-2(1*H*)-yl)ethyl)cyclohexyl)-1*H*-indole-2-carboxamide (SB269652, **1**, **Figure 1**) is a negative allosteric modulator of the D_2R. We presented a novel mechanism of action whereby **1** adopts a bitopic pose at one protomer of a D_2R dimer to modulate the binding of dopamine at the other protomer.[13] We generated fragments of **1** that included the 7-cyano-1,2,3,4-tetrahydroisoquinoline (7-CTHIQ) head-group of **1** to demonstrate that these fragments exhibited competitive antagonism of dopamine and, therefore, that this moiety occupies the orthosteric site of the D_2R. The crystal structure of the D_3R bound to the antagonist: (*S*)-3-chloro-5-ethyl-*N*-((1-ethylpyrrolidin-2-yl)methyl)-6-hydroxy-2-methoxybenzamide (eticlopride, **Figure 1**) and a number of follow-up studies revealed a secondary pocket between transmembrane domains (TMs) 2 and 7 in the receptor structure that can be exploited by extended ligands such as (*R*)-*N*-(4-(4-(2,3-dichlorophenyl)piperazin-1-yl)-3-hydroxybutyl)-1*H*-indole-2-carboxamide (*R*-22, **Figure 1**) to achieve subtype selectivity.[14-16] These studies also revealed

that such ligands extend into a similar secondary pocket in the D_2R. Using mutagenesis in combination with derivatives of **1** we demonstrated that the indole-2-carboxamide moiety of **1** extends into a secondary pocket between the extracellular ends of TM2 and TM7 of the D_2R. We hypothesize that this secondary pocket may an allosteric site that can targeted by allosteric ligands that do not concomitantly engage the orthosteric site unlike the bitopic ligand **1**. In this study we design and synthesise a library of fragments derived from **1** that include and extend from the indole-2-carboxamide moiety of **1** to probe the SAR of this putative allosteric site. *N*-Isopropyl-1*H*-indole-2-carboxamide (**3**), the smallest fragment of **1** containing the indole-2-carboxamide moiety, displays allosteric pharmacology with micromolar affinity for the D_2R. We used mutagenesis to demonstrate that this fragment binds in a similar allosteric pocket as the indole-2-carboxamide moiety of **1**. We then performed an SAR analysis using **3** as our lead compound to identify *N*-butyl-1*H*-indole-2-carboxamide (**11d**), which displayed both 10-fold increased negative cooperativity and 7-fold increased affinity for the D_2R. As such, we report indole-2-carboxamides as a novel scaffold, and attractive starting point for the development of negative allosteric modulators of the D_2R that target an allosteric pocket within the D_2R between TM2 and TM7. These data further confirm the bitopic mode of interaction of **1** and illustrate that fragmentation of extended compounds such as **1** can reveal novel allosteric scaffolds.

RESULTS AND DISCUSSION

Chemistry. The synthesis of the smallest fragment of **1**, *N*-isopropyl-1*H*-indole-2-carboxamide (**3**) was achieved in a good yield, through coupling of commercially available 1*H*-indole-2-carboxylic acid (**2**) and isopropylamine, employing *O*-(1*H*-6-chlorobenzotriazole-1-yl)-1,1,3,3-tetramethyluronium hexafluorophosphate (HCTU) as a coupling reagent (**Scheme 1**).

Scheme 1. Synthesis of fragments of 1[a]

4 **R¹** = OH
5 **R¹** = OEt
6 **R¹** = H

7a **R²** = Me; **R³** = Boc; HCl salt
7b **R²** = Pr; **R³** = Boc
8a **R²** = Me; **R³** = H; di-TFA salt
8b **R²** = Pr; **R³** = H; di-TFA salt

9a **R²** = Me; HCl salt
9b **R²** = Pr

[a] Reagents and conditions: (a) HCTU, isopropylamine, DMF, 75%; (b) i. EtI, K₂CO₃, MeCN, rt to reflux, ii. 50 °C, iii. reflux, 100%; (c) i. dry toluene, -78 °C, ii. DIBAL-H, -78 °C, iii. MeOH, -78 °C, 100%; (d) (R²)₂NH, NaBH(OAc)₃, 1,2-dichloroethane, rt, 50-56%; in the case of **7a**, the product was converted to the corresponding HCl salt form using 1 M HCl/Et₂O (e) TFA/DCM (1:3), rt, 96-99%; (f) DIPEA, BOP, DCM, 36-49%; in the case of **9a**, the product was converted to the corresponding HCl salt form using 1 M HCl (aq).

The larger fragments of **1** (compounds **9a-b**) were accessible through a five-step procedure, initially starting with 2-((*trans*)-4-((*tert*-butoxycarbonyl)amino)cyclohexyl)acetic acid (**4**). Carboxylic acid **4** underwent alkylation with EtI in the presence of K₂CO₃ under reflux conditions in MeCN, to form the corresponding ethyl ester **5** in quantitative yield. The partial reduction of **5** was achieved cleanly in the

presence of DIBAL-H, with quenching at -78°C, to afford aldehyde **6** in quantitative yield. Reductive

amination of **6** with either dimethylamine or dipropylamine using $NaBH(OAc)_3$ in 1,2-dichloroethane,

gave tertiary amine derivatives **7a** and **7b**, respectively. Compounds **7a-b** underwent *N*-Boc

deprotection in the presence of TFA/DCM (1:3), to afford diamines **8a-b** in the bis-trifluoroacetate salt

form. Finally, coupling of **8a-b** with 1*H*-indole-2-carboxylic acid (**1**), employing BOP as the coupling

reagent, furnished the desired fragment compounds **9a-b** (**Scheme 1**). In the case of **9a**, formation of

the HCl salt in 1 M $HCl_{(aq)}$ was carried out prior to pharmacological evaluation.

Scheme 2. Synthesis of *N*-substituted-1*H*-indole-2-carboxamides[a]

R4 =			
a	NH_2	k	azetidin-1-yl
b	NHEt	l	pyrrolidin-1-yl
c	NH^nPr	m	piperidin-1-yl
d	NH^nBu	n	morpholin-4-yl
e	$NHCH_2CH=CH_2$	o	cyclopropylamino
f	$NHCH_2CH_2OH$	p	cyclobutylamino
g	$NHCH(Et)_2$	q	cyclopentylamino
h	NH^tBu	r	cyclohexylamino
i	$N(Me)_2$	s	(piperidin-1-yl)amino
j	$N(^iPr)_2$	t	phenylamino
		u	(cyclopropylmethyl)amino
		v	(cyclohexylmethyl)amino
		w	benzylamino
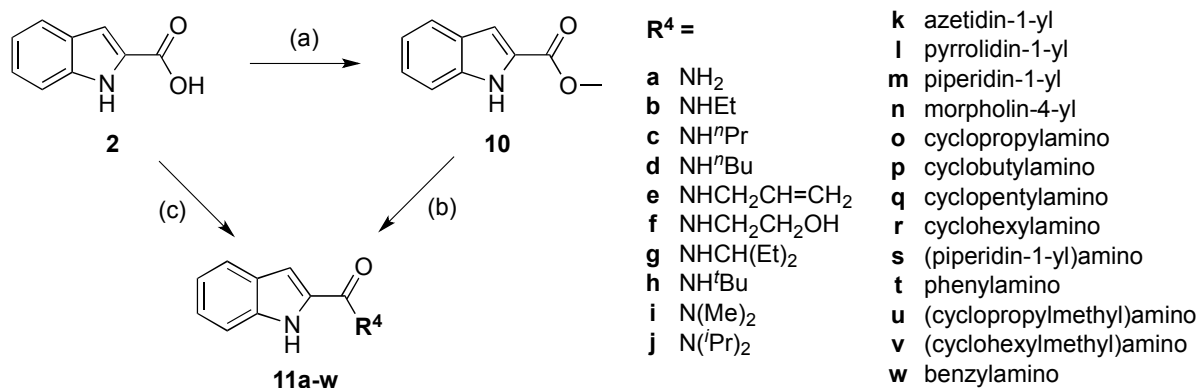
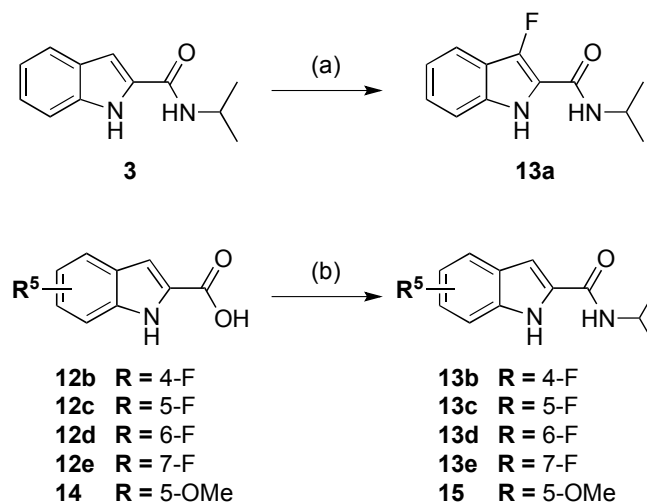[a] Reagents and conditions: (a) MeOH, concentrated H_2SO_4, reflux, 98%; (b) amine/amine solution, EtOH, rt, 34-76%; (c) HCTU, DMF, excess amine or stoichiometric amine and DIPEA, rt, 34-81%.

Our initial library of compounds focused on analogues of **3** varied at the carboxamide moiety.

Synthesis of target amides **11a-w** was achieved by either HCTU-mediated coupling (**11g-h, j-w**), with

a series of commercially available amines (in a similar fashion to the synthesis of **3**), or by direct

aminolysis of the intermediate methyl ester **10** (**Scheme 2**). Methyl ester **10** was obtained from

carboxylic acid **2** in near-quantitative yield, through esterification by reflux in MeOH, in the presence

of catalytic concentrated H_2SO_4. Subsequent direct aminolysis of **10** carried out in EtOH at rt, in the

presence of excess amine or amine solution, afforded **11a-f** and **11i** in modest to good yield. This extensive library of 1*H*-indole-2-carboxamides was comprised of compounds designed to interrogate the effect of introducing increasing size of both linear and branched alkyl chains, saturated and aromatic carbocycles and also amides with varying levels of N-substitution.

The systematic introduction of the electronegative element fluorine into various positions on aromatic ring scaffold, known as a "fluorine walk", has in the past uncovered derivatives of the parent compound with improved potency or physicochemical characteristics; in particular this strategy was employed in SAR studies of the prototypical positive allosteric modulator of the M_1 mAChR – BQCA.[17,18] As a second area of investigation, we sought to generate a small library of mono-fluoro-substituted *N*-isopropyl-1*H*-indole-2-carboxamides (**13a-e**), in addition we synthesized the corresponding 5-methoxy analogue of **3** (**Scheme 3**).
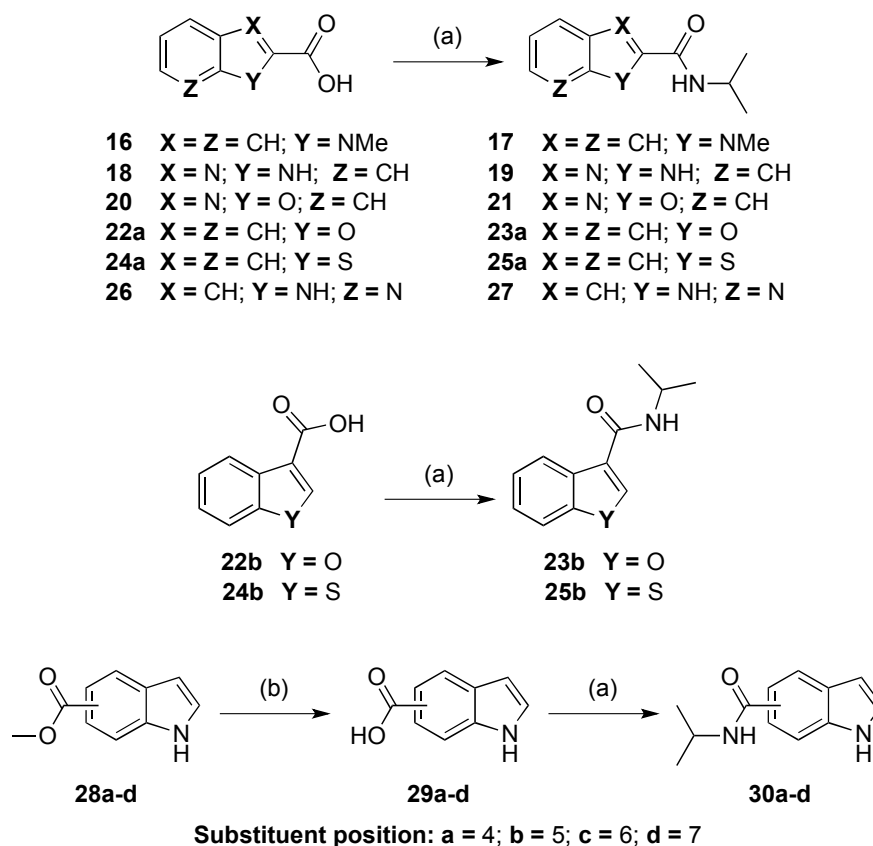
Scheme 3. Synthesis of substituted *N*-isopropyl-1*H*-indole-2-carboxamide[a]

12b	R = 4-F	**13b**	R = 4-F
12c	R = 5-F	**13c**	R = 5-F
12d	R = 6-F	**13d**	R = 6-F
12e	R = 7-F	**13e**	R = 7-F
14	R = 5-OMe	**15**	R = 5-OMe

[a] Reagents and conditions: (a) i. Sat. NaHCO₃ (aq), MeCN, 0 °C, ii. 1-Chloromethyl-4-fluoro-1,4-diazoniabicyclo[2.2.2]octane bis(tetrafluoroborate), rt, 46%; (b) HCTU, isopropylamine, DMF, rt, 7-80%.

3-Fluoro-*N*-isopropyl-1*H*-indole-2-carboxamide (**13a**) was accessed in moderate yield, through fluorination of **3** using the electrophilic fluorine source 1-chloromethyl-4-fluoro-1,4-diazoniabicyclo[2.2.2]octane bis(tetrafluoroborate), adapting literature methodology.[19] The remaining fluoro- and methoxy-substituted analogues (**13b-e, 15**) were obtained through HCTU-mediated coupling the corresponding commercially available carboxylic acid precursors (**12b-e, 14**) with isopropylamine as described above.

Scheme 4. Synthesis of *N*-isopropyl carboxamide-substituted heterocycles*[a]*

16 X = Z = CH; Y = NMe	**17** X = Z = CH; Y = NMe
18 X = N; Y = NH; Z = CH	**19** X = N; Y = NH; Z = CH
20 X = N; Y = O; Z = CH	**21** X = N; Y = O; Z = CH
22a X = Z = CH; Y = O	**23a** X = Z = CH; Y = O
24a X = Z = CH; Y = S	**25a** X = Z = CH; Y = S
26 X = CH; Y = NH; Z = N	**27** X = CH; Y = NH; Z = N

22b Y = O	**23b** Y = O
24b Y = S	**25b** Y = S

28a-d   **29a-d**   **30a-d**

Substituent position: a = 4; b = 5; c = 6; d = 7

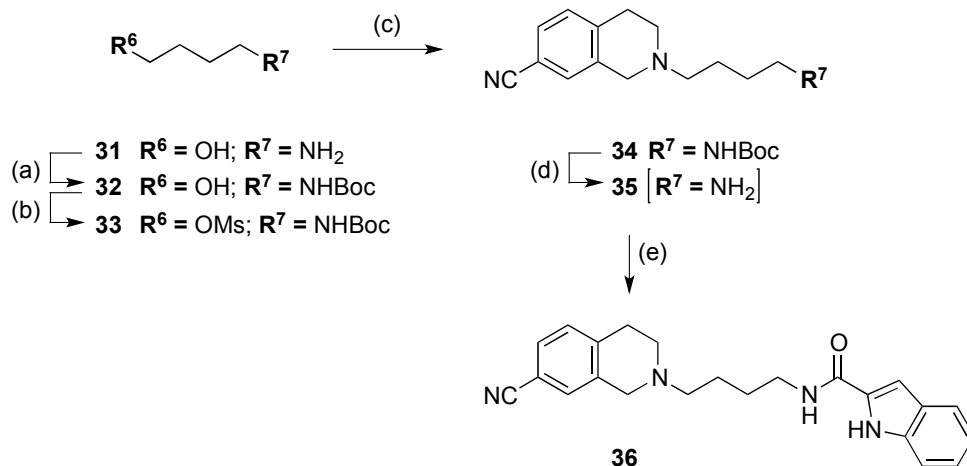*[a]* Reagents and conditions: (a) HCTU, isopropylamine, DMF, rt, 22-90%; (b) LiOH.H$_2$O, THF/water (1:1), rt, 78-100%;

Our final series of fragment analogues used a series of aromatic core replacements to ascertain whether the allosteric modulatory activity of **3** could be affected by the electronic nature of the bicyclic heteroaromatic ring, or the presence of the hydrogen-bond donor moiety of the indole (**Scheme 4**). In addition, we also wanted to investigate positional isomers of **3**, where the attachment point of the *N*-isopropylcarboxamide was varied around the indole scaffold (**Scheme 4**).

The *N*-methyl-1*H*-indole, benzo[*d*]imidazole, benzo[*d*]oxazole, benzofuran, benzo[*b*]thiophene and pyrrolo[2,3-*b*]pyridine analogues of **3** (compounds **17, 19, 21, 23a, 25a** and **27**, respectively) were once again easily synthesized through HCTU-mediated coupling of the parent carboxylic acid with isopropylamine. Considered to be of interest also, were the 3-substituted benzofuran, benzo[*b*]thiophene analogues (**23b** and **25b**) which were obtained in the same manner.

Finally, synthesis of the series of positional isomers of **3** was carried out in a two-step procedure. Attempted direct aminolysis of commercially available methyl esters **28a-d** proved unsuccessful, therefore, initial basic hydrolysis of the esters to give the corresponding carboxylic acids **29a-d** was carried out. Final HCTU-mediated coupling of **29a-d** with isopropylamine gave the desired carboxamides **30a-d** (**Scheme 4**).

Pharmacological analysis of the series of carboxamide fragments revealed the *N*-butyl-1*H*-indole-2-carboxamide **11d**, to have higher affinity for the D_2R and greater negative cooperativity with dopamine as compared to the parent fragment **3** (see below). With this in mind, we sought to synthesise an analogue of **1** incorporating the structure of **11d** (**Scheme 5**), anticipating that combining the 7-CTHIQ and **11d** moieties would proffer a higher affinity D_2R bitopic ligand. The target compound **36** was prepared as described previously (**Scheme 5**).[20]

**Scheme 5. Synthesis of a prospective higher affinity bitopic ligand incorporating fragment 11d**[a]

(a)	31	R^6 = OH; R^7 = NH$_2$
	32	R^6 = OH; R^7 = NHBoc
(b)	33	R^6 = OMs; R^7 = NHBoc

(d)	34	R^7 = NHBoc
	35	[R^7 = NH$_2$]

36

[a] Reagents and conditions: (a) Boc$_2$O, TEA, DCM, rt, 82%; (b) MsCl, TEA, DCM, rt, 93%; (c) 7-CTHIQ, DIPEA, DCM, reflux, 12%; (d) i. TFA/DCM (1:5), rt; ii. neutralization; (e) **2**, HCTU, DIPEA, DMF, rt, 69%.

Pharmacology.

Fragments of 1 containing the indole-2-carboxamide moiety display allosteric pharmacology. In previous work we demonstrated that **1** binds as a bitopic ligand to one protomer of a homodimer of the D$_2$R to modulate the binding of a ligand to the orthosteric site of a second protomer.[13] We previously identified purely orthosteric fragments of **1** containing the 7-CTHIQ moiety that displayed competitive pharmacology with dopamine. This core group comprises the key elements expected to interact with the orthosteric binding site of aminergic receptors (i.e. an aromatic ring in close proximity to a charged nitrogen at physiological pH). In the current study we have derived fragments extending from the indole-2-carboxamide moiety of **1** (distal to the 7-CTHIQ orthosteric head-group), with the aim to provide further validation of the bitopic mode of action of **1**. In addition we wanted to examine whether the approach of dividing bitopic ligands into discrete fragments can unmask novel purely allosteric scaffolds.

Figure 2
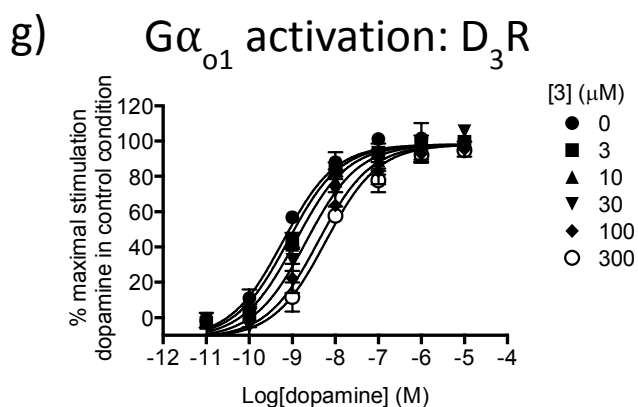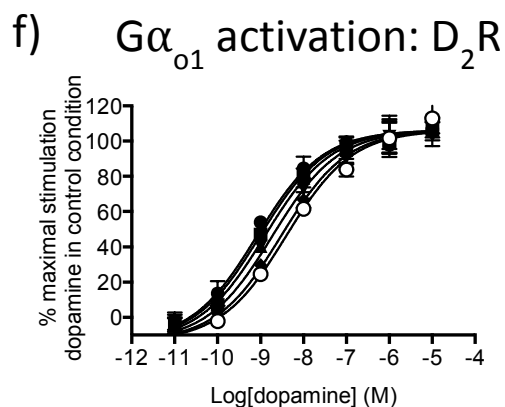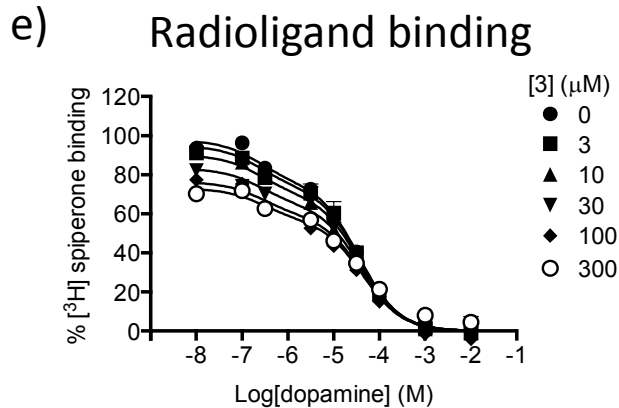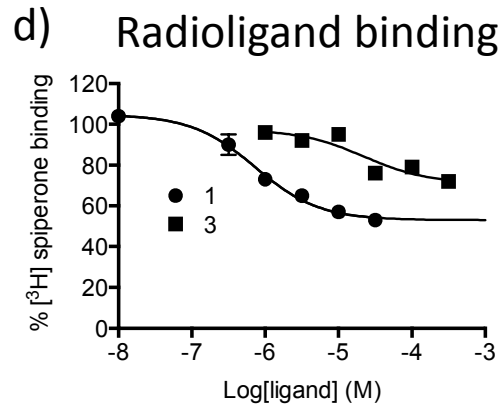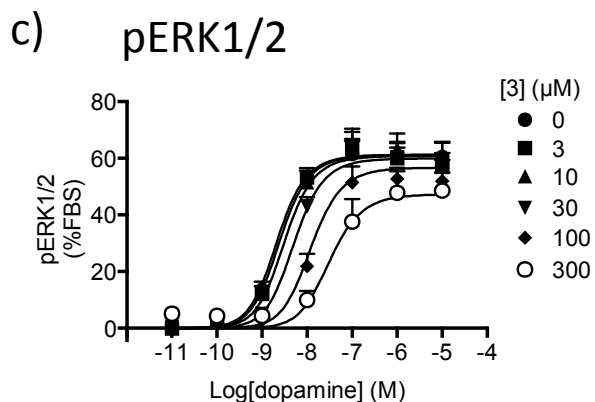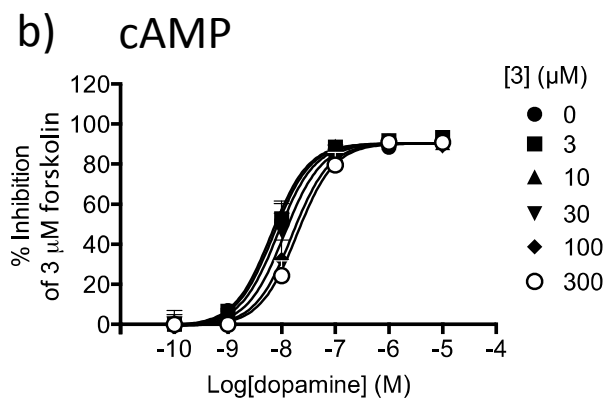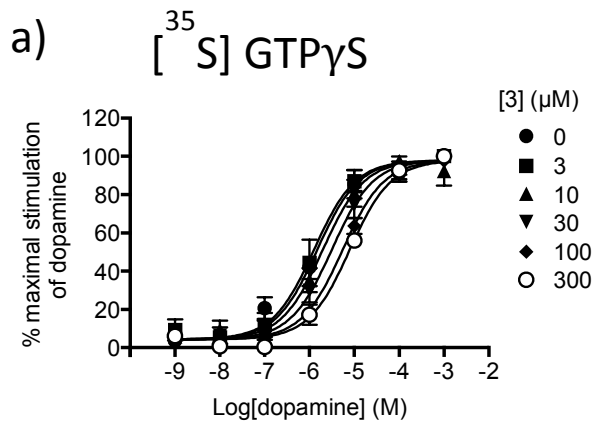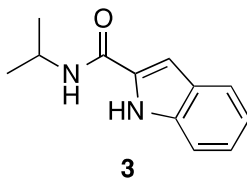
Figure 2. A fragment of **1** containing the indole-2-carboxamide pharmacophore (**3**) inhibited the action of dopamine D_2R in a non-competitive manner, in functional assays measuring: **(a)** D_2R mediated [^{35}S]GTPγS binding; **(b)** inhibition of forskolin stimulated cAMP; **(c)** ERK1/2 phosphorylation. Data were fitted using an allosteric ternary complex model ([^{35}S]GTPγS and cAMP, **Equation 4**) or an operational model of allosterism (pERK1/2, **Equation 5**), to derive values of affinity and cooperativity (**Table 1**). **(d)** Both **1** and **3** caused partial displacement of the binding of [^{3}H]spiperone in an equilibrium binding assay consistent with an allosteric mode of action. **(e)** Dopamine-mediated inhibition of the equilibrium binding of [^{3}H]spiperone in the absence or presence of **3**. Data points represent the mean ± SEM of three experiments performed in duplicate. Curves drawn through the data points represent the best fit of a two-site allosteric ternary complex model (**Equation 1**, **Table 1**). Compound **3** interacts with the D_2R (**f**) and the D_3R (**g**) in an allosteric manner in an assay measuring Ga_{oB} G protein activation.

Table 1. Characterization of fragments of 1 containing the indole-2-carboxamide moiety in terms of binding and function at the D_2R^a

	[^{35}S]GTPγS		cAMP		pERK1/2			[^{3}H]spiperone binding		
	pK_B (K_B, μM)	Log$\alpha\beta$ ($\alpha\beta$)	pK$_B$ (K_B, μM)	Log$\alpha\beta$ ($\alpha\beta$)	pK_B (K_B, μM)	Logα (α)	Logβ	pK_B (K_B, μM)	Logα (α)	Logα' (α')
3	4.89 ± 0.29 (13)	-0.89 ± 0.17 (0.13)	4.72 ± 0.29 (19)	-0.54 ± 0.09 (0.28)	4.35 ± 0.06 (45)	-0.53 ± 0.13 (0.30)	-100	4.88 ± 0.17 (13)	-0.51 ± 0.04 (0.31)	-0.53 ± 0.04 (0.30)
9a	5.54 ± 0.4 (3)	-0.84 ± 0.15 (0.14)	ND	ND	5.54 ± 0.4 (3)	-0.61 ± 0.14 (0.25)	-100	-	-	-

^{a}The ability of **3** or **9a** to modulate the functional effect of agonists or their affinity for the D_2R expressed in Flp-IN CHO cells was tested at various signaling endpoints. For [^{35}S]GTPγS and cAMP assays data was fitted to an allosteric ternary complex model (**Equation 4**) whereas for pERK1/2 assays data was fit to an operational model of allosterism (**Equation 5**) to derive values of affinity (pK_B) and cooperativity. Radioligand binding data were fitted with **Equation 1** to derive values of cooperativity with dopamine (Logα) and [^{3}H]spiperone binding (Logα')

Our previous study demonstrated that the indole-2-carboxamide moiety of **1** extended into a secondary 'allosteric' pocket within the D_2R.[13] Accordingly, we first synthesised the fragment **3**, (**Scheme 1, Figure 2a**) with the hypothesis that this fragment would act as a modulator of dopamine binding and/or function. Our characterization of **3** revealed this small molecule inhibited the action of

dopamine in a manner that was best fit by an allosteric model in both functional and ligand binding assays. When an interaction study with dopamine was performed in either a $[^{35}S]$GTPγS assay (**Figure 2a**) or an assay measuring D_2R-mediated inhibition of forskolin-stimulated cAMP production (**Figure 2b**), **3** caused a limited 8-fold or 3-fold reduction in agonist potency, respectively (**Figure 2b**). Application of an allosteric ternary complex model to the concentration response data yielded estimates of affinity for the unoccupied receptor ($[^{35}S]$GTPγS assay, $K_B = 13$ μM: cAMP assay, $K_B = 19$ μM) and its cooperativity with dopamine ($[^{35}S]$GTPγS assay, $αβ = 0.13$: cAMP assay, $αβ = 0.29$; where $α$ represents cooperativity with dopamine affinity, $β$ represents modulatory effect upon dopamine efficacy and values less than 1 indicate negative cooperativity, **Table 1**). This pattern was distinct from that observed in an assay measuring ERK1/2 phosphorylation, in which **3** caused both a reduction in dopamine potency and a significant decrease in maximal response (**Figure 2c**). This latter observation is consistent with negative modulation of orthosteric ligand efficacy.[21] Accordingly, data were fitted using an operational model of allosterism whereby Log$β$ was fixed to -100 to reflect the high negative modulatory effect of **3** upon dopamine efficacy. This analysis allowed estimation of an affinity value ($K_B = 46$ μM) for **3** and its cooperativity with dopamine binding ($α = 0.29$) (**Table 1**). However, because of the low affinity of **3** and its relatively weak modulatory effect upon dopamine potency we sought additional evidence of an allosteric mode of interaction. Therefore, we extended our characterization to a radioligand-binding assay. We first tested the ability of **3** to antagonize $[^{3}H]$spiperone and found that increasing concentrations of **3** produced only a partial displacement of this radioligand consistent with an allosteric mode of interaction (**Figure 2d**). We extended these studies to perform a binding interaction study to investigate the effect of increasing concentrations of **3** on the affinity of both dopamine and the radiolabeled antagonist $[^{3}H]$spiperone. The value of affinity derived for **3** ($K_B = 13$ μM) was consistent with that determined in each functional assay (**Figure 2e, Table 1**). In addition, **3** was a negative modulator of both dopamine ($α = 0.31$) and $[^{3}H]$spiperone ($α =$

0.30) affinity. These values indicate that, whilst the magnitude of negative allosteric modulation of dopamine affinity is consistent across all assays, the decrease of dopamine E_{max} in the pERK1/2 assay is consistent with additional effects of **3** upon dopamine efficacy. Such a distinct pattern of action may indicate that **3** differentially antagonizes the effect of dopamine at different signalling endpoints. However, the sensitivity of the respective assays and the different assay conditions of the various assays may also underlie this effect although it is interesting to note that the parent compound, **1**, demonstrated a profile of modulation whereby the degree of negative cooperativity with dopamine could be attributed solely to an effect on dopamine affinity and was not significantly different across these different pathways.[14] Compound **1** has been shown to display approximately 50-fold selectivity for the D_3R over the D_2R.[22,23] Furthermore, it was postulated that this subtype selectivity was driven through interaction of the indole-2-carboxamide moiety of **1** with an extended pocket.[15] The D_3R has been shown to selectively couple to the $G\alpha_{o1}$ G protein whereas the D_2R can couple to all members of the $G\alpha_{i/o}$ G protein family.[24] Accordingly, we assessed the action of **3** at the D_2R (**Figure 2f**) compared to the D_3R (**Figure 2g**) in an assay measuring activation of $G\alpha_{o1}$ G protein using a bioluminescence resonance energy transfer (BRET) biosensor.[25] This revealed that **3** displays both affinity (D_2R pK_B = 4.84 ± 0.27 (K_B = 14 μM): D_3R, pK_B = 5.05 ± 0.21 (K_B = 9 μM)) and negative cooperativity (D_2R, logα = -0.77 ± 0.14 (α = 0.17): D_3R, logα = -1.13 ± 0.16 (α = 0.07) that is not significantly different between the D_2R and D_3R.
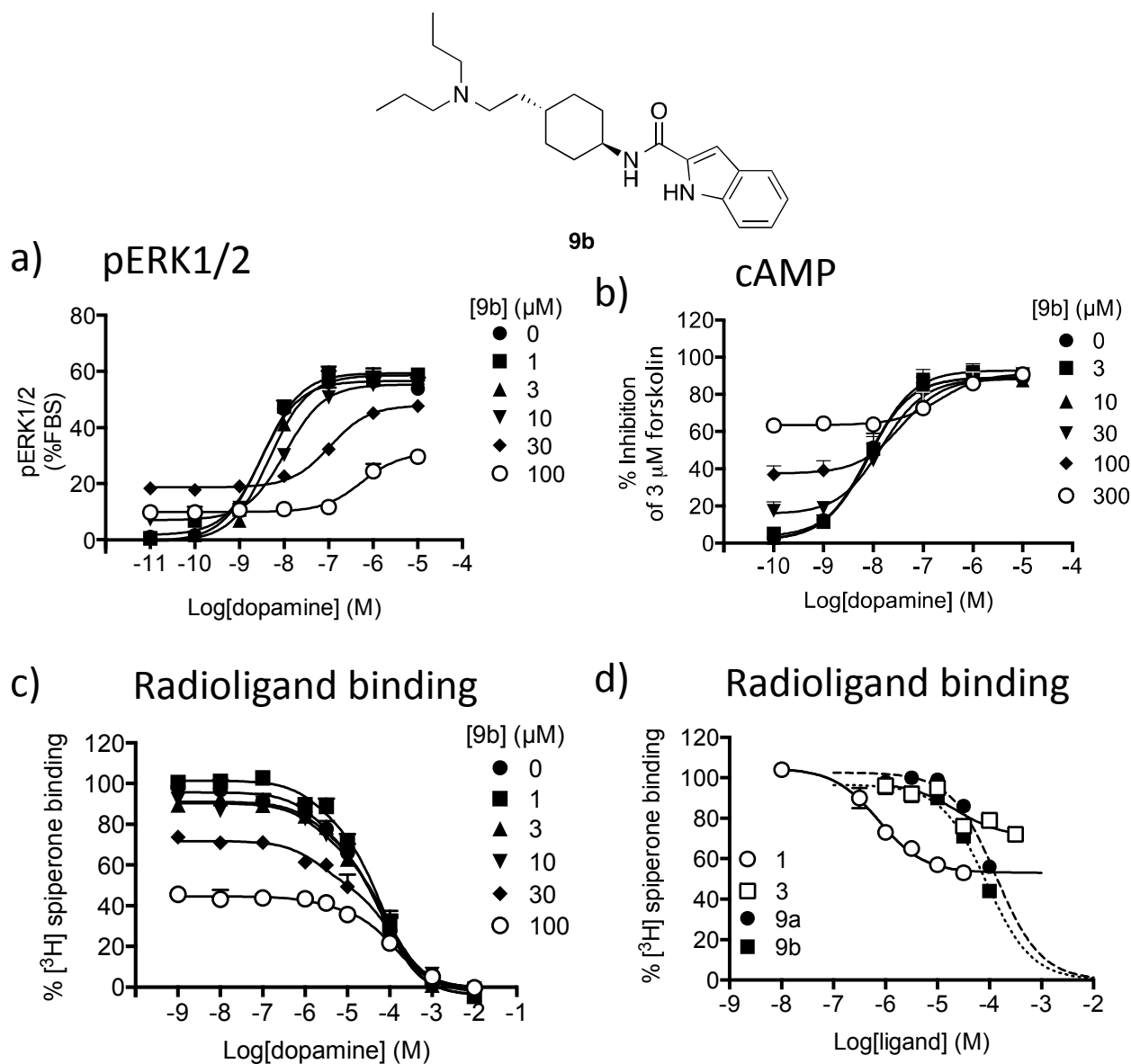
Figure 3
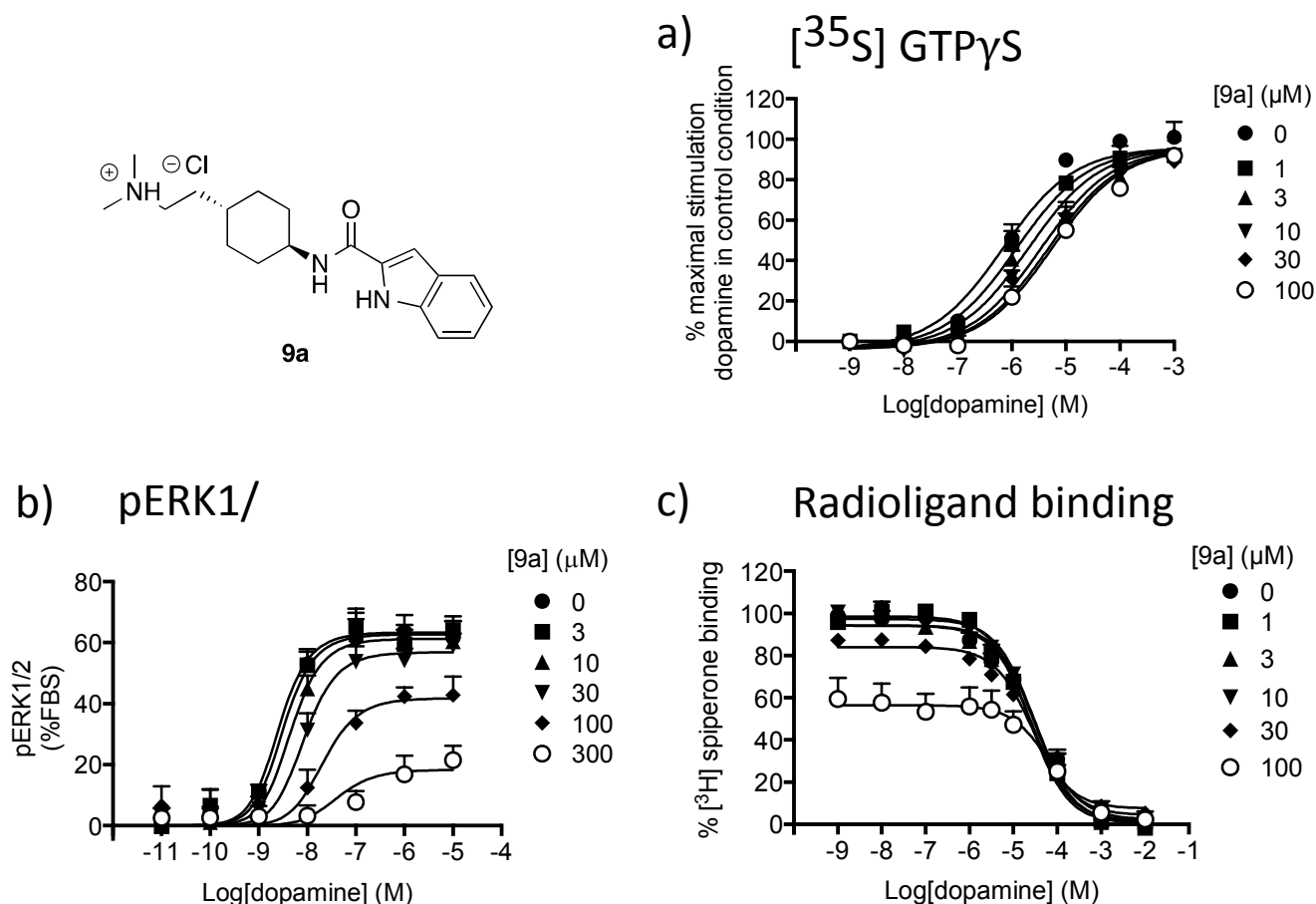
Figure 3. A fragment of **1** containing the indole-2-carboxamide pharmacophore and extending to a tertiary amine (emulating the position of that present on the 7-CTHIQ moiety) interacts with the D_2R in a mixed orthosteric/allosteric manner, in functional assays measuring: **(a)** D_2R mediated $[^{35}S]GTP\gamma S$ binding, and **(b)** ERK1/2 phosphorylation, **9a** inhibited the action of dopamine in a non-competitive manner. Data were fitted using an allosteric ternary complex model ($[^{35}S]GTP_{\gamma}S$, **Equation 4**) or an operational model of allosterism (pERK1/2, **Equation 5**) (**Table 1**). **(c)** Dopamine-mediated inhibition of the equilibrium binding of $[^3H]$spiperone in the absence or presence of **9a**. Data points represent the mean ± SEM of three experiments performed in duplicate. Curves drawn through the data points represent the best fit of a two-site binding model.[26]

One would also expect that extension of the purely allosteric pharmacophore to include structural features of the orthosteric moiety, incorporating a suitable linker moiety in between, would result in the generation of ligands that displayed competitive behaviour with an orthosteric ligand. We generated additional fragments of **1** that extended away from the indole-2-carboxamide moiety and included a

tertiary amine group (emulating that present on the 7-CTHIQ moiety of **1**). Characterisation of **9a** (**Figure 3, Scheme 1**) was consistent with either an allosteric mode of interaction ([^{35}S]GTPγS (**Figure 3a**) and pERK1/2 (**Figure 3b**) or competitive mode of interaction (radioligand binding) (**Figure 3c, Table 1**). This discrepancy is most likely due to the larger molecular size of spiperone as compared to dopamine whereby **9a** may be able to occupy the D_2R simultaneously with dopamine but not with spiperone. Of interest, the allosteric mode of interaction suggests that the protonated amino group of **9a** does not project into the area occupied the protonated amino of dopamine. If one considers the competitive action of fragments of **1** that contain the 7-CTHIQ moiety, this suggests that the orientation of the amino group of **9a** and the amino group within the 7-CTHIQ moiety of **1** must be different. These data also highlight the proximity of the orthosteric and allosteric pockets.

Figure 4. A more extensive fragment of **1** containing the indole-2-carboxamide pharmacophore and extending to a tertiary amine (emulating the position of that present on the 7-CTHIQ moiety, but with longer alkyl chains compared to **9a**) is a partial agonist at the D_2R. To investigate the mode of interaction of **1** with the D_2R we synthesised compound **9b**. In functional assays measuring: **(a)** D_2R-mediated inhibition of forskolin stimulated cAMP production, and **(b)** ERK1/2 phosphorylation, **9b** behaved as a partial agonist. In the pERK1/2 assay, **9b** inhibited the action of dopamine in a non-competitive manner decreasing E_{max} but also displayed agonism in its own right. In contrast in the cAMP assay, **9b** behaved as a competitive partial agonist. **(c)** Dopamine-mediated inhibition of the equilibrium binding of [^{3}H]spiperone in the absence or presence of **9b**. Data points represent the mean ± SEM of three experiments performed in duplicate. Curves drawn through the data points represent the best fit of a two-site binding model[26] (**Supplementary Table 1**). **(d)** The ability of **1** and fragments of **1** to displace [^{3}H]spiperone at the D_2R. Both **1** ($pK_B = 6.29 ± 0.07$, $Log\alpha = -0.46 ± 0.02$) and **3** (pK_B Compound 3 $= 4.75 ± 0.23$, $Log\alpha_{Compound 3} = -0.23 ± 0.03$) demonstrate an inability to completely displace

[^{3}H]spiperone in agreement with an allosteric mode of interaction (**Equation 2**). In contrast, data of both **9a and 9b,** which possess a tertiary amine group (positioned atomically the same distance as that present on the 7-CTHIQ of **1**), were best fitted by a one-site competitive model,[26] with estimated affinity of p$K_{I\_Compound\ 9b}$ = 4.70 ± 0.03.

Extension of the fragment further to generate **9b** (**Figure 4, Scheme 1**) yielded a low affinity partial agonist with a strictly competitive mode of interaction with dopamine in all assays, with the exception of the pERK1/2 assay, in which a concentration-dependent decrease in maximal agonist effect was observed (**Figure 4**). This suggests that the extended alkyl chains of **9b** either reorientate this ligand relative to the position of **9a** so that the protonated amino moiety now occupies and competes directly with the amino moiety of dopamine. Alternatively, if the orientation of **9b** is equivalent to that of **9a** whereby the protonated amine does not compete with that of dopamine the additional length of the alkyl chain substitutions may extend into the binding pocket of dopamine. In either case agonism appears to be concomitant with competition with dopamine.

Compound 3 is modulated by the mutation of residues within a secondary binding pocket of the D$_2$R. While the ability to separate orthosteric and allosteric fragments from **1** is consistent with its bitopic mode of interaction at the D$_2$R, it does not necessarily follow that the allosteric fragment **3** will occupy the same binding pocket as that of the corresponding indole-2-carboxamide moiety of **1**.
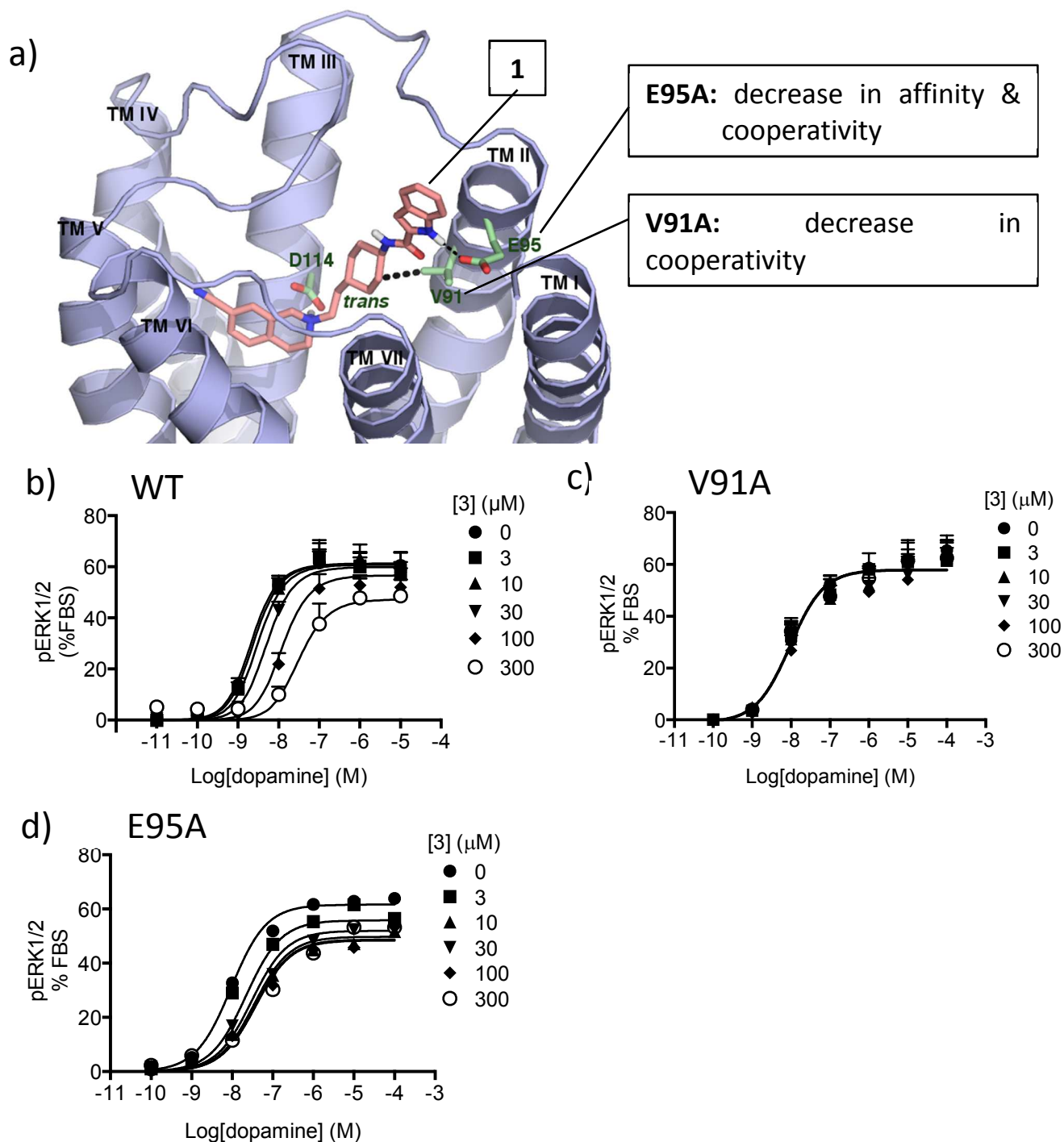
Figure 5. Mutation of residues at the top of TM2 modulates the allosteric action of **3**; **(a)** When docked into a homology model of the D_2R the 7-CTHIQ core of **1** occupies the orthosteric pocket. The 1*H*-indole-2-carboxamide moiety of **1** extends into a secondary pocket between TM2 and TM7, where the indolic NH makes a hydrogen bond interaction with Glu95[2.65], and the 1,4-cyclohexylene group makes a hydrophobic interaction with Val91[2.61] (Figure recreated from modeling studies previously published[14]). Mutation of these residues decreases the affinity or negative cooperativity of **1**.

Interaction studies between **3** and dopamine in an assay measuring D_2R mediated pERK1/2 phosphorylation using CHO cells expressing the **(b)** WT, **(c)** Val91$^{2.61}$Ala or **(d)** Glu95$^{2.65}$Ala.

Table 2: Characterization of binding and function of *N*-isopropyl-1*H*-indole-2-carboxamide (3) at the D_2R^a

	1		**3**		
	pK_B [c] **(K_B, µM)**	**Log$\alpha\beta$** [c] **($\alpha\beta$)**	**pK_B** **(K_B, µM)**	**Logα** **(α)**	**Logβ** **(β)**
Wild Type	6.26 ± 0.09 (0.55)	-1.22 ± 0.11 (0.06)	4.35 ± 0.06 (45)	-0.53 ± 0.13 (0.29)	-100
Val91$^{2.61}$Ala	6.26 ± 0.09 (0.55)	-0.48 ± 0.16 (0.33)	-[b]	-	-
Glu95$^{2.65}$Ala	5.31 ± 0.19 (4.90)	-0.32 ± 0.14 (0.48)	6.38 ± 0.31 (0.04)	0.12 ± 0.12 (1.31)	-0.81 ± 0.11 (0.15)

*[a]*The ability of **3** to modulate the functional effect of agonists or their effect at either the WT D_2R or mutant D_2Rs expressed in Flp-IN CHO cells was tested in a pERK1/2 assay and data was fit to an operational model of allosterism (**Equation 5**) to derive values of affinity (pK_B) and cooperativity with dopamine. *[b]* no effect of **3** was observed up to concentration of 300 µM. *[c]*Values taken from[14].

Our previous study identified two residues at the top of TM2 (Val91$^{2.61}$ and Glu95$^{2.65}$) that interact with the indole-2-carboxamide moiety of **1** and mutation of these residues to alanine reduced the affinity and/or negative cooperativity of **1** (**Figure 5a, Table 2**).[13] We hypothesised that if **3** occupies the same binding pocket as the 1*H*-indole-2-carboxamide moiety of **1**, then one would expect a similar sensitivity to mutation of these residues. Mutation of Val91$^{2.61}$Ala removed any effect of **3** up to a concentration of 300 µM upon a dopamine in a pERK1/2 assay, indicating this residue is key for **3** binding or function (**Figure 5b, Table 2**). This mutation caused no change in affinity of **1** but caused a 5-fold decrease in negative cooperativity with dopamine. This indicates that **1** makes additional

interactions, most likely within the orthosteric pocket of the D2R, which are the main contibutors to affinity. In contrast, the mutation of Glu95$^{2.65}$Ala caused a 100-fold increase in affinity and a complete abolition of negative cooperativity with dopamine affinity (**Figure 5d, Table 2**). In addition, while **3** at the WT D$_2$R (**Figure 2c**) displayed high negative modulation of dopamine efficacy (Logβ = -100) this modulatory effect was more limited at the Glu95$^{2.65}$Ala (β = 0.15) (**Figure 5b & d, Table 2**). This is quite different to the effect of this mutation upon **1**, where both an 8-fold decrease in negative cooperativity and a 9-fold decrease in affinity was observed. It is important to note that these mutations caused no change in the affinity of dopamine. Therefore, these results suggest that **3** occupies a similar binding site between TM2 and TM7 of the D$_2$R to the 1*H*-indole-2-carboxamide moiety of **1** although it is important to note the individual contribution of the different residues to binding affinity and cooperativity differ between **1** and **3**. Therefore, we must acknowledge the possibility that the orientation of **3** within this pocket may be different to that of 1*H*-indole-2-carboxamide moiety of **1**. Furthermore, because we cannot measure binding of **3** directly (i.e with a radiolabelled derivative) then we must also consider the possibility that the effects of such mutations, rather than indicating a direct residue-ligand interaction, may result from an allosteric effect i.e. mediated by a global change in receptor conformation.

We then conducted a detailed SAR study to understand the structural determinants of the allosteric action of **3** and to generate derivatives with higher affinity and/or negative cooperativity.
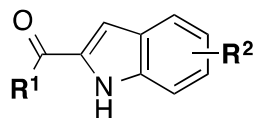

Preliminary investigation into the SAR of indole and related heterocycle carboxamide derivatives

The most complex allosteric behaviour for compound **3** was observed in the pERK1/2 phosphorylation assay in which increasing concentrations of the modulator caused both a decrease in dopamine affinity and maximal effect. Moreover, this assay provides a robust, medium-throughput measurement of D$_2$R activation. As such, all derivatives of compound **3** were screened using this assay. We observed four
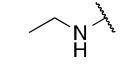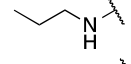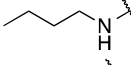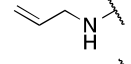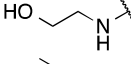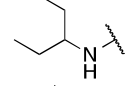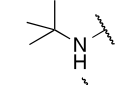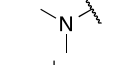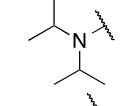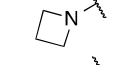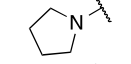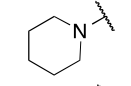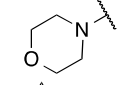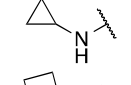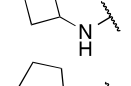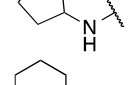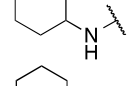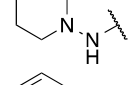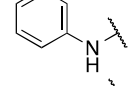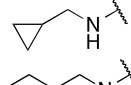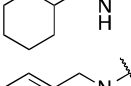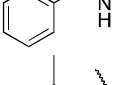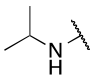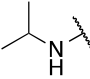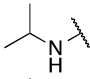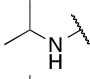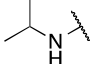
distinct patterns of ligand action across the entire series of compounds (**Table 3 & 4**). A number of compounds caused both a rightward displacement of the dopamine concentration-response curve and a decrease in the maximal response of dopamine that did not reach a limit within the concentration range used. These data were analyzed according to an operational model of allosterism (as for compound **3**, **Figure 1**) to determine a value of affinity (K_B) and binding cooperativity parameter (α) between dopamine and the allosteric ligand (where Logβ was constrained to -100 to represent high negative modulation of dopamine efficacy). Other compounds caused a limited rightward shift of the dopamine dose-response curve but no decrease in E_{max}. These data were fit using an operational model of allosterism where Logβ was constrained to 0 to represent no effect upon dopamine efficacy. A number of compounds produced an unlimited rightward shift of a dopamine dose-response curve within the concentration range of test compound used. Accordingly, data were fit with a competitive model to allow an estimate of affinity for the D_2R. However, because the concentration range used to test these compounds was restricted by compound solubility we cannot exclude the possibility that these compounds also act by binding to an allosteric pocket while maintaining high negative cooperativity with dopamine. Finally, some compounds had no effect upon the dopamine dose-response curve within the range of compound tested.

Table 3. Characterization of analogues of compound 3, varied at the carboxamide *N*-substituent and indole-substitution in terms of binding and function at the D_2R^a

No.	R^1	R^2	pK_B (K_B, μM)	Logα (α)
3^b		H	4.35 ± 0.07 (45)	-0.53 ± 0.09 (0.29)
11a		H	ND	ND

Compound		R		
11b[b]		H	3.67 ± 0.14 (214)	-0.35 ± 0.21 (0.45)
11c[b]		H	4.21 ± 0.06 (62)	-0.60 ± 0.09 (0.25)
11d[b]		H	5.21 ± 0.07 (6)	-1.63 ± 0.11 (0.02)
11e[b]		H	5.33 ± 0.21 (5)	-0.26 ± 0.06 (0.55)
11f		H	ND	ND
11g[d]		H	4.41 ± 0.14 (39)	NA
11h[b]		H	4.30 ± 0.06 (50)	-0.58 ± 0.13 (0.26)
11i		H	ND	ND
11j[b]		H	4.72 ± 0.10 (19)	-1.39 ± 0.11 (0.04)
11k		H	ND	ND
11l[d]		H	3.08 ± 0.11 (831)	NA
11m		H	ND	ND
11n		H	ND	ND
11o[d]		H	3.81 ± 0.08 (154)	NA
11p[c]		H	4.77 ± 0.13 (17)	-1.77 ± 0.27 (0.02)
11q[b]		H	4.72 ± 0.26 (19)	-0.63 ± 0.11 (0.23)
11r		H	ND	ND
11s[b]		H	4.04 ± 0.10 (91)	-0.53 ± 0.13 (0.30)
11t[d]		H	4.73 ± 0.34 (19)	NA
11u[b]		H	4.53 ± 0.07 (30)	-1.01 ± 0.08 (0.10)
11v		H	ND	ND
11w		H	ND	ND
13a[b]		3-F	4.35 ± 0.29 (45)	-0.72 ± 0.35 (0.19)

Compound	Structure	R	pKB (α)	Logβ (β)
13b[b]		4-F	4.74 ± 0.10 (18)	-1.14 ± 0.10 (0.07)
13c[d]		5-F	4.04 ± 0.08 (91)	NA
13d[d]		6-F	4.26 ± 0.17 (55)	NA
13e[b]		7-F	4.74 ± 0.11 (18)	-0.96 ± 0.12 (0.11)
15[d]		5-OMe	3.98 ± 0.20 (104)	NA

[a]Interaction studies between compounds and dopamine were performed using an ERK1/2 phosphorylation assay upon FlpIn CHO cells stably expressing the $D_{2L}R$ as in **Figure 1c**. [b]For compounds that caused a decrease in the maximal response of dopamine, data were analysed according to an operational model of allosterism where K_B is the equilibrium dissociation constant of the allosteric ligand, α is the binding cooperativity parameter between the orthosteric and allosteric ligand, and β (Logβ constrained to -100 to represent high negative cooperativity with dopamine efficacy) denotes the magnitude of the allosteric effect of the modulator on the efficacy of the orthosteric agonist. [c]For compounds that caused a limited rightward shift of the dopamine dose-response curve but no decrease in E_{max}, data were fit using an operational model of allosterism where Logβ was constrained to 0, to represent neutral cooperativity with dopamine efficacy. [d]For compounds that produced an unlimited rightward shift of a dopamine dose-response curve within the concentration range of test compound used data were fit using model of competitive antagonism (**Equation 6**) . As such a value of cooperativity could not be derived (denoted NA). ND signifies no effect of compound was observed even at the highest concentration of 300 μM. Data represent the mean ± SEM of three experiments performed in duplicate apart from compounds with no effect, which were tested in two separate experiments.

The subtle differences and stepwise structural changes introduced to members of the fragment library reveal some interesting SAR in terms of both their binding and function at the D_2R (**Table 3**). Considering analogues of **3** varied only at the carboxamide *N*-substituent, substitution appears to be essential for binding to the receptor, as the primary amide derivative **11a** does not exhibit receptor binding at even the highest concentrations employed. Furthermore, the degree of N-substitution of the carboxamide moiety is also a key determinant of affinity (K_B), with mono-substituted derivatives (**3, 11b-e, g-h, o-q, t-u**) exhibiting activity, whereas the majority of di-substituted derivatives (**11i, k, m-n**) did not.

Comparing the mono-substituted carboxamide analogues of **3** bearing non-cyclic N-substituents (**11b-h**), increasing the size of linear alkyl substituents from *N*-ethyl (**11b** K_B = 214 μM, $α$ = 0.45), to *N*-propyl (**11c** K_B = 62 μM, $α$ = 0.25), to *N*-butyl (**11d** K_B = 6 μM, $α$ = 0.02), improved both affinity and increased negative cooperativity in a progressive fashion. This demonstrates the importance of *N*-substituent chain length to both binding and negative cooperativity. Interestingly, the *N*-allyl analogue **11e** (K_B = 5 μM, $α$ = 0.55) is of comparable size to **11c**, but differs only in the degree of saturation in the N-substituent. However, this subtle structural difference results in around a 10-fold increase in affinity, but approximately 2-fold decrease in negative cooperativity; suggesting that affinity and negative cooperativity are driven by different structural features of these allosteric fragments, i.e. simply increasing fragment affinity does not automatically result in increased negative cooperativity. The inactivity of the ethanolamide analogue **11f** indicates that polarity in the carboxamide *N*-substituent is not tolerated, suggesting that this region of the molecule may largely interact with hydrophobic residues. The two branched amide analogues **11g** (K_B = 39 μM) and **11h** (K_B = 50 μM, $α$ = 0.26) both displayed similar affinity to **3**, however *N*-(pentan-3-yl) analogue **11g** lacked determinable negative cooperativity. These data, when combined with the activity profile of *N*-ethyl analogue **11b,** suggest that an optimal degree of branching may be present on the *N*-isopropyl substituent of **3** both in terms of degree of substitution of the carbon atom adjacent to the carboxamide nitrogen in addition to branch length. Further branching to the *N*-*tert*-butyl present on **11h** does not appear to impact affinity or cooperativity. Extending the branch length of the *N*-isopropyl group of **3** to the *N*-(pentan-3-yl) group of **11g** did not affect affinity and the effect on negative cooperativity was indeterminable. In comparison, reducing branching (i.e. **3** vs **11b**) causes both affinity and negative cooperativity to reduce.

Di-substituted carboxamide derivatives largely comprised of aliphatic heterocycle bearing analogues (**11k-n**). Of these, only pyrrolidyl analogue **11l** (K_B = 831 μM) displayed some, albeit weak affinity,

with no detectable negative cooperativity. Although the di-substituted amide derivatives generally lacked affinity, the *N*-diisopropyl analogue **11j** (K_B = 19 μM, α = 0.04) possessed both higher affinity and almost 10-fold higher negative cooperativity than **3**. This activity is difficult to rationalize amidst the data for other compounds in the library. However, given the fragment-size nature of these compounds, the possibility of alternative binding poses should not be discounted.

The remaining analogues in this series comprised cyclic moieties with the linking nitrogen atom external to the ring. In the *N*-carbocycle series, ring size influenced both affinity and negative cooperativity when comparing *N*-cyclopropyl **11o** (K_B = 154 μM), *N*-cyclobutyl **11p** (K_B = 17 μM, α = -0.02), *N*-cyclopentyl **11q** (K_B = 19 μM, α = 0.23) and *N*-cyclohexyl **11r** (no determinable activity) analogues. The optimal size in terms of affinity and highest level of negative cooperativity is exhibited by the *N*-cyclobutyl bearing **11p**. Incrementing ring size by a single methylene unit to give **11q** does not affect affinity, but causes approximately 10-fold reduction in negative cooperativity. This data supports the SAR discussed above, of the acyclic substituents, with **11o-p** being most similar in size and shape to **3**, whereas **11q-r** are more comparable to **11g**. The inactivity of **11r** may initially seem counterintuitive, given a common cyclohexyl moiety present on the relatively high affinity parent compound **1**. This apparent discrepancy can be reconciled if the bitopic nature of **1** is taken into account, i.e. the high affinity of **1** is derived from concomitant salt-bridge interaction with the orthosteric binding site of the D$_2$R. Without the strong 'orthosteric anchor' interaction, the allosteric fragments are more sensitive to subtle structural changes.

Though substituent size is important for both the affinity and negative cooperativity exhibited by these compounds, the nature of the carboxamide NH may also be key. Both the acidity of the NH bond (i.e. its ability to donate a hydrogen bond) and steric crowding around the NH bond is also important. The *N*-(1-piperidyl) analogue **11s** (K_B = 91 μM, α = 0.30) differs from **11r** only by replacement of the ring methine by a nitrogen atom but bears an allosteric activity profile similar to **3**. Also, the *N*-phenyl

analogue **11t** (K_B = 19 µM) regains affinity compared to **11r**, where the saturated cyclohexyl group is replaced with a planar phenyl ring. In both **11s** and **11t**, the carboxamide NH would be expected to be a better hydrogen bond donor (due to substituent electron-withdrawing effect) than that of **11r**. Finally, compounds **11u-w** also support the importance of access to the carboxamide NH combined with sensitivity to substituent size. Insertion of a methylene spacer on **11o** to give cyclopropylmethyl analogue **11u** (K_B = 30 µM, α = 0.10) improves affinity around 10-fold, as well as imparting determinable negative cooperativity. In comparison, no activity for **11v-w** was observed up to a concentration of 300 µM, possibly due to these compounds bearing larger substituents causing a sterically unfavourable interaction with the receptor.

Compounds **13a-e** and **15** (**Table 3**) were based on the structure of **3**, however introduced either fluoro- or methoxy- substituents on to the indole core. Whilst all analogues in this series retained activity at the D_2R, the 5-fluoro analogue **13c** (K_B = 91 µM) and 5-methoxy analogue **15** (K_B = 104 µM) exhibited reduced affinity. In comparison the 4-fluoro analogue **13b** (K_B = 18 µM, α = 0.07) and 7-fluoro analogue **13e** (K_B = 18 µM, α = 0.11) both displayed slightly improved affinity and displayed higher negative cooperativity with dopamine compared to **3**. The SAR of this series is difficult to extrapolate without examining a wider range of compounds, though substitution at the 5- and 6-positions of the ring appears to be less well tolerated. The effect of substitution at other ring positions is likely to be determined by both regional and electronic influence of each substituent.

Table 4. Characterization of analogues of compound 3, varying the nature of the bicyclic heteroaromatic ring, and substitution position of the carboxamide, in terms of binding and function at the D_2R^a

1
2
3
4
5
6
7
8
9
10

No.	Heterocycle	pK_B (K_B, µM)	Logα (α)
3[b]	(indole)	4.35 ± 0.07 (45)	-0.53 ± 0.09 (0.29)
17	(N-methyl indole)	ND	ND
19[c]	(benzimidazole)	5.69 ± 0.38 (2)	-1.07 ± 0.22 (0.08)
21	(benzoxazole)	ND	ND
23a	(benzofuran)	ND	ND
23b	(benzofuran)	ND	ND
25a[d]	(benzothiophene)	4.31 ± 0.20 (49)	NA
25b	(benzothiophene)	ND	ND
27	(7-azaindole)	ND	ND
30a	(indole)	ND	ND
30b[b]	(indole)	3.91 ± 0.5 (123)	-1.27 ± 0.3 (0.05)
30c[c]	(indole)	5.16 ± 0.5 (7)	-1.1 ± 0.3 (0.08)
30d	(indole)	ND	ND

[a]Interaction studies between compounds and dopamine were performed using an ERK1/2 phosphorylation assay upon FlpIn CHO cells stably expressing the $D_{2L}R$ as in **Figure 1c**. [b]For compounds that caused a decrease in the maximal response of dopamine, data were analysed according to an operational model of allosterism where K_B is the equilibrium dissociation constant of the allosteric ligand, α is the binding cooperativity parameter between the orthosteric and allosteric ligand, and β (Logβ constrained to -100 to represent high negative cooperativity with dopamine efficacy) denotes the magnitude of the allosteric effect of the modulator on the efficacy of the orthosteric

agonist. [c] For compounds that caused a limited rightward shift of the dopamine dose-response curve but no decrease in E_{max}, data were fit using an operational model of allosterism where Logβ was constrained to 0, to represent neutral cooperativity with dopamine efficacy. [d] For compounds that produced an unlimited rightward shift of a dopamine dose-response curve within the concentration range of test compound used data were fit using a model of competitive antagonism (equation 6). As such a value of cooperativity could not be derived (denoted NA). ND signifies no effect of compound was observed even at the highest concentration of 300 μM. Data represent the mean ± SEM of three experiments performed in duplicate apart from compounds with no effect, which were tested in two separate experiments.

In order to evaluate the importance of the indole core of **3**, we also synthesized a set of analogues bearing alternative bicyclic heterocyclic cores (**Table 4**). Compounds (**17, 21, 23a-b, 25b**) lacking the ability to donate a hydrogen bond (compared to the indolic NH of **3**) did not show activity up to a concentration of 300 μM. We were surprised to note that benzothiophene **25a** (K_B = 49 μM) retained affinity for the D_2R comparable with that of **3**. However, an unlimited rightward shift of the dopamine concentration-response curve within the concentration range of **25a** employed meant a measure of negative cooperativity could not be determined.

The benzimidazole based compound **19** (K_B = 2 μM, α = 0.08) had both higher affinity and negative cooperativity relative to **3**. This may be explained by the differing acidity of the indolic NH bond (pK_a = 21)[27] compared to that of benzimidazole (pK_a = 16.4)[28], with the more acidic benzimidazole acting as a better hydrogen bond donor.

The lack of activity exhibited by the 7-azaindole analogue **27** is somewhat surprising. However the ability to interact with the receptor may be complicated by a number of factors, including the complex interaction between the two nitrogen atoms, intermolecular dimer formation, and the ability to form efficient hydrogen bonds with water.

Finally, the positional isomers **30a-d** support the importance of an NH bond and relative position to the carboxamide moiety. Whereas 4- and 7-substituted analogues **30a** and **30d** were devoid of detectable activity, the corresponding 5- and 6-substitited analogues **30b** (K_B = 123 μM, α = 0.05) and

30c (K_B = 7 µM, α = 0.08) exhibited both affinity and negative cooperativity. Though both **30b-c** showed a higher degree of negative cooperativity relative to **3**, they were divergent in their relative affinities, with **30b** having weaker affinity and **30c** having higher affinity than **3.**

A possible explanation for the ability of **30b-c** to maintain activity as negative allosteric modulators relative to **3**, (in comparison to **30a** and **30d**, which are devoid of detectable activity) is that these regioisomers could maintain key interactions with the receptor. In particular **30c** may be able to maintain the carboxamide-associated and indole NH-associated interactions that appear to be key to activity, based on our above SAR analysis. It is conceivable that **30b** might not be able to participate in these interactions as efficiently resulting in a weaker affinity. It is clear that the position of the carboxamide and indolic NH within this set of regioisomers are key determinants of activity, though the precise nature of these interactions is yet to be determined.

The activity of Compound 11d is modulated by mutation of residues within the secondary pocket of the D₂R. We then selected **11d** as the promising compound from this SAR study based upon both a 7-fold increase in affinity and a 10-fold increase in negative cooperativity for further characterization. In particular we tested the activity of **11d** at the two secondary pocket mutant D₂R receptors Glu95$^{2.65}$Ala and Val91$^{2.61}$Ala (**Figure 6, Table 5**).
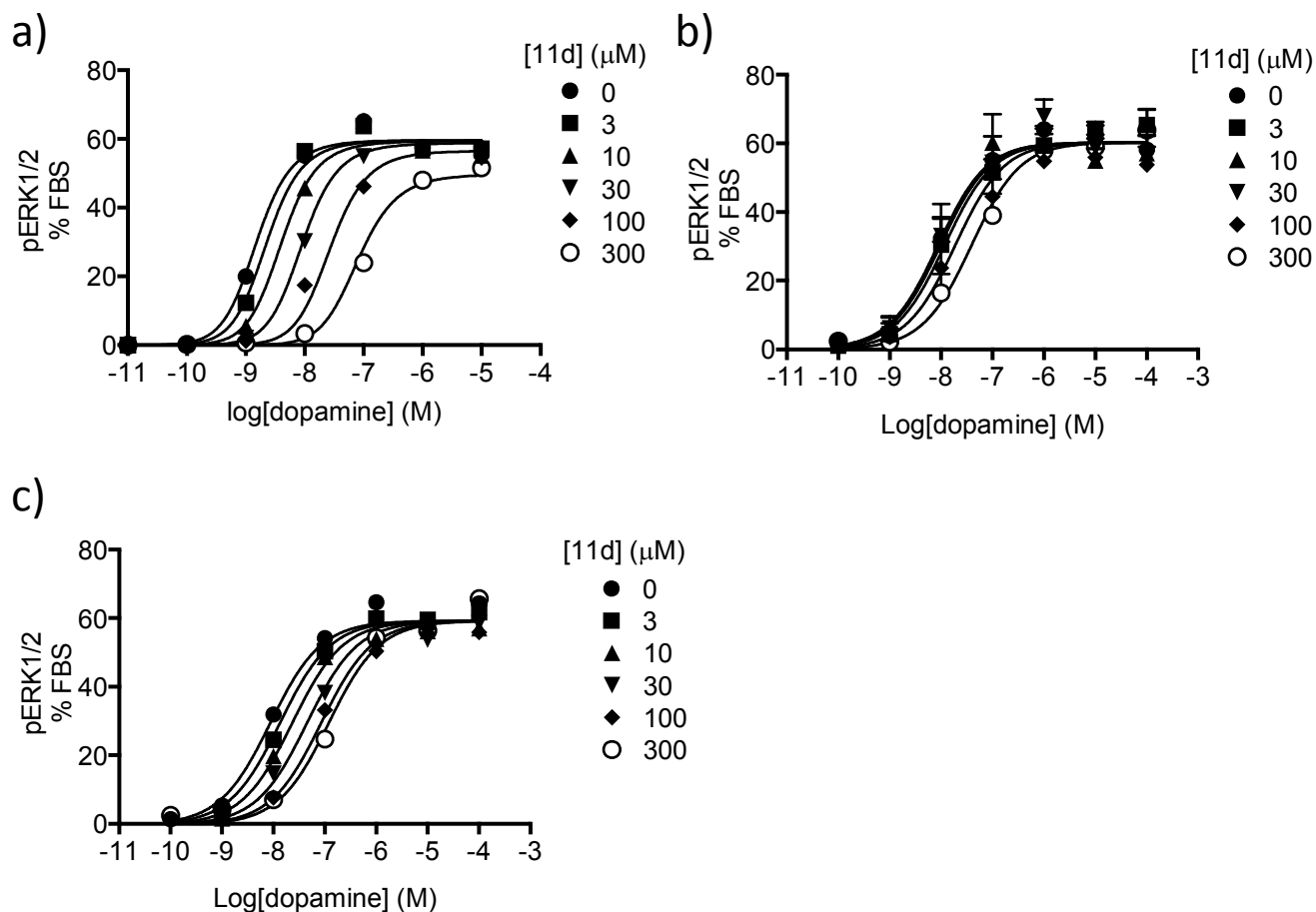
Figure 6. Mutation of residues at the top of TM2 modulates the allosteric action of **11d**. Interaction studies between dopamine and **11d** in an assay measuring D_2R mediated pERK1/2 phosphorylation using CHO cells expressing the **(a)** WT, **(b)** Val91$^{2.61}$Ala or **(c)** Glu95$^{2.65}$Ala.

This compound displayed a reduced activity at the Val91$^{2.61}$Ala mutant, with a 14-fold decrease in affinity (**Figure 6b, Table 5**). Most likely because of this reduced affinity, while **11d** did cause a decrease in dopamine potency at the highest concentrations used, this rightward shift did not reach a limit. Furthermore, in contrast to the action of the compound in this assay at the WT receptor, the E_{max} of dopamine was not reduced. Therefore, a value of negative cooperativity with dopamine binding affinity could not be determined for **11d**. A reduced affinity at this mutant was also observed for **3** suggesting that these compounds bind in the same secondary pocket within the D_2R. Of interest, at the Glu95$^{2.65}$Ala mutant, **11d** displayed similar affinity and negative cooperativity with dopamine binding,

as compared to its action at the WT D_2R. However, no decrease in dopamine E_{max} was observed, consistent with no modulation of dopamine efficacy. It is interesting to note that this mutation had quite a different effect upon the pharmacology of **3** (100-fold increase in affinity and complete loss of negative cooperativity with dopamine affinity). This suggests that the *N*-substituent attached to the carboxamide nitrogen (*N*-isopropyl in **3** compared to *N*-butyl in **11d**) plays an important role in determining the effect of the mutation of Glu95$^{2.65}$ to alanine.

Table 5. Characterization of the binding and function of *N*-butyl-1*H*-indole-2-carboxamide (11d) at the D_2R^a

	pK_B (K_B, nM)	Logα (α)	Logβ
Wild Type	5.21 ± 0.07 (6)	-1.63 ± 0.11 (0.02)	-100
Val91$^{2.61}$Ala	4.07 ± 0.18 (85)	-	-
Glu95$^{2.65}$Ala	5.30 ± 0.24 (5)	-1.24 ± 0.17 (0.05)	0

^{a} The ability of **11d** to modulate the functional effect of agonists or their effect at either the WT D_2R or mutant D_2Rs expressed in Flp-IN CHO cells was tested in a pERK1/2 assay and data was fit to an operational model of allosterism (**Equation 5**) to derive values of affinity (pK_B) and cooperativity with dopamine.

Given that **11d** displayed 10-fold increased affinity compared to **3**, we hypothesised that if we combined the structural features of **11d** (as an allosteric moiety), with the orthosteric 7-CTHIQ head-group, the resultant compound might exhibit a bitopic mode of interaction with the D_2R in a similar manner to **1**. Additionally, we anticipated the increased affinity displayed by the allosteric fragment **11d** might be translated into this putative bitopic ligand and confer a gain of affinity and/or negative cooperativity with dopamine, compared to that exhibited by **1**. Accordingly we synthesised **36**. This

bitopic ligand displayed a 10-fold increase in affinity and similar magnitude of negative cooperativity

with dopamine as compared to **1** (**Figure 7**).
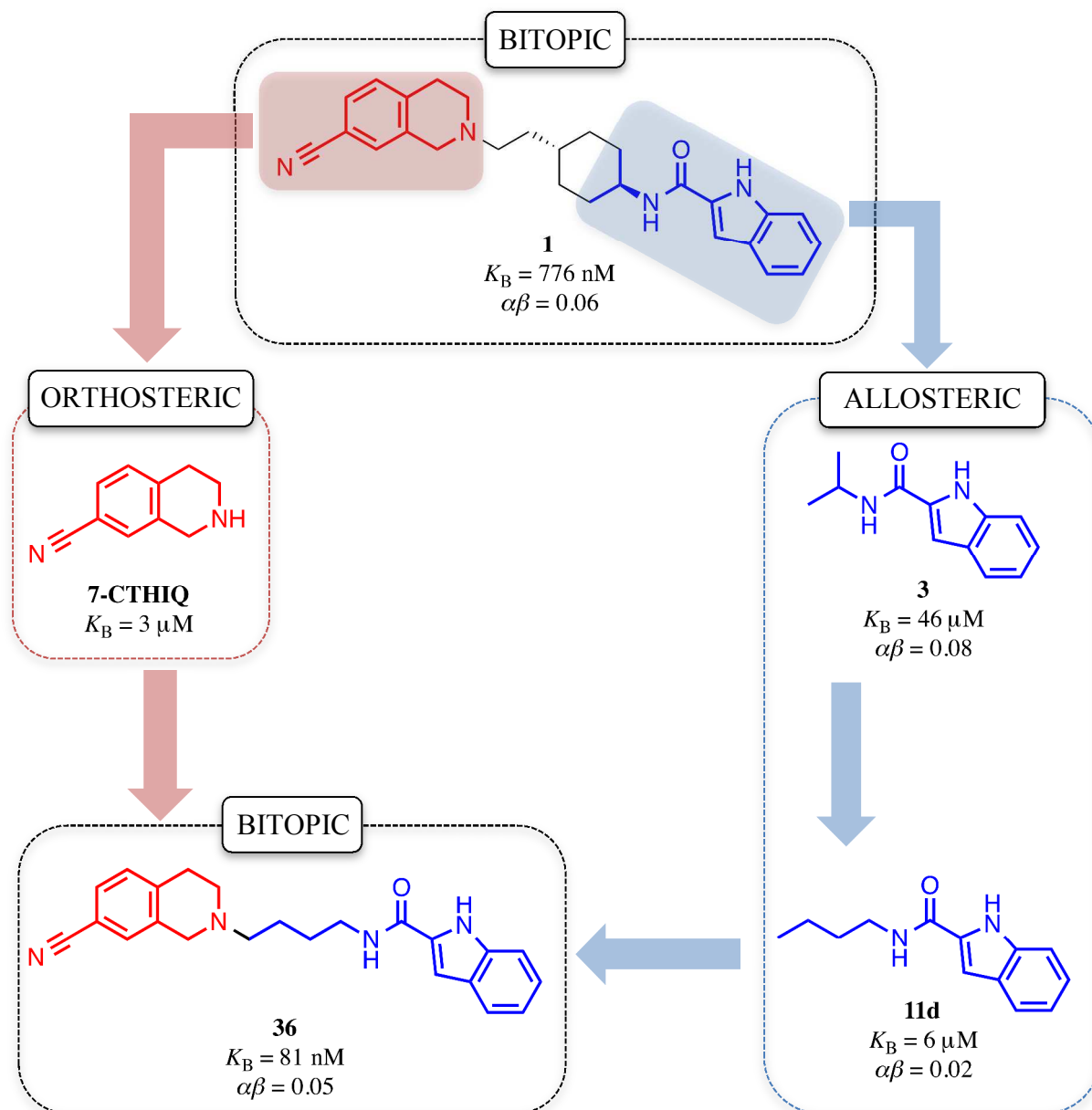
Figure 7. Incorporation of an optimized allosteric moiety (**11d**) into the bitopic pharmacophore of **1**, to generate a novel bitopic ligand **36**, conferring a 10-fold increase in affinity and no change in negative cooperativity with dopamine ($pK_B = 7.09 \pm 0.14$, $Log\alpha\beta = -1.32 \pm 0.09$) as compared to **1**. Compound **1** binds the D_2R in a bitopic mode and acts as an allosteric modulator across a D_2R dimer. Compound **1** can be separated into an orthosteric moiety (7-CTHIQ) and an allosteric moiety (**3**). Optimisation of **3** yielded **11d**, an allosteric modulator with 10-fold higher affinity. Incorporation of **11d** into the bitopic pharmacophore of **1**, generated **36** that displayed 10-fold higher affinity as compared to **1**.

This is in line with our hypothesis and is consistent with both the allosteric moieties of **1** and **36** occupying the same secondary pocket that includes residues extracellular at the extracellular end of TM2. This demonstrates that this pocket can be targeted for the development of both novel allosteric and bitopic ligands. It should be noted though that while 1 displays modest selectivity for the D$_3$R, the allosteric fragment, 3, displayed similar affinity and allosteric action at both the D$_3$R and D$_2$R. This is perhaps not surprising given the high homology between these two receptors and in particular that the two residues (Val91 and Glu95) shown to modulate the binding and/or effect of 3 and 11d are conserved between these two subtypes. This suggests that the putative allosteric pocket may be very similar at the D$_2$R and D$_3$R.

CONCLUSIONS

To date, studies of bitopic ligands have been largely restricted to the muscarinic and adenosine receptor families.[3,4] This is largely due to the rich allosteric pharmacology that exists for these two receptor families. Until recently, examples of small molecule allosteric modulators were lacking for the D$_2$R. We previously demonstrated that **1** bound the D$_2$R in a bitopic mode and acted as a negative allosteric modulator of dopamine binding and function across a D$_2$R dimer.[13] Studies at the mAChRs have used ligand fragmentation approaches to isolate orthosteric and allosteric pharmacophores from a bitopic ligand.[10,11] In this study we were able to isolate **3** an allosteric fragment of **1**, derived from the indole-2-carboxamide moiety of the parent compound. Furthermore, we demonstrate that the action of **3** is modulated by mutation of the same residues at the top of TM2 shown to interact with the indole-carboxamide moiety of **1**. Compound **3** bound the receptor with a relatively low affinity (48 µM) and displayed 4-fold lower negative cooperativity with dopamine affinity as to that observed for **1** (α =

0.29). This provides further evidence of a bitopic mode of interaction for **1** at the D_2R. One would expect a bitopic ligand to display competitive behaviour with an orthosteric agonist because the orthosteric head-group (in this case the 7-CTHIQ moiety) would compete to bind at the orthosteric site. To accommodate the bitopic binding mode of **1** with its purely allosteric pharmacology, we had to extend our mechanism of action to modulation across a D_2R dimer. In the case of **3**, this ligand possesses no established orthosteric pharmacophore and our mutagenesis studies suggest that it binds to residues within a secondary pocket at the top of TM2. Therefore, its allosteric action can be accommodated within a simple ternary complex of a single D_2R protomer, the orthosteric agonist dopamine and the allosteric ligand **3**. Such a mechanism of action has been validated for allosteric modulators of the muscarinic M_2 receptor through the crystallization of such a ternary complex.[29] However, without similar structural evidence we cannot discount that **3** or its derivatives act across a D_2R dimer as we have shown for **1**. Finally, our preliminary SAR studies of the indole-2-carboxamide scaffold yielded **11d** an allosteric modulator that displayed a 10-fold improvement of affinity as compared to **3**. Furthermore, by combining this optimised allosteric moiety with the 7-CTHIQ orthosteric head-group of **1**, we developed a novel bitopic ligand (compound **36**) that displayed 10-fold improvement in affinity as compared to **1**. If the orientation of the indole-2-carboxamide scaffold of **11d** is equivalent to that of **1**, then the *N*-butyl substituent of **11d** is equivalent to the linker region of **1**. Therefore, the higher affinity of **36** may result from the greater flexibility of the alkyl chain linker allowing optimal binding of the orthosteric and allosteric moieties at their respective sites. For a bitopic ligand to simultaneously occupy both orthosteric and allosteric sites then these sites must proximal to each other and connected. It follows then that the allosteric and linker moieties will be necessarily integrated. Thus it is not surprising that allosteric fragments derived from bitopic ligands can be optimised through substitution in the direction that corresponds to the linker region. However, it is interesting to note that the nature of the substituent, where alkyl chains were tolerated but larger cyclic

or aromatic substitutions were not, was important for maintaining the allosteric action of the fragment. Thus this SAR may dictate what can be tolerated or is preferable within the linker region of the bitopic molecule.

Combined, this study reveals the indole-2-carboxamide scaffold as a novel pharmacophore for negative allosteric modulators of the dopamine D_2R. Furthermore, this study highlights an allosteric pocket within the D_2R between TM2 and TM7, which can be exploited for the design of novel allosteric modulators and bitopic ligands for this therapeutically attractive receptor.

EXPERIMENTAL SECTION

Chemistry. Chemicals and solvents were purchased from standard suppliers and used without further purification. Davisil® silica gel (40-63µm), for flash column chromatography (FCC) was supplied by Grace Davison Discovery Sciences (Victoria, Australia) and deuterated solvents were purchased from Cambridge Isotope Laboratories, Inc. (USA, distributed by Novachem Pty Ltd, Victoria, Australia).

Unless otherwise stated, reactions were carried out at ambient temperature. All microwave reactions took place in a Biotage Initiator Microwave Synthesiser. Reactions were monitored by thin layer chromatography on commercially available precoated aluminium-backed plates (Merck Kieselgel 60 F_{254}). Visualisation was by examination under UV light (254 and 366 nm). General staining carried out with $KMnO_4$ or phosphomolybdic acid. A solution of Ninhydrin (in ethanol) was used to visualize primary and secondary amines. All organic extracts collected after aqueous work-up procedures were dried over anhydrous $MgSO_4$ or Na_2SO_4 before gravity filtering and evaporation to dryness. Organic solvents were evaporated *in vacuo* at ≤ 40°C (water bath temperature). Purification using preparative layer chromatography (PLC) was carried out on Analtech preparative TLC plates (200 mm × 200 mm × 2 mm).

^{1}H NMR and ^{13}C NMR spectra were recorded on a Bruker Avance Nanobay III 400MHz Ultrashield Plus spectrometer at 400.13 MHz and 100.62 MHz respectively. Chemical shifts (δ) are recorded in parts per million (ppm) with reference to the chemical shift of the deuterated solvent. Coupling constants (J) and carbon-fluorine coupling constants (J_{CF}) are recorded in Hz and the significant multiplicities described by singlet (s), doublet (d), triplet (t), quadruplet (q), broad (br), multiplet (m), doublet of doublets (dd), doublet of triplets (dt). Spectra were assigned using appropriate COSY, distortionless enhanced polarisation transfer (DEPT), HSQC and HMBC sequences.

Analytical reverse-phase HPLC was performed on a Waters HPLC system coupled directly to a photodiode array detector and fitted with a Phenomenex® Luna C8(2) 100 Å column (150 mm × 4.6

mm, 5 μm) using a binary solvent system; solvent A: 0.1% TFA/H$_2$O; solvent B: 0.1% TFA/80% CH$_3$CN/H$_2$O. Gradient elution was achieved using 100% solvent A to 100% solvent B over 20 min at a flow rate of 1 mL/min.

LCMS were run to verify reaction outcome and purity using either system A or B. **System A:** an Agilent 6100 Series Single Quad coupled to an Agilent 1200 Series HPLC. The following buffers were used; buffer A: 0.1% formic acid in H$_2$O; buffer B: 0.1% formic acid in MeCN. The following gradient was used with a Phenomenex Luna 3μM C8 (2) 15 × 4.6 mm column, and a flow rate of 0.5 mL/min and total run time of 12 min; 0–4 min 95% buffer A and 5% buffer B, 4–7 min 0% buffer A and 100% buffer B, 7–12 min 95% buffer A and 5% buffer B. Mass spectra were acquired in positive and negative ion mode with a scan range of 0–1000 *m/z* at 5V. UV detection was carried out at 254 nm. **System B:** an Agilent 6120 Series Single Quad coupled to an Agilent 1260 Series HPLC. The following buffers were used; buffer A: 0.1% formic acid in H$_2$O; buffer B: 0.1% formic acid in MeCN. The following gradient was used with a Poroshell 120 EC-C18 50 × 3.0 mm 2.7 micron column, and a flow rate of 0.5 mL/min and total run time of 5 min; 0–1 min 95% buffer A and 5% buffer B, from 1-2.5 min up to 0% buffer A and 100% buffer B, held at this composition until 3.8 min, 3.8–4 min 95% buffer A and 5% buffer B, held until 5 min at this composition. Mass spectra were acquired in positive and negative ion mode with a scan range of 100–1000 *m/z*. UV detection was carried out at 214 and 254 nm. All retention times (t_R) are quoted in min. High resolution mass spectra (HRMS) were obtained on a Waters LCT Premier XE (TOF) using electrospray ionization (ESI) at a cone voltage of 50 V. All tested compounds were of > 95% purity.

General Procedure A: Substituted 1*H*-indole-2-carboxamide synthesis through direct aminolysis of methyl 1*H*-indole-2-carboxylate. Methyl 1*H*-indole-2-carboxylate (**10**) (100 mg, 0.57 mmol) was dispersed in EtOH (1 mL) at rt. To this was added either neat amine or a solution of amine (1 mL) and stirring continued until TLC analysis (EtOAc/PE 3:7) indicated ester had been consumed.

The mixture was diluted with water and the resulting precipitate collected by filtration (vacuum) and washed with water. Where necessary, further purification was achieved by FCC (see individual monographs).

General procedure B: HCTU-mediated coupling of carboxylic acids with amines in DMF (using excess amine as base). Carboxylic acid and HCTU (1.1 eq) were dissolved in DMF (1 mL) with stirring at rt. To this was added amine (2.5-3 eq), and mixture stirred at rt overnight. TLC analysis (EtOAc/PE 1:1 or EtOAc) was used to confirm reaction completion after this period. The mixture was diluted with water (10 mL) and allowed to stir at rt for 10 min, before collecting the resultant precipitate by filtration (vacuum), then washing with water. Further purification was achieved by aqueous workup and FCC as detailed under each monologue.

General procedure C: Ester hydrolysis of methyl indole carboxylates with LiOH.H$_2$O. Ester (100 mg, 0.57 mmol) and LiOH.H$_2$O (72 mg, 1.71 mmol, 3 eq) was stirred in THF/water (1:1, 2 mL) at rt for 90 h. LCMS analysis after this time indicated complete hydrolysis had taken place. The mixture was diluted with water (20 mL) and washed with Et$_2$O (20 mL). After discarding the Et$_2$O washings, the aqueous layer was acidified with 2 M HCl$_{(aq)}$ to pH~2. The aqueous layer was then extracted with EtOAc (3 × 20 mL), and the combined organic extracts washed with brine (20 mL). On concentration, the desired carboxylic acid was obtained, requiring no further purification.

N-Isopropyl-1*H*-indole-2-carboxamide (**3**).[30] Indole-2-carboxylic acid (**1**) (1.00 g, 6.21 mmol) and HCTU (2.82 g, 6.82 mmol, 1.1 eq) were dissolved in DMF (10 mL) at rt with stirring. To this was added isopropylamine (1.59 mL, 18.6 mmol, 3 eq), and the mixture stirred at rt overnight. TLC analysis (EtOAc/PE 1:1) indicated complete conversion, so the reaction was quenched with water (100 mL), and the resulting precipitate collected by filtration (vacuum). After drying, the precipitate was further purified by FCC (eluent EtOAc/PE 0:100 to 30:70), to give 940 mg of white solid (75%). ^{1}H NMR (*d$_6$*-DMSO) δ 11.50 (s, 1H), 8.20 (d, *J* = 7.8 Hz, 1H), 7.59 (d, *J* = 7.9 Hz, 1H), 7.41 (dd, *J* = 8.2/0.8 Hz,

1H), 7.23–7.08 (m, 2H), 7.02 (ddd, J = 8.0/7.0/1.0 Hz, 1H), 4.28–3.94 (m, 1H), 1.19 (d, J = 6.6 Hz,

6H); ^{13}C NMR (d_6-DMSO) δ 160.2, 136.3, 132.0, 127.1, 123.1, 121.4, 119.6, 112.2, 102.4, 40.6, 22.4;

m/z MS (TOF ES$^+$) $C_{12}H_{15}N_2O$ [MH]$^+$ calcd 203.1; found 203.1; LCMS t_R: 3.20 min (system B).

Ethyl 2-((*trans*)-4-((*tert*-butoxycarbonyl)amino)cyclohexyl)acetate (5). 2-((*trans*)-4-((*tert*-butoxycarbonyl)amino)cyclohexyl)acetic acid (**4**) (1.00 g, 3.89 mmol) and K_2CO_3 (644 mg, 4.66 mmol, 1.2 eq) were dispersed in MeCN (30 mL). To this was added EtI (0.344 mL, 4.28 mmol, 1.1 eq), and the mixture stirred at rt for 1.75 h. LCMS analysis indicated no progress, and the mixture had formed a gel, so MeCN (20 mL) was added, and the mixture heated under reflux for 3 h. EtI (0.156 mL, 1.95 mmol, 0.5 eq) was added and the mixture heated at 50 °C overnight. LCMS analysis indicated almost complete conversion, so EtI (0.156 mL, 1.95 mmol, 0.5 eq) was added and the mixture heated under reflux for 2 h. The mixture was cooled, and concentrated under reduced pressure to remove MeCN and EtI. The residue was taken up into EtOAc (30 mL) and washed with water (30 mL), sat. NaHCO$_3$ $_{(aq)}$ (30 mL) and brine (30 mL). After concentration, 1.11 g of white solid was obtained (quantitative yield). ^{1}H NMR (CDCl$_3$) δ 4.60–4.19 (m, 1H), 4.19–3.98 (m, 2H), 3.37 (s, 1H), 2.18 (d, J = 6.8 Hz, 2H), 1.98 (dd, J = 14.1/9.4 Hz, 2H), 1.87–1.55 (m, 3H), 1.43 (s, 9H), 1.33–1.21 (m, 3H), 1.19–0.98 (m, 4H); ^{13}C NMR (CDCl$_3$) δ 173.0, 155.4, 79.2, 60.4, 49.7, 41.6, 34.2, 33.3, 31.7, 28.6, 14.4; m/z MS (TOF ES$^+$) $C_{15}H_{27}NNaO_4$ [MNa]$^+$ calcd 308.2; found 308.2; LCMS t_R: 3.40 min (system B).

***tert*-Butyl ((*trans*)-4-(2-oxoethyl)cyclohexyl)carbamate (6).** Ethyl 2-((*trans*)-4-((*tert*-butoxycarbonyl)amino)cyclohexyl)acetate (**5**) (1.059 g, 3.71 mmol) was dissolved in dry toluene (15 mL) under an atmosphere of N$_2$. The reaction mixture was degassed with a stream of N$_2$, before cooling to -78 °C (dry ice/acetone). DIBAL-H in toluene (1M, 7.5 mL, ~2 eq) was added, and the mixture maintained at -78 °C with stirring for 3.5 h (TLC analysis (EtOAc/PE 3:7) after 1.5 h indicated complete consumption of starting material). The mixture was quenched with care using MeOH (7.5 mL), whilst maintaining the temperature at -78 °C. After complete addition of MeOH, the mixture was

warmed to rt, then stirred for 15 min, before addition of saturated potassium sodium tartrate (Rochelle's salt) solution (35 mL), and continuing stirring at rt for a further 30 min. The reaction mixture was then extracted with Et_2O (4 × 30 mL), and the combined organic extracts concentrated under reduced pressure, to give 913 mg of white solid (quantitative yield). ^{1}H NMR ($CDCl_3$) δ 9.75 (t, J = 2.0 Hz, 1H), 4.36 (s, 1H), 3.37 (s, 1H), 2.32 (dd, J = 6.6/2.0 Hz, 2H), 2.10–1.92 (m, 2H), 1.91–1.70 (m, 3H), 1.43 (s, 9H), 1.22–0.99 (m, 4H); ^{13}C NMR ($CDCl_3$) δ 202.3, 155.4, 79.2, 50.8, 49.6, 33.3, 31.9, 31.8, 28.6; m/z MS (TOF ES$^+$) $C_9H_{16}NO_3$ [M+2H-^{t}Bu]$^+$ calcd 186.1; found 186.2; LCMS t_R: 6.70 min (system A).

tert-Butyl ((_trans_)-4-(2-(dimethylamino)ethyl)cyclohexyl)carbamate hydrochloride (7a). _tert_-Butyl ((_trans_)-4-(2-oxoethyl)cyclohexyl)carbamate (**6**) (165 mg, 0.68 mmol) was dissolved in 1,2-dichloroethane (3 mL) with stirring at rt, before adding _N,N_-dimethylamine hydrochloride (56 mg, 0.68 mmol, 1 eq) and Na(OAc)$_3$BH (219 mg, 1.03 mmol, 1.5 eq). The mixture was stirred under an inert atmosphere for 16 h at rt, after which LCMS analysis indicated the reaction was complete. The mixture was then diluted with DCM (15 mL), before washing with 1 M K_2CO_3 $_{(aq)}$ (3 × 20 mL) and brine (15 mL). The DCM layer was then dried over anhydrous Na_2SO_4 before concentration under reduced pressure. The crude residue was purified by FCC (eluent MeOH/CHCl$_3$ 2:8) to give the desired compound in the free-amine form as a clear oil (105 mg, 50%). ^{1}H NMR (400 MHz, CDCl$_3$) δ 4.39 (br s, 1H), 3.70–3.62 (m, 3H), 3.37 (br s, 1H), 2.04–1.96 (m, 2H), 1.82–1.72 (m, 2H), 1.65–1.28 (m, 17H), 1.14–0.97 (m, 4H). ^{13}C NMR (CDCl$_3$) δ 155.4, 79.1, 57.6, 50.5, 45.2, 35.2, 34.2, 33.4, 32.0, 28.5. m/z MS (TOF ES$^+$) $C_{15}H_{31}N_2O_2$ [MH]$^+$ calcd 271.2; found 271.2; LCMS: no visible UV absorbance at 254 nm.

The free-amine product was then converted to the hydrochloride salt by taking up in CHCl$_3$ (10 mL), before adding 1 M HCl/Et$_2$O, and then solvents removed to give a colourless solid.

tert-Butyl ((trans)-4-(2-(dipropylamino)ethyl)cyclohexyl)carbamate (7b). *tert*-Butyl ((*trans*)-4-(2-oxoethyl)cyclohexyl)carbamate (**6**) (170 mg, 0.70 mmol) was dissolved in 1,2-dichloroethane (3 mL) with stirring at rt, before adding *N,N*-dipropylamine (71 mg, 0.70 mmol, 1 eq) and NaBH(OAc)$_3$ (223 mg, 1.05 mmol, 1.5 eq). The mixture was stirred under an inert atmosphere for 16 h at rt, after which LCMS analysis indicated the reaction was complete. The mixture was then diluted with DCM (15 mL), before washing with 1M K$_2$CO$_3$ $_{(aq)}$ (3 × 20 mL) and brine (15 mL). The DCM layer was then dried over anhydrous Na$_2$SO$_4$ before concentration under reduced pressure. The crude residue was purified by FCC (eluent MeOH/CHCl$_3$ 2:8) to give the desired compound as a clear oil (128 mg, 56%). ^{1}H NMR (CDCl$_3$) δ 4.39 (br s, 1H), 3.36 (br s, 1H), 2.46–2.39 (m, 2H), 2.39–2.30 (m, 4H), 2.02–1.92 (m, 2H), 1.78–1.71 (m, 2H), 1.50–1.39 (m, 13H), 1.36–1.30 (m, 2H), 1.22–1.18 (m, 1H), 1.11–0.97 (m, 4H), 0.87 (dd, *J* = 9.3/5.4 Hz, 2 × 3H); ^{13}C NMR (CDCl$_3$) δ 155.4, 79.1, 56.3, 51.9, 50.0, 35.4, 33.8, 33.6, 32.1, 28.5, 20.2, 12.1;

(trans)-4-(2-(Dimethylammonio)ethyl)cyclohexan-1-aminium   di-(2,2,2-trifluoroacetate)   (8a). *tert*-Butyl ((*trans*)-4-(2-(dimethylamino)ethyl)cyclohexyl)carbamate hydrochloride (**7a**) (105 mg, 0.34 mmol) was taken up in DCM (3 mL) and TFA (1 mL), and the colourless solution allowed to stir at rt for 15 min. The solvents were then evaporated to dryness under reduced pressure, to give the title compound as a colourless oil (quantitative yield). ^{1}H NMR (MeOD) δ 3.10–3.02 (m, 2H), 3.01–2.90 (m, 1H), 2.77 (s, 6H), 2.04–1.90 (m, 2H), 1.85–1.72 (m, 2H), 1.59–1.49 (m, 2H), 1.39–1.22 (m, 3H), 1.12–0.96 (ddd, *J* = 25.3/13.3/3.2 Hz, 2H); ^{13}C NMR (MeOD) δ 162.7 (q, J_{CF} = 34.9 Hz), 116.0 (q, J_{CF} = 284 Hz), 57.1, 51.3, 43.4, 35.2, 31.9, 31.5, 31.4.

(trans)-4-(2-(Dipropylammonio)ethyl)cyclohexan-1-aminium   di-(2,2,2-trifluoroacetate)   (8b). *tert*-Butyl ((*trans*)-4-(2-(dipropylamino)ethyl)cyclohexyl)carbamate (**7b**) (128 mg, 0.39 mmol) was taken up in DCM (3 mL) and TFA (1 mL), and the colourless solution allowed to stir at rt for 15 min. The solvents were then evaporated to dryness under reduced pressure, to give the title compound as a

colourless oil (85 mg, 96%). ^{1}H NMR (MeOD) δ 3.22–3.13 (m, 2H), 3.13–3.01 (m, 5H), 2.12–2.01 (m, 2H), 1.95–1.85 (m, 2H), 1.80–1.68 (m, 4H), 1.68–1.59 (m, 2H), 1.49–1.32 (m, 3H), 1.22–1.08 (m, 2H), 1.01 (t, J = 7.4 Hz, 2 × 3H). ^{13}C NMR (MeOD) δ 161.5 (q, J_{CF} = 37.5 Hz), 117.4 (q, J_{CF} = 289 Hz), 55.6, 52.4, 51.3, 35.4, 31.5, 31.4, 31.0, 18.3, 11.1.

***N*-((*trans*)-4-(2-(Dimethylamino)ethyl)cyclohexyl)-1*H*-indole-2-carboxamide   hydrochloride (9a).** (*trans*)-4-(2-(Dimethylamino)ethyl)cyclohexan-1-amine (**8a**) (60 mg, 0.35 mmol) and indole-2-carboxylic acid (**2**) (114 mg, 0.71 mmol, 2 eq) were taken up in DCM (5 mL) before DIPEA (1.23 mL, 7.05 mmol, 10 eq), and BOP (234 mg, 0.53 mmol, 1.5 eq) were added. The clear yellow solution turned cloudy after 5 min of stirring at rt, and after 1 h, the reaction was complete by LCMS analysis. The reaction mixture was then diluted with DCM (20 mL), washed with 1 M K$_2$CO$_{3\ (aq)}$ (2 × 20 mL), brine (20 mL), dried over anhydrous Na$_2$SO$_4$, then evaporated to dryness. The resulting crude solid was recrystallised from MeOH/water to give the product as a pale yellow solid, which was then converted to the hydrochloride salt in 1 M HCl solution, then lyophilized to give the title compound as a pale yellow solid (44 mg, 36%). Mp: 271–273 °C; ^{1}H NMR (d_6-DMSO) δ 11.54 (s, 1H) 10.49 (s, 1H), 8.31 (d, J = 8.0 Hz, 1H), 7.59 (d, J = 7.9 Hz, 1H), 7.42 (dd, J = 8.2/0.7 Hz, 1H), 7.19–7.13 (m, 2H), 7.05–6.99 (t, J = 7.9 Hz, 1H), 3.77 (dtt, J = 15.4/7.8/3.8 Hz, 1H), 3.10–2.99 (m, 2H), 2.71 (s, 6H), 1.88 (d, J = 10.1 Hz, 2H), 1.77 (d, J = 11.8 Hz, 2H), 1.62–1.54 (m, 2H), 1.45–1.25 (m, 3H), 1.14–0.98 (m, 2H); ^{13}C NMR (d_6-DMSO) δ 160.2, 136.3, 132.0, 127.0, 123.1, 121.4, 119.6, 112.2, 102.7, 54.8, 48.0, 41.9, 34.2, 32.0, 31.2, 30.4; LCMS t_R: 4.66 min (system A); HPLC (λ = 254, 214 nm) t_R = 7.99 min; HRMS (*m/z*): [MH]$^+$ calcd. for C$_{19}$H$_{27}$N$_3$O, 314.2227; found 314.2228.

***N*-((*trans*)-4-(2-(Dipropylamino)ethyl)cyclohexyl)-1*H*-indole-2-carboxamide (9b).** (*trans*)-4-(2-(Dipropylamino)ethyl)cyclohexan-1-amine (**8b**) (85 mg, 0.38 mmol) was taken up in DCM (5 mL) before DIPEA (0.653 mL, 3.75 mmol, 10 eq), BOP (252 mg, 0.57 mmol, 1.5 eq) and indole-2-carboxylic acid (**2**) (61 mg, 0.38 mmol, 1eq) were added. The yellow solution was allowed to stir at rt

for 4 h, after which time a precipitate formed and was collected by filtration to afford the title compound as a white solid. The filtrate was then concentrated to effect further solid precipitation, which was collected by filtration and washed with methanol (5 mL), to give a second crop of the title compound as a white solid (45 mg, 49%). Mp: 226–228 °C; ^{1}H NMR (d_6-DMSO) δ 11.49 (s, 1H), 8.17 (d, J = 8.0 Hz, 1H), 7.59 (d, J = 7.9 Hz, 1H), 7.42 (d, J = 8.2 Hz, 1H), 7.19–7.11 (m, 2H), 7.02 (t, J = 7.5 Hz, 1H), 3.82–3.67 (m, 1H), 2.59–2.27 (m, 6H), 1.87 (d, J = 11.4 Hz, 2H), 1.77 (d, J = 12.1 Hz, 2H), 1.48–1.18 (m, 9H), 1.10–0.93 (m, 2H), 0.85 (t, J = 7.3 Hz, 6H); ^{13}C NMR (d_6-DMSO) δ 160.2, 136.3, 132.0, 127.1, 123.1, 121.4, 119.6, 112.2, 102.4, 55.3, 51.1, 48.2, 34.6, 33.4, 32.4, 31.7, 19.6, 11.7; LCMS t_R: 4.82 min (system A); HPLC (λ = 214 nm) t_R = 9.01 min; HRMS (m/z): [MH]$^+$ calcd. for $C_{23}H_{35}N_3O$, 370.2853; found 370.2871.

Methyl 1H-indole-2-carboxylate (10). Indole-2-carboxylic acid (**2**) (1.038 g, 6.44 mmol) was dissolved in MeOH (30 mL), and concentrated sulfuric acid (0.5 mL) added. The mixture was heated under reflux for 5.75 h, then stirred at rt overnight. TLC analysis (EtOAc/PE 1:1) indicated almost complete conversion, so reflux was continued for a further 7 h. The mixture was concentrated, and the residue dispersed in sat. NaHCO$_3$ $_{(aq)}$, causing a beige solid to precipitate. This was collected by filtration (vacuum) and washed with water before drying, to give 1.101 g (98%) of beige solid. ^{1}H NMR (CDCl$_3$) δ 8.92 (s, 1H), 7.70 (dd, J = 8.1/0.9 Hz, 1H), 7.43 (dd, J = 8.3/0.9 Hz, 1H), 7.33 (ddd, J = 8.3/7.0/1.1 Hz, 1H), 7.23 (dd, J = 2.1/0.9 Hz, 1H), 7.16 (ddd, J = 8.0/7.0/1.0 Hz, 1H), 3.96 (s, 3H); ^{13}C NMR (CDCl$_3$) δ 162.6, 137.0, 127.6, 127.3, 125.6, 122.8, 121.0, 112.0, 109.0, 52.2; m/z MS (TOF ES$^+$) $C_{10}H_{10}NO_2$ [MH]$^+$ calcd 176.1; found 176.1; LCMS t_R: 3.60 min (system B)

1H-Indole-2-carboxamide (11a). The title compound was synthesised according to general procedure A, using NH$_4$OH$_{(aq)}$. After stirring for 2 nights, further NH$_4$OH$_{(aq)}$ (2 mL) was added, and stirring continued for a further 4 nights. The compound was isolated as 61 mg of white solid (67%). ^{1}H NMR (d_6-DMSO) δ 11.51 (s, 1H), 7.93 (s, 1H), 7.59 (d, J = 8.0 Hz, 1H), 7.41 (dd, J = 8.2/0.8 Hz, 1H),

7.33 (s, 1H), 7.17 (ddd, J = 8.2/7.0/1.1 Hz, 1H), 7.11 (d, J = 1.3 Hz, 1H), 7.02 (ddd, J = 8.0/7.0/1.0 Hz, 1H); ^{13}C NMR (d_6-DMSO) δ 162.8, 136.5, 131.8, 127.1, 123.2, 121.5, 119.6, 112.3, 103.0; m/z MS (TOF ES$^+$) $C_9H_9N_2O$ [MH]$^+$ calcd 161.1; found 161.1; LCMS t_R: 2.93 min (system B).

N-Ethyl-1H-indole-2-carboxamide (11b).[31] The title compound was synthesised according to general procedure A, initially using 33% EtNH$_2$ in EtOH. After overnight stirring, TLC analysis indicated minimal progress, so 70% EtNH$_2$ (aq) (2 mL) was added, and stirring continued for a further 2 nights. After diluting with water, the crude precipitate was collected and further purified by FCC (eluent MeOH/DCM 0:100 to 5:95), to give 45 mg of white solid (42%); ^{1}H NMR (CDCl$_3$) δ 9.34 (s, 1H), 7.65 (d, J = 8.0 Hz, 1H), 7.44 (dd, J = 8.3/0.8 Hz, 1H), 7.29 (ddd, J = 8.2/7.0/1.1 Hz, 1H), 7.14 (ddd, J = 8.0/7.0/1.0 Hz, 1H), 6.82 (d, J = 1.1 Hz, 1H), 6.17 (s, 1H), 3.55 (td, J = 10.7/7.1 Hz, 2H), 1.29 (t, J = 7.3 Hz, 3H); ^{13}C NMR (CDCl$_3$) δ 160.9, 139.6, 137.3, 127.9, 124.6, 122.0, 120.8, 112.1, 101.7, 34.8, 15.2; m/z MS (TOF ES$^+$) $C_{11}H_{13}N_2O$ [MH]$^+$ calcd 189.1; found 189.1; LCMS t_R: 3.12 min (system B).

N-Propyl-1H-indole-2-carboxamide (11c).[32] The title compound was synthesised according to general procedure A, using n-propylamine. After stirring for 2 nights, further n-propylamine (2 mL) was added, and stirring continued for a further 4 nights. After diluting with water, the crude precipitate was collected and further purified by FCC (eluent EtOAc/PE 0:100 to 50:50), to give 87 mg of white solid (76%); ^{1}H NMR (d_6-DMSO) δ 11.52 (s, 1H), 8.44 (t, J = 5.7 Hz, 1H), 7.59 (d, J = 7.9 Hz, 1H), 7.41 (dd, J = 8.2/0.8 Hz, 1H), 7.16 (ddd, J = 8.2/7.0/1.1 Hz, 1H), 7.10 (dd, J = 2.1/0.7 Hz, 1H), 7.02 (ddd, J = 8.0/7.0/1.0 Hz, 1H), 3.29–3.17 (m, 2H), 1.63–1.46 (m, 2H), 0.91 (t, J = 7.4 Hz, 3H); ^{13}C NMR (d_6-DMSO) δ 161.0, 136.3, 131.9, 127.1, 123.1, 121.4, 119.6, 112.2, 102.2, 40.5, 22.5, 11.4; m/z MS (TOF ES$^+$) $C_{12}H_{15}N_2O$ [MH]$^+$ calcd 203.1; found 203.2; LCMS t_R: 3.23 min (system B).

N-Butyl-1H-indole-2-carboxamide (11d).[31] The title compound was synthesised according to general procedure A, using n-butylamine. After stirring for 2 nights, further n-butylamine (2 mL) was

added, and stirring continued for a further 4 nights. After diluting with water, the crude precipitate was collected and further purified by FCC (eluent EtOAc/PE 0:100 to 50:50), to give 62 mg of white solid (50%); ^{1}H NMR (d_6-DMSO) δ 11.51 (s, 1H), 8.41 (t, J = 5.6 Hz, 1H), 7.59 (d, J = 7.9 Hz, 1H), 7.41 (dd, J = 8.2/0.8 Hz, 1H), 7.16 (ddd, J = 8.2/7.0/1.1 Hz, 1H), 7.09 (d, J = 1.4 Hz, 1H), 7.02 (ddd, J = 8.0/7.1/0.9 Hz, 1H), 3.28 (dt, J = 6.9/6.9 Hz, 2H), 1.59–1.46 (m, 2H), 1.41–1.28 (m, 2H), 0.91 (t, J = 7.3 Hz, 3H); ^{13}C NMR (d_6-DMSO) δ 161.0, 136.3, 131.9, 127.1, 123.1, 121.4, 119.6, 112.2, 102.1, 38.4, 31.4, 19.6, 13.7; m/z MS (TOF ES$^+$) $C_{13}H_{17}N_2O$ [MH]$^+$ calcd 217.1; found 217.2; LCMS t_R: 3.34 min (system B).

N-Allyl-1*H*-indole-2-carboxamide (11e).[33] The title compound was synthesised according to general procedure A, using allylamine. After stirring for 2 nights, further allylamine (2 mL) was added. Stirring was continued for a further 7 nights, before adding in allylamine (2 mL) and stirring over the weekend. After diluting with water, the crude precipitate was collected and further purified by FCC (eluent EtOAc/PE 0:100 to 30:70), to give 41 mg of white solid (36%); ^{1}H NMR (d_6-DMSO) δ 11.56 (s, 1H), 8.66 (t, J = 5.7 Hz, 1H), 7.60 (d, J = 8.0 Hz, 1H), 7.42 (dd, J = 8.2/0.8 Hz, 1H), 7.27–7.10 (m, 2H), 7.03 (ddd, J = 8.0/7.0/0.9 Hz, 1H), 5.92 (ddt, J = 17.2/10.3/5.2 Hz, 1H), 5.20 (ddt, J = 17.2/1.7/1.7 Hz, 1H), 5.11 (ddt, J = 10.3/1.6/1.6 Hz, 1H), 4.02–3.85 (m, 2H); ^{13}C NMR (d_6-DMSO) δ 160.9, 136.4, 135.5, 131.6, 127.1, 123.2, 121.5, 119.7, 115.2, 112.3, 102.4, 41.0; m/z MS (TOF ES$^+$) $C_{12}H_{13}N_2O$ [MH]$^+$ calcd 201.1; found 201.1; LCMS t_R: 3.12 min (system B).

N-(2-Hydroxyethyl)-1*H*-indole-2-carboxamide (11f).[34] The title compound was synthesised according to general procedure A, using ethanolamine. After stirring for 2 nights, the mixture was diluted with water. The crude precipitate was collected and further purified by FCC (eluent MeOH/DCM 0:100 to 5:95), to give 42 mg of white solid (36%); ^{1}H NMR (d_6-DMSO) δ 11.54 (s, 1H), 8.44 (t, J = 5.6 Hz, 1H), 7.60 (d, J = 7.9 Hz, 1H), 7.41 (dd, J = 8.2/0.7 Hz, 1H), 7.16 (ddd, J = 8.2/7.0/1.1 Hz, 1H), 7.11 (d, J = 1.4 Hz, 1H), 7.07–6.96 (m, 1H), 4.76 (t, J = 5.5 Hz, 1H), 3.53 (q, J =

6.1 Hz, 2H), 3.41–3.34 (m, 2H); ^{13}C NMR (d_6-DMSO) δ 161.2, 136.4, 131.8, 127.1, 123.2, 121.4, 119.6, 112.3, 102.4, 59.9, 41.7; *m/z* MS (TOF ES$^+$) $C_{11}H_{13}N_2O_2$ [MH]$^+$ calcd 205.1; found 205.1; LCMS t_R: 2.91 min (system B).

N-(Pentan-3-yl)-1*H*-indole-2-carboxamide (11g). Indole-2-carboxylic acid (100 mg, 0.62 mmol) was coupled to 1-ethylpropylamine according to general procedure B. The crude precipitate was dissolved in EtOAc (30 mL) and washed with sat. NaHCO$_3$ $_{(aq)}$ (30 mL), before concentrating and further purifying the residue by FCC (eluent EtOAc/PE 0:100 to 50:50), to give 116 mg of white solid (76%). ^{1}H NMR (d_6-DMSO) δ 11.49 (s, 1H), 8.01 (d, *J* = 8.8 Hz, 1H), 7.68–7.52 (m, 1H), 7.42 (dd, *J* = 8.2/0.8 Hz, 1H), 7.26–7.09 (m, 2H), 7.02 (ddd, *J* = 8.0/7.0/1.0 Hz, 1H), 3.81 (dtt, *J* = 8.6/8.6/5.1 Hz, 1H), 1.64–1.40 (m, 4H), 0.88 (t, *J* = 7.4 Hz, 2 × 3H); ^{13}C NMR (d_6-DMSO) δ 160.9, 136.3, 132.0, 127.1, 123.1, 121.3, 119.6, 112.2, 102.3, 51.7, 27.0, 10.6; *m/z* MS (TOF ES$^+$) $C_{14}H_{19}N_2O$ [MH]$^+$ calcd 231.2; found 231.2; LCMS t_R: 3.36 min (system B).

N-(*tert*-Butyl)-1*H*-indole-2-carboxamide (11h).[32] Indole-2-carboxylic acid (100 mg, 0.62 mmol) was coupled to *tert*-butylamine according to general procedure B. The crude precipitate was dissolved in EtOAc (30 mL) and washed with sat. NaHCO$_3$ $_{(aq)}$ (30 mL), before concentrating and further purifying the residue by FCC (eluent EtOAc/PE 0:100 to 50:50), to give 89 mg of white solid (66%). ^{1}H NMR (d_6-DMSO) δ 11.45 (s, 1H), 7.71 (s, 1H), 7.58 (dd, *J* = 7.9/0.6 Hz, 1H), 7.41 (dd, *J* = 8.2/0.8 Hz, 1H), 7.23–7.09 (m, 2H), 7.01 (ddd, *J* = 8.0/7.0/1.0 Hz, 1H), 1.41 (s, 9H); ^{13}C NMR (d_6-DMSO) δ 160.8, 136.2, 132.6, 127.1, 123.1, 121.3, 119.6, 112.1, 102.7, 50.8, 28.7; *m/z* MS (TOF ES$^+$) $C_{13}H_{17}N_2O$ [MH]$^+$ calcd 217.1; found 217.2; LCMS t_R: 3.35 min (system B).

N,N-Dimethyl-1*H*-indole-2-carboxamide (11i). The title compound was synthesised according to general procedure A, using 40% Me$_2$NH$_{(aq)}$. After stirring for 2 nights, further Me$_2$NH$_{(aq)}$ (2 mL) was added, and stirring continued for a further 4 nights. After diluting with water, the crude precipitate was collected and further purified by FCC (eluent EtOAc/PE 20:80 to 100:0), to give 36 mg of white solid

(34%). ^{1}H NMR (d_6-DMSO) δ 11.51 (s, 1H), 7.61 (dd, J = 7.9/0.8 Hz, 1H), 7.42 (dd, J = 8.2/0.9 Hz, 1H), 7.18 (ddd, J = 8.2/7.0/1.2 Hz, 1H), 7.03 (ddd, J = 8.0/7.0/1.0 Hz, 1H), 6.87 (dd, J = 2.2/0.8 Hz, 1H), 3.65–2.83 (m, 6H); ^{13}C NMR (d_6-DMSO) δ 162.6, 135.7, 130.2, 127.0, 123.2, 121.4, 119.6, 112.1, 104.6, 38.89; m/z MS (TOF ES$^+$) $C_{11}H_{13}N_2O$ [MH]$^+$ calcd 189.1; found 189.1; LCMS t_R: 3.14 min (system B).

N,N-Diisopropyl-1H-indole-2-carboxamide (11j).[35] Indole-2-carboxylic acid (100 mg, 0.62 mmol) was coupled to diisopropylamine according to general procedure B. The crude precipitate was dissolved in EtOAc (30 mL) and washed with sat. NaHCO$_3$ $_{(aq)}$ (30 mL), before concentrating and further purifying the residue by FCC (eluent EtOAc/PE 0:100 to 50:50, then recolumn in MeOH/DCM 0:100 to 5:95), to give 52 mg of white solid (34%). ^{1}H NMR (d_6-DMSO) δ 11.50 (s, 1H), 7.58 (d, J = 7.9 Hz, 1H), 7.38 (dd, J = 8.2/0.8 Hz, 1H), 7.15 (ddd, J = 8.2/7.0/1.1 Hz, 1H), 7.02 (ddd, J = 7.9/7.1/0.9 Hz, 1H), 6.60 (d, J = 1.4 Hz, 1H), 4.12 (s, 2H), 1.34 (d, J = 6.0 Hz, 12H); ^{13}C NMR (d_6-DMSO) δ 162.6, 137.4, 135.6, 132.2, 122.6, 121.1, 119.6, 111.8, 101.3, 52.2, 20.7; m/z MS (TOF ES$^+$) $C_{15}H_{21}N_2O$ [MH]$^+$ calcd 245.2; found 245.1; LCMS t_R: 3.52 min (system B).

Azetidin-1-yl(1H-indol-2-yl)methanone (11k). Indole-2-carboxylic acid (100 mg, 0.62 mmol) was coupled to azetidine according to general procedure B. The crude precipitate was further purified by FCC (eluent EtOAc/PE 0:100 to 100:0) to give a white solid (contaminated with 6-chloro-1H-benzo[d][1,2,3]triazol-1-ol). This was dissolved in EtOAc (30 mL) and washed with sat. NaHCO$_3$ $_{(aq)}$ (30 mL) and brine (30 mL), before concentrating to give 47 mg of white solid (38%); ^{1}H NMR (d_6-DMSO) δ 11.57 (s, 1H), 7.62 (d, J = 8.0 Hz, 1H), 7.43 (dd, J = 8.2/0.7 Hz, 1H), 7.19 (ddd, J = 8.2/7.0/1.1 Hz, 1H), 7.04 (ddd, J = 7.9/7.2/0.9 Hz, 1H), 6.79 (d, J = 1.4 Hz, 1H), 4.51 (t, J = 7.1 Hz, 2H), 4.09 (t, J = 7.2 Hz, 2H), 2.43–2.23 (m, 2H); ^{13}C NMR (d_6-DMSO) δ 161.5, 135.9, 129.3, 127.4, 123.5, 121.6, 119.7, 112.3, 104.2, 52.5, 48.5, 15.9; m/z MS (TOF ES$^+$) $C_{12}H_{13}N_2O$ [MH]$^+$ calcd 201.1; found 201.1; LCMS t_R: 3.16 min (system B).

(1*H*-Indol-2-yl)(pyrrolidin-1-yl)methanone (11l).[36] Indole-2-carboxylic acid (100 mg, 0.62 mmol) was coupled to pyrrolidine according to general procedure B. The crude precipitate was further purified by FCC (eluent EtOAc/PE 0:100 to 100:0) to give a white solid (contaminated with 6-chloro-1*H*-benzo[*d*][1,2,3]triazol-1-ol). This was dissolved in EtOAc (30 mL) and washed with sat. NaHCO$_3$ (aq) (30 mL) and brine (30 mL), before concentrating to give 87 mg of white solid (65%). ^{1}H NMR (d_6-DMSO) δ 11.52 (s, 1H), 7.62 (dd, J = 7.9/0.6 Hz, 1H), 7.44 (dd, J = 8.2/0.8 Hz, 1H), 7.18 (ddd, J = 8.2/7.0/1.1 Hz, 1H), 7.03 (ddd, J = 8.0/7.0/1.0 Hz, 1H), 6.95 (d, J = 1.5 Hz, 1H), 3.82 (t, J = 6.6 Hz, 2H), 3.55 (t, J = 6.8 Hz, 2H), 2.10–1.92 (m, 2H), 1.93–1.79 (m, 2H); ^{13}C NMR (d_6-DMSO) δ 160.3, 135.8, 131.1, 127.4, 123.4, 121.6, 119.6, 112.2, 104.5, 48.0, 47.0, 26.2, 23.5; *m/z* MS (TOF ES$^+$) C$_{13}$H$_{15}$N$_2$O [MH]$^+$ calcd 215.1; found 215.1; LCMS t_R: 3.27 min (system B).

(1*H*-Indol-2-yl)(piperidin-1-yl)methanone (11m).[37] Indole-2-carboxylic acid (100 mg, 0.62 mmol) was coupled to piperidine according to general procedure B. The crude precipitate was further purified by FCC (eluent EtOAc/PE 0:100 to 50:50) to give a white solid (contaminated with 6-chloro-1*H*-benzo[*d*][1,2,3]triazol-1-ol). This was dissolved in EtOAc (30 mL) and washed with sat. NaHCO$_3$ (aq) (30 mL) and brine (30 mL), before concentrating to give 112 mg of white solid (79%). ^{1}H NMR (d_6-DMSO) δ 11.53 (s, 1H), 7.60 (dd, J = 7.9/0.6 Hz, 1H), 7.41 (dd, J = 8.2/0.8 Hz, 1H), 7.17 (ddd, J = 8.2/7.0/1.1 Hz, 1H), 7.03 (ddd, J = 8.0/7.0/1.0 Hz, 1H), 6.73 (dd, J = 2.1/0.7 Hz, 1H), 3.70 (s, 4H), 1.86–1.38 (m, 6H); ^{13}C NMR (d_6-DMSO) δ 161.9, 135.8, 130.3, 126.8, 123.0, 121.2, 119.6, 112.0, 103.3, 47.1, 25.8, 24.1; *m/z* MS (TOF ES$^+$) C$_{14}$H$_{17}$N$_2$O [MH]$^+$ calcd 229.1; found 229.1; LCMS t_R: 3.37 min (system B).

(1*H*-Indol-2-yl)(morpholino)methanone (11n).[38] Indole-2-carboxylic acid (100 mg, 0.62 mmol) was coupled to morpholine according to general procedure B. The crude precipitate was dissolved in EtOAc (30 mL) and washed with sat. NaHCO$_3$ (aq) (30 mL), before concentrating and further purifying the residue by FCC (eluent EtOAc/PE 10:90 to 100:0), to give 107 mg of white solid (75%). ^{1}H NMR

(d_6-DMSO) δ 11.58 (s, 1H), 7.60 (d, J = 7.8 Hz, 1H), 7.42 (dd, J = 8.2/0.8 Hz, 1H), 7.18 (ddd, J =

8.2/7.0/1.1 Hz, 1H), 7.04 (ddd, J = 7.9/7.2/0.9 Hz, 1H), 6.81 (d, J = 1.3 Hz, 1H), 3.96–3.48 (m, 8H);

^{13}C NMR (d_6-DMSO) δ 162.1, 135.9, 129.6, 126.8, 123.2, 121.3, 119.7, 112.0, 104.1, 66.2, 47.9; m/z

MS (TOF ES$^+$) $C_{13}H_{15}N_2O_2$ [MH]$^+$ calcd 231.1; found 231.2; LCMS t_R: 3.09 min (system B).

N-Cyclopropyl-1H-indole-2-carboxamide (11o). Indole-2-carboxylic acid (100 mg, 0.62 mmol)

was coupled to cyclopropylamine according to general procedure B. The crude precipitate was further

purified by FCC (eluent EtOAc/PE 0:100 to 50:50) to give a white solid (contaminated with 6-chloro-

1H-benzo[d][1,2,3]triazol-1-ol). This was dissolved in EtOAc (30 mL) and washed with sat.

NaHCO$_{3(aq)}$ (30 mL) and brine (30 mL), before concentrating to give 100 mg of white solid (81%). ^{1}H

NMR (d_6-DMSO) δ 11.52 (s, 1H), 8.44 (d, J = 3.9 Hz, 1H), 7.58 (dd, J = 7.9/0.5 Hz, 1H), 7.41 (dd, J =

8.2/0.8 Hz, 1H), 7.16 (ddd, J = 8.2/7.0/1.1 Hz, 1H), 7.08 (d, J = 1.4 Hz, 1H), 7.02 (ddd, J = 8.0/7.0/1.0

Hz, 1H), 2.85 (ddddd, J = 7.9/7.9/7.9/4.0/4.0 Hz, 1H), 0.80 – 0.49 (m, 4H); ^{13}C NMR (d_6-DMSO) δ

162.2, 136.4, 131.7, 127.1, 123.2, 121.4, 119.6, 112.3, 102.4, 22.6, 5.8; m/z MS (TOF ES$^+$) $C_{12}H_{13}N_2O$

[MH]$^+$ calcd 201.1; found 201.2; LCMS t_R: 3.14 min (system B).

N-Cyclobutyl-1H-indole-2-carboxamide (11p). Indole-2-carboxylic acid (100 mg, 0.62 mmol) was

coupled to cyclobutylamine according to general procedure B. The crude precipitate was dissolved in

EtOAc (30 mL) and washed with sat. NaHCO$_3$ $_{(aq)}$ (30 mL), before concentrating and further purifying

the residue by FCC (eluent EtOAc/PE 0:100 to 50:50), to give 52 mg of white solid (39%). ^{1}H NMR

(d_6-DMSO) δ 11.51 (s, 1H), 8.59 (d, J = 7.8 Hz, 1H), 7.60 (d, J = 7.9 Hz, 1H), 7.41 (dd, J = 8.2/0.8 Hz,

1H), 7.25–7.08 (m, 2H), 7.02 (ddd, J = 8.0/7.0/1.0 Hz, 1H), 4.57–4.33 (m, 1H), 2.31–2.17 (m, 2H),

2.16–2.01 (m, 2H), 1.77–1.61 (m, 2H); ^{13}C NMR (d_6-DMSO) δ 160.0, 136.4, 131.7, 127.1, 123.2,

121.4, 119.6, 112.3, 102.5, 44.1, 30.2, 14.7; m/z MS (TOF ES$^+$) $C_{13}H_{15}N_2O$ [MH]$^+$ calcd 215.1; found

215.2; LCMS t_R: 6.00 min (system A).

***N*-Cyclopentyl-1*H*-indole-2-carboxamide (11q).**[32] Indole-2-carboxylic acid (100 mg, 0.62 mmol) was coupled to cyclopentylamine according to general procedure B. The crude precipitate was dissolved in EtOAc (30 mL) and washed with sat. $NaHCO_3$ (aq) (30 mL), before concentrating and further purifying the residue by FCC (eluent EtOAc/PE 0:100 to 50:50), to give 103 mg of off-white solid (73%). ^{1}H NMR (d_6-DMSO) δ 11.49 (s, 1H), 8.25 (d, J = 7.4 Hz, 1H), 7.59 (dd, J = 7.9/0.5 Hz, 1H), 7.41 (dd, J = 8.2/0.8 Hz, 1H), 7.21–7.10 (m, 2H), 7.02 (ddd, J = 8.0/7.0/1.0 Hz, 1H), 4.35–4.12 (m, 1H), 1.98–1.80 (m, 2H), 1.80–1.38 (m, 6H); ^{13}C NMR (d_6-DMSO) δ 160.6, 136.3, 132.0, 127.1, 123.1, 121.4, 119.6, 112.2, 102.5, 50.6, 32.2, 23.6; m/z MS (TOF ES[+]) $C_{14}H_{17}N_2O$ [MH][+] calcd 229.1; found 229.1; LCMS t_R: 3.34 min (system B).

***N*-Cyclohexyl-1*H*-indole-2-carboxamide (11r).**[31] Indole-2-carboxylic acid (100 mg, 0.62 mmol) was coupled to cyclohexylamine according to general procedure B. The crude precipitate was dissolved in EtOAc (30 mL) and washed with sat. $NaHCO_3$ (aq) (30 mL), before concentrating and further purifying the residue by FCC (eluent EtOAc/PE 0:100 to 50:50), to give 116 mg of off-white solid (77%). ^{1}H NMR (d_6-DMSO) δ 11.50 (s, 1H), 8.17 (d, J = 8.0 Hz, 1H), 7.59 (d, J = 7.9 Hz, 1H), 7.42 (dd, J = 8.2/0.7 Hz, 1H), 7.22–7.10 (m, 2H), 7.02 (ddd, J = 7.9/ 7.1/0.9 Hz, 1H), 3.94–3.53 (m, 1H), 1.97–1.52 (m, 5H), 1.46–0.98 (m, 5H); ^{13}C NMR (d_6-DMSO) δ 160.1, 136.3, 132.0, 127.1, 123.1, 121.4, 119.6, 112.2, 102.5, 47.9, 32.6, 25.3, 24.9; m/z MS (TOF ES[+]) $C_{15}H_{19}N_2O$ [MH][+] calcd 243.2; found 243.2; LCMS t_R: 6.36 min (system A).

***N*-(Piperidin-1-yl)-1*H*-indole-2-carboxamide (11s).** Indole-2-carboxylic acid (100 mg, 0.62 mmol) was coupled to 1-aminopiperidne according to general procedure B. The crude precipitate was dissolved in EtOAc (30 mL) and washed with sat. $NaHCO_3$ (aq) (30 mL), before concentrating and further purifying the residue by FCC (eluent EtOAc/PE 10:90 to 100:0), to give 91 mg of off-white solid (60%). ^{1}H NMR (d_6-DMSO) δ 11.53 (s, 1H), 9.37 (s, 1H), 7.59 (d, J = 7.9 Hz, 1H), 7.41 (d, J = 8.2 Hz, 1H), 7.16 (dd, J = 7.6/7.6 Hz, 1H), 7.09 (d, J = 1.1 Hz, 1H), 7.06–6.97 (m, 1H), 3.19–2.71 (m,

4H), 1.87–1.26 (m, 6H); ^{13}C NMR (d_6-DMSO) δ 158.9, 136.3, 130.9, 127.0, 123.2, 121.4, 119.7, 112.2, 102.3, 55.4, 40.2, 39.9, 39.7, 39.5, 39.3, 39.1, 38.9, 25.4, 23.1; *m/z* MS (TOF ES$^+$) $C_{14}H_{18}N_3O$ [MH]$^+$ calcd 244.1; found 244.2; LCMS t_R: 3.13 min (system B).

N-Phenyl-1H-indole-2-carboxamide (11t).[39] Indole-2-carboxylic acid (100 mg, 0.62 mmol), HCTU (282 mg, 0.68 mmol, 1.1 eq) and aniline (0.068 mL, 0.74 mmol, 1.2 eq) were dissolved in DMF (1 mL) at rt, before adding DIPEA (0.129 mL, 0.74 mmol, 1.2 eq). The mixture was stirred at rt overnight, before adding water (10 mL), and allowed to stir for 10 min. The resulting precipitate was collected by filtration (vacuum), then redissolved in EtOAc (30 mL). This solution was then washed with sat. NaHCO$_3$ $_{(aq)}$ (30 mL), before concentrating and further purifying the residue by FCC (eluent EtOAc/PE 0:100 to 50:50), to give 118 mg of yellow solid (81%). ^{1}H NMR (d_6-DMSO) δ 11.74 (s, 1H), 10.20 (s, 1H), 7.81 (dd, J = 8.6/1.0 Hz, 2H), 7.68 (d, J = 8.0 Hz, 1H), 7.52–7.41 (m, 2H), 7.38 (dd, J = 10.8/5.1 Hz, 2H), 7.22 (ddd, J = 8.2/7.0/1.1 Hz, 1H), 7.16–7.01 (m, 2H); ^{13}C NMR (d_6-DMSO) δ 159.7, 139.0, 136.8, 131.5, 128.7, 127.0, 123.8, 123.5, 121.7, 120.1, 119.9, 112.4, 103.9; *m/z* MS (TOF ES$^+$) $C_{15}H_{13}N_2O$ [MH]$^+$ calcd 237.1; found 237.1; LCMS t_R: 3.37 min (system B).

N-(Cyclopropylmethyl)-1H-indole-2-carboxamide (11u). Indole-2-carboxylic acid (100 mg, 0.62 mmol) was coupled to cyclopropylmethylamine according to general procedure B. The mixture was diluted with water/sat. NaHCO$_3$ $_{(aq)}$ (1:1), and the resulting precipitate collected by filtration (vacuum), and washed with water. After drying, 73 mg of white solid was obtained, requiring no further purification. ^{1}H NMR (d_6-DMSO) δ 11.54 (s, 1H), 8.54 (t, J = 5.7 Hz, 1H), 7.60 (d, J = 7.9 Hz, 1H), 7.42 (dd, J = 8.2/0.8 Hz, 1H), 7.16 (ddd, J = 8.2/7.0/1.1 Hz, 1H), 7.13–7.07 (m, 1H), 7.02 (ddd, J = 8.0/7.0/1.0 Hz, 1H), 3.17 (dd, J = 6.3/6.3 Hz, 2H), 1.15–0.94 (m, 1H), 0.55–0.35 (m, 2H), 0.34–0.15 (m, 2H); ^{13}C NMR (d_6-DMSO) δ 161.0, 136.3, 131.9, 127.1, 123.1, 121.4, 119.6, 112.2, 102.3, 43.1, 11.1, 3.3; *m/z* MS (TOF ES$^+$) $C_{13}H_{15}N_2O$ [MH]$^+$ calcd 215.1; found 215.1; LCMS t_R: 3.24 min (system B).

N-(Cyclohexylmethyl)-1H-indole-2-carboxamide (11v). Indole-2-carboxylic acid (100 mg, 0.62 mmol) was coupled to cyclohexylmethylamine according to general procedure B. The crude precipitate was dissolved in EtOAc (30 mL) and washed with sat. $NaHCO_3$ (aq) (30 mL), before concentrating and further purifying the residue by FCC (eluent EtOAc/PE 0:100 to 50:50), to give 102 mg of white solid (64%). ^1H NMR (d_6-DMSO) δ 11.50 (s, 1H), 8.40 (t, J = 5.8 Hz, 1H), 7.59 (d, J = 7.9 Hz, 1H), 7.41 (dd, J = 8.2/0.8 Hz, 1H), 7.16 (ddd, J = 8.2/7.0/1.1 Hz, 1H), 7.12 (dd, J = 2.0/0.6 Hz, 1H), 7.02 (ddd, J = 8.0/7.1/0.9 Hz, 1H), 3.13 (dd, J = 6.4/6.4 Hz, 2H), 1.83–1.43 (m, 6H), 1.36–1.05 (m, 3H), 1.03–0.82 (m, 2H); ^{13}C NMR (d_6-DMSO) δ 161.1, 136.3, 131.9, 127.1, 123.1, 121.4, 119.6, 112.2, 102.2, 45.0, 37.6, 30.5, 26.1, 25.4; m/z MS (TOF ES$^+$) $C_{16}H_{21}N_2O$ [MH]$^+$ calcd 257.2; found 257.2; LCMS t_R: 3.50 min (system B).

N-Benzyl-1H-indole-2-carboxamide (11w).[31,32] Indole-2-carboxylic acid (100 mg, 0.62 mmol) was coupled to benzylamine according to general procedure B. The crude precipitate was dissolved in EtOAc (30 mL) and washed with sat. $NaHCO_3$ (aq) (30 mL), before concentrating and further purifying the residue by FCC (eluent EtOAc/PE 0:100 to 50:50), to give 116 mg of white solid (74%). ^1H NMR (d_6-DMSO) δ 11.59 (s, 1H), 9.02 (t, J = 6.1 Hz, 1H), 7.61 (d, J = 7.9 Hz, 1H), 7.46–7.39 (m, 1H), 7.39–7.30 (m, J = 4.4 Hz, 4H), 7.29–7.21 (m, 1H), 7.21–7.13 (m, 2H), 7.03 (ddd, J = 8.0/7.0/1.0 Hz, 1H), 4.52 (d, J = 6.1 Hz, 2H); ^{13}C NMR (d_6-DMSO) δ 161.1, 139.6, 136.5, 131.6, 128.3, 127.2, 127.1, 126.8, 123.3, 121.5, 119.7, 112.3, 102.6, 42.1; m/z MS (TOF ES$^+$) $C_{16}H_{15}N_2O$ [MH]$^+$ calcd 251.1; found 251.1; LCMS t_R: 3.34 min (system B).

3-Fluoro-N-isopropyl-1H-indole-2-carboxamide (13a). N-Isopropyl-1H-indole-2-carboxamide (**3**) (113 mg, 0.56 mmol) as dissolved in MeCN (5 mL), before adding sat. $NaHCO_3$ (aq) (1 mL), and cooling to 0 °C. Once cooled, 1-chloromethyl-4-fluoro-1,4-diazoniabicyclo[2.2.2]octane bis(tetrafluoroborate) (Selectfluor$^®$) (238 mg, 0.67 mmol, 1.2 eq) was added gradually, and the mixture stirred at rt for 5 h. TLC analysis (EtOAc/PE 3:7) indicated reaction progression had stopped, so the

mixture was quenched with water (30 mL), before extracting with EtOAc (3 × 20 mL), and the combined organic extracts washed with brine (30 mL). After concentration, the crude residue was purified by FCC (eluent EtOAc/PE 0:100 to 30:70) to give 56 mg of off-white solid (46%). ^{1}H NMR (d_6-DMSO) δ 11.37 (s, 1H), 7.60 (d, J = 8.0 Hz, 1H), 7.53 (d, J = 6.3 Hz, 1H), 7.39 (ddd, J = 8.4/1.5/0.9 Hz, 1H), 7.25 (ddd, J = 8.3/7.0/1.1 Hz, 1H), 7.10 (ddd, J = 7.9/7.0/0.9 Hz, 1H), 4.31–3.96 (m, 1H), 1.21 (d, J = 6.6 Hz, 6H); ^{19}F NMR (376 MHz, d_6-DMSO) δ -164.67; ^{13}C NMR (d_6-DMSO) δ 158.5 (d, J_{CF} = 3.5 Hz), 142.7 (d, J_{CF} = 250.4 Hz), 131.8 (d, J_{CF} = 6.5 Hz), 124.6, 120.1, 117.2 (d, J_{CF} = 2.6 Hz), 115.2 (d, J_{CF} = 15.8 Hz), 114.9 (d, J_{CF} = 18.7 Hz), 112.7, 40.9, 22.2; m/z MS (TOF ES[+]) $C_{12}H_{14}FN_2O$ [MH][+] calcd 221.1; found 221.2; LCMS t_R: 3.38 min (system B).

4-Fluoro-*N*-isopropyl-1*H*-indole-2-carboxamide (13b). 4-Fluoroindole-2-carboxylic acid **(12b)** (100 mg, 0.56 mmol) and isopropylamine (0.142 mL, 1.67 mmol, 3 eq), were coupled according to general procedure B. Sat. NaHCO$_3$ (aq) (1 mL) was added, followed by water. The resulting precipitate was collected by vacuum filtration, then washed with water, dried and further purified by FCC (eluent EtOAc/PE 0:100 to 40:60) to give 18 mg of yellow solid (15%). ^{1}H NMR (d_6-DMSO) δ 11.86 (s, 1H), 8.30 (d, J = 7.8 Hz, 1H), 7.30–7.20 (m, 2H), 7.14 (td, J = 8.0, 5.4 Hz, 1H), 6.80 (ddd, J = 10.8/7.8/0.5 Hz, 1H), 4.22–4.06 (m, 1H), 1.19 (d, J = 6.6 Hz, 6H); ^{19}F NMR (376 MHz, d_6-DMSO) δ -121.88; ^{13}C NMR (d_6-DMSO) δ 159.7, 156.1 (d, J_{CF} = 245.7 Hz), 138.8 (d, J_{CF} = 10.8 Hz), 132.4, 123.6 (d, J_{CF} = 7.8 Hz), 116.2 (d, J_{CF} = 22.0 Hz), 108.8 (d, J_{CF} = 3.5 Hz), 103.9 (d, J_{CF} = 18.4 Hz), 97.9, 40.7, 22.4; m/z MS (TOF ES[+]) $C_{12}H_{14}FN_2O$ [MH][+] calcd 221.1; found 221.1; LCMS t_R: 3.26 min (system B).

5-Fluoro-*N*-isopropyl-1*H*-indole-2-carboxamide (13c). 5-Fluoroindole-2-carboxylic acid (**12c**) (100 mg, 0.56 mmol) and isopropylamine (0.142 mL, 1.67 mmol, 3 eq), were coupled according the general procedure B. The crude was purified by FCC (eluent EtOAc/PE 0:100 to 50:50) to give 90 mg of white solid (73%). ^{1}H NMR (d_6-DMSO) δ 11.61 (s, 1H), 8.25 (d, J = 7.8 Hz, 1H), 7.46–7.32 (m, 2H), 7.13 (d, J = 1.5 Hz, 1H), 7.02 (ddd, J = 9.3/9.3/2.6 Hz, 1H), 4.28–3.96 (m, 1H), 1.18 (d, J = 6.6

Hz, 1H); ^{19}F NMR (376 MHz, d_6-DMSO) δ -124.2; ^{13}C NMR (d_6-DMSO) δ 159.9, 157.1 (d, J_{CF} = 232.3 Hz), 133.8, 133.0, 127.1 (d, J_{CF} = 10.5 Hz), 113.4 (d, J_{CF} = 9.8 Hz), 111.7 (d, J_{CF} = 26.5 Hz), 105.6 (d, J_{CF} = 23.0 Hz), 102.4 (d, J_{CF} = 5.1 Hz), 40.7, 22.4; m/z MS (TOF ES$^+$) $C_{12}H_{14}FN_2O$ [MH]$^+$ calcd 221.1; found 221.1; LCMS t_R: 3.25 min (system B).

6-Fluoro-*N*-isopropyl-1*H*-indole-2-carboxamide (13d). 6-Fluoroindole-2-carboxylic acid (**12d**) (100 mg, 0.56 mmol) isopropylamine (0.142 mL, 1.67 mmol, 3 eq), were coupled according to general procedure B. The crude was purified by FCC (eluent EtOAc/PE 0:100 to 50:50) to give 30 mg of pink solid (24%). ^{1}H NMR (d_6-DMSO) δ 11.58 (s, 1H), 8.21 (d, J = 7.8 Hz, 1H), 7.62 (dd, J = 8.7/5.5 Hz, 1H), 7.15 (dd, J = 2.2/0.8 Hz, 1H), 7.13 (dd, J = 10.1/2.4 Hz, 1H), 6.89 (ddd, J = 9.8/8.8/2.4 Hz, 1H), 4.27–3.98 (m, 1H), 1.18 (d, J = 6.6 Hz, 7H); ^{19}F NMR (376 MHz, d_6-DMSO) δ -119.0; ^{13}C NMR (d_6-DMSO) δ 159.9, 159.8 (d, J_{CF} = 236.7 Hz), 136.2 (d, J_{CF} = 12.9 Hz), 132.8 (d, J_{CF} = 3.7 Hz), 123.9, 122.8 (d, J_{CF} = 10.4 Hz), 108.6 (d, J_{CF} = 24.8 Hz), 102.5, 97.7 (d, J_{CF} = 25.5 Hz), 40.7, 22.4; m/z MS (TOF ES$^+$) $C_{12}H_{14}FN_2O$ [MH]$^+$ calcd 221.1; found 221.1; LCMS t_R: 3.25 min (system B).

7-Fluoro-*N*-isopropyl-1*H*-indole-2-carboxamide (13e). 7-Fluoroindole-2-carboxylic acid (**12e**) (100 mg, 0.56 mmol) and isopropylamine (0.142 mL, 1.67 mmol, 3 eq) were coupled according to general procedure B. The mixture was quenched with sat. NaHCO$_{3 (aq)}$/water (1:1, 10 mL) and stirred at rt for a further 5 min, causing precipitate formation. This was collected by filtration (vacuum), then washed with water, dried and further purified by FCC (eluent EtOAc/PE 0:100 to 50:50) to give 8 mg of white solid (7%). ^{1}H NMR (d_6-DMSO) δ 11.93 (s, 1H), 8.23 (d, J = 7.7 Hz, 1H), 7.51–7.36 (m, 1H), 7.19 (dd, J = 3.2/2.1 Hz, 1H), 7.09–6.91 (m, 2H), 4.26–3.95 (m, 1H), 1.19 (d, J = 6.6 Hz, 6H); ^{19}F NMR (376 MHz, d_6-DMSO) δ -131.50; ^{13}C NMR (d_6-DMSO) δ 159.5, 149.3 (d, J_{CF} = 245.1 Hz), 133.5, 130.8 (d, J_{CF} = 5.7 Hz), 124.6 (d, J_{CF} = 13.3 Hz), 119.9 (d, J_{CF} = 6.0 Hz), 117.5 (d, J_{CF} = 3.6 Hz), 107.8 (d, J_{CF} = 15.9 Hz), 104.1 (d, J_{CF} = 2.1 Hz), 40.8, 22.4; m/z MS (TOF ES$^+$) $C_{12}H_{14}FN_2O$ [MH]$^+$ calcd 221.1; found 221.1; LCMS t_R: 3.25 min (system B).

5-Methoxy-*N*-isopropyl-1*H*-indole-2-carboxamide (15). 5-Methoxyindole-2-carboxylic acid (**14**) (191 mg, 1.00 mmol) and isopropylamine (0.255 mL, 3.00 mmol, 3 eq) were coupled according to general procedure B. The mixture was quenched with sat. NaHCO$_3$ $_{(aq)}$/water (1:1, 10 mL) and stirred at rt for a further 5 min, causing precipitate formation. This was collected by filtration (vacuum), then washed with water, dried and further purified by FCC (eluent EtOAc/PE 0:100 to 50:50) to give 185 mg of off-white solid (80%). ^{1}H NMR (d_6-DMSO) δ 11.34 (s, 1H), 8.15 (d, J = 7.8 Hz, 1H), 7.30 (d, J = 8.9 Hz, 1H), 7.05 (d, J = 2.4 Hz, 1H), 7.03 (dd, J = 2.1/0.7 Hz, 1H), 6.81 (dd, J = 8.9/2.5 Hz, 1H), 4.18–4.05 (m, 1H), 3.75 (s, 3H), 1.18 (d, J = 6.6 Hz, 6H); ^{13}C NMR (d_6-DMSO) δ 160.2, 153.7, 132.4, 131.6, 127.4, 114.2, 113.0, 102.1, 102.0, 55.3, 40.6, 22.5; *m/z* MS (TOF ES$^+$) C$_{13}$H$_{17}$N$_2$O$_2$ [MH]$^+$ calcd 233.3; found 233.2; LCMS t_R: 3.53 min (system B).

***N*-Isopropyl-1-methyl-1*H*-indole-2-carboxamide (17).**[40] 1-Methyl-1*H*-indole-2-carboxylic acid (**16**) (175 mg, 1.00 mmol) and isopropylamine (0.255 mL, 3.00 mmol, 3 eq) were coupled according to general procedure B. The mixture was quenched with sat. NaHCO$_3$ $_{(aq)}$/water (1:1, 10 mL) and stirred at rt for a further 5 min, causing precipitate formation. This was collected by filtration (vacuum), then washed with water, dried and further purified by FCC (eluent EtOAc/PE 0:100 to 50:50), to give 195 mg of yellow solid (90%). ^{1}H NMR (d_6-DMSO) δ 8.26 (d, J = 7.9 Hz, 1H), 7.66–7.56 (m, 1H), 7.51 (dd, J = 8.4/0.7 Hz, 1H), 7.26 (ddd, J = 8.3/7.0/1.2 Hz, 1H), 7.14–6.99 (m, 2H), 4.17–4.03 (m, 1H), 3.97 (s, 3H), 1.18 (d, J = 6.6 Hz, 6H); ^{13}C NMR (d_6-DMSO) δ 161.0, 138.3, 132.5, 125.6, 123.3, 121.4, 120.0, 110.4, 104.1, 40.6, 31.3, 22.3; *m/z* MS (TOF ES$^+$) C$_{13}$H$_{17}$N$_2$O [MH]$^+$ calcd 217.1; found 217.2; LCMS t_R: 3.73 min (system B).

***N*-Isopropyl-1*H*-benzo[*d*]imidazole-2-carboxamide (19).**[41] 1*H*-Benzo[*d*]imidazole-2-carboxylic acid (**18**) (162 mg, 1.00 mmol) and isopropylamine (0.255 mL, 3.00 mmol, 3 eq) were coupled according to general procedure B. The mixture was quenched with sat. NaHCO$_3$ $_{(aq)}$/water (1:1, 10 mL) and stirred at rt for a further 5 min, causing precipitate formation. This was collected by filtration

(vacuum), then washed with water, dried and further purified by FCC (eluent EtOAc/PE 0:100 to 50:50) to give 45 mg of off-white solid (22%). ^{1}H NMR (d_6-DMSO) δ 13.19 (s, 1H), 8.68 (d, J = 8.4 Hz, 1H), 7.71 (d, J = 7.6 Hz, 1H), 7.58–7.45 (m, 1H), 7.33–7.28 (m, 1H), 7.28–7.22 (m, 1H), 4.32–4.08 (m, 1H), 1.21 (d, J = 6.6 Hz, 6H); ^{13}C NMR (d_6-DMSO) δ 157.8, 145.9, 142.5, 134.4, 124.0, 122.5, 119.8, 112.5, 40.8, 22.1; m/z MS (TOF ES$^+$) $C_{11}H_{14}N_3O$ [MH]$^+$ calcd 204.1; found 204.2; LCMS t_R: 3.42 min (system B).

N-Isopropylbenzo[d]oxazole-2-carboxamide (21).[42] Potassium benzo[d]oxazole-2-carboxylate (**20**) (141 mg, 0.70 mmol) and isopropylamine (0.178 mL, 2.09 mmol, 3 eq) were coupled according to general procedure B. The mixture was quenched with sat. NaHCO$_{3 (aq)}$/water (1:1, 10 mL) and stirred at rt for a further 5 min, before extraction with EtOAc (3 × 20 mL). The combined organic layers were washed with brine (20 mL), before concentration under reduced pressure, and further purified by FCC (eluent EtOAc/PE 0:100 to 50:50) to give 42 mg of off-white solid (30%). ^{1}H NMR (d_6-DMSO) δ 9.11 (d, J = 8.2 Hz, 1H), 7.92–7.81 (m, 2H), 7.60–7.53 (m, 1H), 7.53–7.46 (m, 1H), 4.23–4.01 (m, 1H), 1.20 (d, J = 6.6 Hz, 6H); ^{13}C NMR (d_6-DMSO) δ 155.9, 154.2, 150.1, 139.8, 127.3, 125.6, 120.9, 111.8, 41.3, 21.9; m/z MS (TOF ES$^+$) $C_{11}H_{13}N_2O_2$ [MH]$^+$ calcd 205.2; found 205.1; LCMS t_R: 3.54 min (system B).

N-Isopropylbenzofuran-2-carboxamide (23a).[43] Benzofuran-2-carboxylic acid (**22a**) (162 mg, 1.00 mmol) and isopropylamine (0.255 mL, 3.00 mmol, 3 eq) were coupled according to general procedure B. The mixture was quenched with sat. NaHCO$_{3 (aq)}$/water (1:1, 10 mL) and stirred at rt for a further 5 min, causing precipitate formation. This was collected by filtration (vacuum), then washed with water, to give 160 mg of white solid (79%). ^{1}H NMR (CDCl$_3$) δ 7.67 (ddd, J = 7.8/1.2/0.7 Hz, 1H), 7.50 (dd, J = 8.3/0.8 Hz, 1H), 7.45 (d, J = 0.9 Hz, 1H), 7.41 (ddd, J = 8.4/7.2/1.3 Hz, 1H), 7.29 (ddd, J = 8.1/7.3/1.0 Hz, 1H), 6.46 (d, J = 5.7 Hz, 1H), 4.49–4.17 (m, 1H), 1.31 (d, J = 6.6 Hz, 6H); ^{13}C NMR

(CDCl$_3$) δ 158.2, 154.8, 149.1, 127.9, 126.9, 123.8, 122.9, 111.8, 110.3, 41.6, 23.0; *m/z* MS (TOF ES$^+$) C$_{12}$H$_{14}$NO$_2$ [MH]$^+$ calcd 204.1; found 204.2; LCMS t_R: 3.62 min (system B).

N-Isopropylbenzofuran-3-carboxamide (23b). Benzofuran-3-carboxylic acid (**22b**) (162 mg, 1.00 mmol) and isopropylamine (0.255 mL, 3.00 mmol, 3 eq) were coupled according to general procedure B. The mixture was quenched with sat. NaHCO$_3$ $_{(aq)}$/water (1:1, 10 mL) and stirred at rt for a further 5 min, causing precipitate formation. This was collected by filtration (vacuum), then washed with water, dried and further purified by FCC (eluent EtOAc/PE 0:100 to 50:50), to give 117 mg of yellow solid (58%). ^{1}H NMR (*d*$_6$-DMSO) δ 8.54 (s, 1H), 8.10 (d, *J* = 7.5 Hz, 1H), 8.08–8.01 (m, 1H), 7.68–7.58 (m, 1H), 7.42–7.28 (m, 2H), 4.32–3.86 (m, 1H), 1.18 (d, *J* = 6.6 Hz, 6H); ^{13}C NMR (*d*$_6$-DMSO) δ 161.2, 154.6, 147.0, 125.4, 125.0, 123.6, 122.0, 117.1, 111.5, 40.5, 22.4; *m/z* MS (TOF ES$^+$) C$_{12}$H$_{14}$NO$_2$ [MH]$^+$ calcd 204.1; found 204.2; LCMS t_R: 3.61 min (system B).

N-Isopropylbenzo[b]thiophene-2-carboxamide (25a).[44] Benzo[b]thiophene-2-carboxylic acid (**24a**) (178 mg, 1.00 mmol) and isopropylamine (0.255 mL, 3.00 mmol, 3 eq) were coupled according to general procedure B. The mixture was quenched with sat. NaHCO$_3$ $_{(aq)}$/water (1:1, 10 mL) and stirred at rt for a further 5 min, causing precipitate formation. This was collected by filtration (vacuum), then washed with water, to give 164 mg of white solid (75%). ^{1}H NMR (CDCl$_3$) δ 7.92–7.78 (m, 2H), 7.74 (s, 1H), 7.47–7.34 (m, 2H), 5.89 (d, *J* = 5.5 Hz, 1H), 4.42–4.18 (m, 1H), 1.29 (d, *J* = 6.6 Hz, 6H); ^{13}C NMR (CDCl$_3$) δ 161.6, 148.7, 140.9, 139.3, 126.4, 125.1, 125.1, 125.0, 122.9, 42.4, 23.0; *m/z* MS (TOF ES$^+$) C$_{12}$H$_{14}$NOS [MH]$^+$ calcd 220.1; found 220.1; LCMS t_R: 3.70 min (system B).

N-Isopropylbenzo[b]thiophene-3-carboxamide (25b). Benzo[b]thiophene-3-carboxylic acid (**24b**) (178 mg, 1.00 mmol) and isopropylamine (0.255 mL, 3.00 mmol, 3 eq) were coupled according to general procedure B. The mixture was quenched with sat. NaHCO$_3$ $_{(aq)}$/water (1:1, 10 mL) and stirred at rt for a further 5 min, causing precipitate formation. This was collected by filtration (vacuum), then washed with water, to give 195 mg of white solid (89%). ^{1}H NMR (CDCl$_3$) δ 8.34 (d, *J* = 7.8 Hz, 1H),

7.86 (ddd, J = 7.9/1.2/0.7 Hz, 1H), 7.82 (s, 1H), 7.46 (ddd, J = 8.2/7.1/1.3 Hz, 1H), 7.43–7.37 (m, 1H),

5.84 (s, 1H), 4.53–4.15 (m, 1H), 1.30 (d, J = 6.6 Hz, 6H); ^{13}C NMR (CDCl$_3$) δ 166.8, 143.2, 140.4,

136.9, 128.8, 125.2, 124.3, 122.7, 118.7, 41.9, 23.1; *m/z* MS (TOF ES$^+$) C$_{12}$H$_{14}$NOS [MH]$^+$ calcd

220.1; found 220.1; LCMS t_R: 3.68 min (system B).

N-Isopropyl-1H-pyrrolo[2,3-b]pyridine-2-carboxamide **(27).** 1H-Pyrrolo[2,3-b]pyridine-2-

carboxylic acid (**26**) (103 mg, 0.64 mmol) and isopropylamine (0.164 mL, 1.92 mmol, 3 eq) were

coupled together according to general procedure B. After an overnight period of stirring, the carboxylic

acid starting material had disappeared, however, the isouronium intermediate was still present, and

appeared to be only partially soluble in the reaction mixture. DCM (1 mL) and further isopropylamine

(0.273 mL, 3.2 mmol, 5 eq) was added and stirring continued for a further overnight period. The

mixture was quenched with sat. NaHCO$_3$ $_{(aq)}$/water (1:1, 10 mL) and stirred at rt for a further 5 min,

causing precipitate formation. This was collected by filtration (vacuum), then washed with water, to

give 86 mg of white solid (66%). ^{1}H NMR (d_6-DMSO) δ 12.03 (s, 1H), 8.32 (dd, J = 4.6/1.5 Hz, 1H),

8.24 (d, J = 7.6 Hz, 1H), 8.05 (dd, J = 7.9/1.4 Hz, 1H), 7.20–7.02 (m, 2H), 4.42–3.72 (m, 1H), 1.19 (d,

J = 6.6 Hz, 6H); ^{13}C NMR (d_6-DMSO) δ 159.6, 148.3, 145.1, 132.5, 129.9, 119.3, 116.3, 101.7, 40.8,

22.4; *m/z* MS (TOF ES$^+$) C$_{11}$H$_{14}$N$_3$O [MH]$^+$ calcd 204.1; found 204.2; LCMS t_R: 4.98 min (system A).

1H-Indole-4-carboxylic acid (29a). Methyl 1H-indole-4-carboxylate (**28a**) underwent hydrolysis

according to general procedure C, to give 72 mg (78%) of pale orange solid.

^{1}H NMR (d_6-DMSO) δ 11.38 (s, 1H), 7.71 (dd, J = 7.4/1.0 Hz, 1H), 7.65 (ddd, J = 8.0/0.9/0.9 Hz,

1H), 7.49 (dd, J = 2.8/2.8 Hz, 1H), 7.22–7.08 (m, 1H), 6.95 (ddd, J = 3.0/2.0/0.9 Hz, 1H); ^{13}C NMR

(d_6-DMSO) δ 168.5, 136.7, 127.3, 127.2, 122.3, 121.4, 120.1, 116.2, 102.3; *m/z* MS (TOF ES$^-$)

C$_9$H$_6$NO$_2$ [M-H]$^-$ calcd 160.0; found 160.1; LCMS t_R: 3.21 min (system B).

1H-Indole-5-carboxylic acid (29b). Methyl 1H-indole-5-carboxylate (**28b**) underwent hydrolysis

according to general procedure C, to give 95 mg (quantitative) of pale orange solid.

^{1}H NMR (d_6-DMSO) δ 11.42 (s, 1H), 8.23 (s, 1H), 7.70 (dd, J = 8.5/1.6 Hz, 1H), 7.52–7.35 (m, 2H), 6.65–6.49 (m, 1H); ^{13}C NMR (d_6-DMSO) δ 168.4, 138.3, 127.2, 126.9, 122.8, 122.2, 121.4, 111.1, 102.47; m/z MS (TOF ES$^-$) $C_9H_6NO_2$ [M-H]$^-$ calcd 160.0; found 160.1; LCMS t_R: 3.23 min (system B).

1*H*-Indole-6-carboxylic acid (29c). Methyl 1*H*-indole-6-carboxylate (**28c**) underwent hydrolysis according to general procedure C, to give 94 mg (quantitative) of pale orange solid. ^{1}H NMR (d_6-DMSO) δ 11.44 (s, 1H), 8.04 (ddd, J = 1.0/1.0/1.0 Hz, 1H), 7.62–7.58 (m, 2H), 7.58–7.54 (m, 1H), 6.51 (ddd, J = 2.9/1.9/0.9 Hz, 1H); ^{13}C NMR (d_6-DMSO) δ 168.4, 135.2, 131.0, 128.9, 123.1, 119.8, 119.6, 113.5, 101.4; m/z MS (TOF ES$^-$) $C_9H_6NO_2$ [M-H]$^-$ calcd 160.0; found 160.1; LCMS t_R: 3.35 min (system B).

1*H*-Indole-7-carboxylic acid (29d). Methyl 1*H*-indole-7-carboxylate (**28d**) underwent hydrolysis according to general procedure C, to give 100 mg (quantitative) of orange solid. ^{1}H NMR (d_6-DMSO) δ 11.05 (s, 1H), 7.83 (d, J = 7.8 Hz, 1H), 7.74 (dd, J = 7.5/1.0 Hz, 1H), 7.36 (dd, J = 2.8/2.8 Hz, 1H), 7.10 (dd, J = 7.6/7.6 Hz, 1H), 6.54 (dd, J = 3.1/2.0 Hz, 1H); ^{13}C NMR (d_6-DMSO) δ 168.0, 134.6, 129.3, 126.8, 125.6, 123.8, 118.4, 113.5, 101.5; m/z MS (TOF ES$^-$) $C_9H_6NO_2$ [M-H]$^-$ calcd 160.0; found 160.1; LCMS t_R: 3.48 min (system B).

N-Isopropyl-1*H*-indole-4-carboxamide (30a). 1*H*-Indole-4-carboxylic acid (**29a**) (64 mg, 0.40 mmol) and isopropylamine (0.102 mL, 1.20 mmol, 3 eq) were coupled together according to general procedure B. The mixture was quenched with sat. NaHCO$_3$ $_{(aq)}$/water (1:1, 10 mL) and stirred at rt for 30 min, causing precipitate formation. This was collected by filtration (vacuum), then washed with water, to give 32 mg (40%) of off-white solid, requiring no further purification. ^{1}H NMR (d_6-DMSO) δ 11.24 (s, 1H), 7.95 (d, J = 7.9 Hz, 1H), 7.51 (ddd, J = 8.1/0.8/0.8 Hz, 1H), 7.46–7.38 (m, 1H), 7.37 (dd, J = 7.3/0.8 Hz, 1H), 7.16–7.04 (m, 1H), 6.80 (ddd, J = 2.9/2.0/0.8 Hz, 1H), 4.31–3.99 (m, 1H), 1.19 (d, J = 6.6 Hz, 6H); ^{13}C NMR (d_6-DMSO) δ 167.0, 136.5, 127.2, 126.2, 125.9, 120.1, 118.3, 113.8, 101.8,

40.6, 22.4; *m/z* MS (TOF ES$^+$) C$_{12}$H$_{15}$N$_2$O [MH]$^+$ calcd 203.1; found 203.2; LCMS t_R: 3.36 min

(system B).

N-Isopropyl-1H-indole-5-carboxamide (30b).[45] 1*H*-Indole-5-carboxylic acid (**29b**) (80 mg, 0.50

mmol) and isopropylamine (0.128 mL, 1.50 mmol, 3 eq) were coupled together according to general

procedure B. The mixture was quenched with sat. NaHCO$_3$ (aq)/water (1:1, 10 mL) and stirred at rt for

30 min, before extraction with EtOAc (3 × 20 mL). The combined organic layers were washed with

brine (20 mL), before concentration under reduced pressure, and further purification by FCC (eluent

EtOAc/PE 0:100 to 100:0), to give 180 mg of clear colourless oil. This was diluted with DCM, and the

resulting precipitate removed by filtration. After concentration of the filtrate, the resulting residue was

triturated with water to give 66 mg (65%) of glassy solid. ^{1}H NMR (*d$_6$*-DMSO) δ 11.27 (s, 1H), 8.17–

8.07 (m, 1H), 8.02 (d, *J* = 7.8 Hz, 1H), 7.62 (dd, *J* = 8.5/1.7 Hz, 1H), 7.49–7.31 (m, 2H), 6.51 (ddd, *J* =

2.9/1.9/0.8 Hz, 1H), 4.24–3.99 (m, 1H), 1.17 (d, *J* = 6.6 Hz, 6H); ^{13}C NMR (*d$_6$*-DMSO) δ 166.4, 137.3,

126.9, 126.5, 125.9, 120.6, 119.8, 110.7, 102.0, 40.8, 22.5; *m/z* MS (TOF ES$^+$) C$_{12}$H$_{15}$N$_2$O [MH]$^+$ calcd

203.1; found 203.1; LCMS t_R: 3.37 min (system B).

N-Isopropyl-1H-indole-6-carboxamide (30c). 1*H*-Indole-6-carboxylic acid (**29c**) (70 mg, 0.43

mmol) and isopropylamine (0.111 mL, 1.29 mmol, 3 eq) were coupled together according to general

procedure B. The mixture was quenched with sat. NaHCO$_3$ (aq)/water (1:1, 10 mL) and stirred at rt for

30 min, before extraction with EtOAc (3 × 20 mL). The combined organic layers were washed with

brine (20 mL), before concentration under reduced pressure, and further purification by FCC (eluent

EtOAc/PE 0:100 to 100:0), to give 105 mg of clear colourless oil. This was triturated with water to give

52 mg (60%) of glassy solid. ^{1}H NMR (*d$_6$*-DMSO) δ 11.32 (s, 1H), 8.09 (d, *J* = 7.2 Hz, 1H), 7.93 (s,

1H), 7.76–7.16 (m, 3H), 6.47 (s, 1H), 4.41–3.80 (m, 1H), 1.17 (d, *J* = 6.5 Hz, 6H); ^{13}C NMR (*d$_6$*-

DMSO) δ 166.3, 135.2, 129.6, 127.8, 123.6, 119.2, 118.1, 111.2, 101.1, 40.8, 22.5; *m/z* MS (TOF ES$^+$)

C$_{12}$H$_{15}$N$_2$O [MH]$^+$ calcd 203.1; found 203.1; LCMS t_R: 3.41 min (system B).

N-**Isopropyl-1*H*-indole-7-carboxamide (30d).** 1*H*-Indole-7-carboxylic acid (**29d**) (70 mg, 0.43 mmol) and isopropylamine (0.111 mL, 1.29 mmol, 3 eq) were coupled together according to general procedure B. The mixture was quenched with sat. NaHCO$_3$ $_{(aq)}$/water (1:1, 10 mL) and stirred at rt for 30 min, causing precipitate formation. This was collected by filtration (vacuum), then washed with water, to give 66 mg (76%) of orange solid, requiring no further purification. ^{1}H NMR (*d*$_6$-DMSO) δ 11.11 (s, 1H), 8.26 (d, *J* = 7.7 Hz, 1H), 7.71 (d, *J* = 7.8 Hz, 1H), 7.66 (d, *J* = 7.5 Hz, 1H), 7.33 (dd, *J* = 2.8/2.8 Hz, 1H), 7.05 (dd, *J* = 7.6/7.6 Hz, 1H), 6.47 (dd, *J* = 3.1/2.1 Hz, 1H), 4.34–4.04 (m, 1H), 1.21 (d, *J* = 6.6 Hz, 6H); ^{13}C NMR (*d*$_6$-DMSO) δ 166.2, 134.2, 129.1, 126.5, 123.5, 119.8, 117.9, 117.2, 100.9, 40.6, 22.4; *m/z* MS (TOF ES[+]) C$_{12}$H$_{15}$N$_2$O [MH][+] calcd 203.1; found 203.2; LCMS *t*$_R$: 3.65 min (system B).

***tert*-Butyl (4-hydroxybutyl)carbamate (32).** 4-Aminopentanol (**31**) (196 mg, 2.20 mmol, 1.1 eq) was stirred in DCM (30 mL) at rt, before adding TEA (0.307 mL, 2.20 mmol, 1.1 eq) followed by dropwise addition of di-*tert*-butyl dicarbonate (437 mg, 2.00 mmol) solution in DCM (5 mL). After 24 h, the mixture was washed with 1 M KHSO$_4$ $_{(aq)}$ (2 × 20 mL), brine (20 mL), dried over Na$_2$SO$_4$ then concentrated under reduced pressure to give the title compound as a colourless oil (286 mg, 82%).^{1}H NMR (CDCl$_3$) δ 4.65 (s, 1H), 3.67 (t, *J* = 6.0 Hz, 2H), 3.16 (dd, *J* = 12.1/6.2 Hz, 2H), 1.78 (s, 1H), 1.68–1.51 (m, 4H), 1.51–1.38 (m, 9H). ^{13}C NMR (CDCl$_3$) δ 156.3, 79.2, 62.6, 40.4, 29.9, 28.6, 26.8.

4-((*tert*-Butoxycarbonyl)amino)butyl methanesulfonate (33). To a solution of *tert*-butyl (4-hydroxybutyl)carbamate (**32**) (150 mg, 0.79 mmol) in DCM (20 mL) was added TEA (0.220 mL, 1.58 mmol, 2 eq), followed by methanesulfonyl chloride (109 mg, 0.95 mmol, 1.2 eq). After 16 h stirring at rt, the solution was washed with 1 M NaOH $_{(aq)}$ (20 mL), 1 M KHSO$_4$ $_{(aq)}$ (20 mL), brine (20 mL), then dried over Na$_2$SO$_4$ and concentrated under reduced pressure to afford the title compound as a yellow oil (196 mg, 93%). ^{1}H NMR (CDCl$_3$) δ 4.66 (br s, 1H), 4.25 (t, *J* = 6.4 Hz, 2H), 3.22–3.11 (m, 2H), 3.02

(s, 3H), 1.84–1.74 (m, 2H), 1.68–1.52 (m, 2H), 1.43 (s, 9H). ^{13}C NMR (CDCl$_3$) δ 156.1, 79.3, 69.7, 39.8, 37.4, 28.5, 26.5, 26.3.

***tert*-Butyl (4-(7-cyano-3,4-dihydroisoquinolin-2(1*H*)-yl)butyl)carbamate (34).** To a solution of 4-((*tert*-butoxycarbonyl)amino)butyl methanesulfonate (**33**) (202 mg, 0.76 mmol) in DCM (15 mL) was added 7-cyano-1,2,3,4-tetrahydroisoquinoline (131 mg, 0.83 mmol, 1.1eq), followed by *N,N*-diisopropylethylamine (156 µL, 0.91 mmol, 1.2eq). The solution was heated at reflux for 3 d, then concentrated under reduced pressure and the product purified by FCC (EtOAc) to give the title compound as a yellow oil (36 mg, 12%). ^{1}H NMR (CDCl$_3$) δ 7.40 (dd, *J* = 7.9/1.6 Hz, 1H), 7.32 (s, 1H), 7.19 (d, *J* = 7.9 Hz, 1H), 4.99 (s, 1H), 3.62 (s, 2H), 3.15 (dd, *J* = 12.2/6.1 Hz, 2H), 2.96 (t, *J* = 5.8 Hz, 2H), 2.74 (t, *J* = 5.9 Hz, 2H), 2.54 (t, *J* = 7.0 Hz, 2H), 1.71–1.50 (m, 4H), 1.42 (s, 9H). ^{13}C NMR (CDCl$_3$) δ 156.2, 140.4, 136.3, 130.5, 129.73, 129.65, 119.2, 109.5, 79.1, 57.8, 55.5, 50.3, 40.5, 29.5, 28.5, 28.0, 24.5.

N-(4-(7-Cyano-3,4-dihydroisoquinolin-2(1*H*)-yl)butyl)-1*H*-indole-2-carboxamide (36).

tert-Butyl (4-(7-cyano-3,4-dihydroisoquinolin-2(1*H*)-yl)butyl)carbamate (**34**) (36 mg, 0.11 mmol) was taken up in DCM (5 mL) and TFA (1 mL) and stirred at rt for 16 h. After this, the mixture was diluted with DCM (20 mL) and water (5 mL) added. The pH of the aqueous layer was adjusted to ~10 by dropwise addition of NH$_4$OH (approximately 3 mL). Subsequently, the aqueous layer was extracted further with DCM (2 × 15 mL). The combined organic layers were washed with brine (20 mL), then dried over Na$_2$SO$_4$ and concentrated under reduced pressure to give the free amine intermediate **35.** This was immediately taken up in DMF (5 mL) under a nitrogen atmosphere. 1*H*-Indole-2-carboxylic acid (21 mg, 0.13 mmol, 1.2 eq), HCTU (68 mg, 0.17 mmol, 1.5 eq) and DIPEA (0.096 mL, 0.55 mmol, 5 eq) were added, and the mixture stirred at rt for 16 h. The mixture was concentrated under reduced pressure, before adding 2M NaHCO$_3$ $_{(aq)}$, then extracting the resulting aqueous slurry with EtOAc (20 mL). The organic layer was washed with 2M NaHCO$_3$ $_{(aq)}$ (2 × 20 mL), brine (20 mL), then

dried over Na_2SO_4 before concentrating under reduced pressure. The resulting crude product was purified by FCC (eluent MeOH/CHCl$_3$ 5:95) to give 28 mg of white solid (69%). ^{1}H NMR (d_6-DMSO) δ 8.44 (t, J = 5.7 Hz, 1H), 7.58 (d, J = 7.9 Hz, 1H), 7.57–7.53 (m, 2H), 7.41 (dq, J = 8.3/0.9 Hz, 1H), 7.30 (d, J = 8.5 Hz, 1H), 7.16 (ddd, J = 8.2/7.0/1.1 Hz, 1H), 7.08 (dd, J = 2.1/0.7 Hz, 1H), 7.02 (ddd, J = 8.0/7.0/1.0 Hz, 1H), 3.57 (s, 2H), 3.32–3.28 (m, 2H), 2.87 (t, J = 6.2 Hz, 2H), 2.66 (t, J = 5.8 Hz, 2H), 2.49–2.46 (m, 2H), 1.59 (dt, J = 6.7/3.5 Hz, 4H). ^{13}C NMR (d_6-DMSO) δ 161.0, 140.7, 136.7, 136.3, 131.9, 130.3, 129.7, 129.4, 127.1, 123.1, 121.4, 119.6, 119.1, 112.3, 108.2, 102.2, 57.0, 54.8, 49.7, 38.7, 28.9, 27.1, 23.9. HRMS (m/z): [MH]$^+$ calcd. for $C_{23}H_{24}N_4O$, 373.2023; found 373.2022; HPLC t_R = 7.2 min.

Pharmacology.

Materials: Dulbecco's modified Eagle's medium, Flp-In CHO cells, and hygromycin B were purchased from Invitrogen (Carlsbad, CA). Fetal bovine serum (FBS) was purchased from ThermoTrace (Melbourne, VIC, Australia). [^{3}H]spiperone, [^{35}S]GTPγS (1000 Ci/mmol), AlphaScreen reagents and Ultima gold scintillation cocktail were from PerkinElmer (Boston, MA). pcDNA3L-His-CAMYEL was purchased from ATCC. All other reagents were purchased from Sigma Aldrich (St. Louis, MO). The G protein BRET constructs were generated by Dr. Céline Galés (Paul Sabatier University, France).

Cell culture and membrane preparation: was performed as described previously.[46]

Molecular Biology: cDNA in pcDNA3.1+ encoding the long isoform of the wild-type human D$_2$ dopamine receptor (D$_{2L}$R) was obtained from Missouri University of Science and Technology (http://www.cdna.org). Oligonucleotides were purchased from GeneWorks (Hindmarsh, Australia). An N-terminal c-myc epitope tag (EQKLISEEDL) was introduced to the sequence of the D$_{2L}$R and flanking AttB sites were introduced to the WT D$_{2L}$R by overlap extension polymerase chain reaction to

allow sub-cloning into the pDONR201[TM] vector. The WT or c-myc tagged wildtype (WT) $D_{2L}R$

receptor construct in pDONR201™ were subsequently transferred into the pEF5/frt/V5/dest vector

using the LR clonase enzyme mix (Invitrogen). Desired mutations were introduced using the

Quikchange™ site-directed mutagenesis kit (Agilent). Receptor constructs in pEF5/frt/V5/dest were

used to transfect Flp-In CHO cells (Invitrogen). Cells were transfected using linear polyethyleneimine

(PEI, Polysciences, Warrington, PA) as described previously.[47]

ERK1/2 phosphorylation assay: Experiments were performed as described previously.[46] Concentration-

response stimulation or inhibition curves were generated by exposure of the cells to antagonist ligand

for 30 min and then dopamine for 5 min. Data were normalized to the response generated by 10% fetal

bovine serum.

BRET cAMP assay: $D_{2L}R$-Flp-In CHO cells were transfected with 2μg of pcDNA3L-His-CAMYEL.

The assay was performed as described previously[13] with the following difference: 30 min prior to

agonist addition appropriate concentrations of **1** or fragment ligand were added. 5 min following

agonist addition 10 μL of forskolin was added to a final concentration of 3 μM. Data were normalized

to the level of cAMP generated by 3 μM forskolin.

[^{35}S]GTPγS Binding Assay: Cell membranes (5 μg D_{2L}-Flp-In CHO or 20 μg rat striatal tissue) were

equilibrated for 60 min at 30 °C with varying concentrations of ligands in binding buffer (20 mM

HEPES, 10 mM $MgCl_2$, 100 mM NaCl 1 mM EGTA, 1 mM EDTA, 0.1% ascorbic acid, 1 mM DTT;

pH 7.4) containing 3 μM GDP. [^{35}S]GTPγS (0.1 nM) was added to a final volume of 0.2 mL (D_{2L}-Flp-

In CHO) and membranes were incubated for further 60 min at 30 °C. 5 μg of saponin was added per

assay point. For experiments using D_{2L}-Flp-In CHO membranes termination of [^{35}S]GTPγS binding

was by rapid filtration with a Packard plate harvester onto 96-well GF/C filter plates followed by three

washes with ice cold 0.9% NaCl. Bound radioactivity was measured in a Microbeta microplate counter (Perkin Elmer). Data were normalized to the maximal response of dopamine in the control condition.

[^{3}H]spiperone binding assay: Experiments were performed using a methodology described previously[46].

β-arrestin recruitment: HEK293T cells were transfected with a 2:2:4 ratio of cDNA coding for D_{2L}-Rluc8, GRK2 and β-arrestin 2-YFP. Experiments were performed as described previously.[48] Antagonists were added 30 min prior to coelenterazine-h. Data were normalised to the maximal response of dopamine in the control condition.

G Protein Activation: Flp-In-CHO cells stably expressing the $D_{2L}R$ were seeded at a density of 2,000,000 cells per 10cm dish and were transfected the following day using polyethylenimine as transfection reagent. To measure the activation of $G\alpha_{i1}$ and $G\alpha_{OB}$ G proteins the cells were transfected with either 0.3 μg Rluc8-tagged $G\alpha_{i1}$, 1.2 μg Gβ and 1.35 μg Venus-tagged Gγ; or 0.14 μg Rluc8-tagged $G\alpha_{OB}$ 1.2 μg Gβ and 0.6 μg Venus-tagged Gγ. 24 h after transfection the cells were plated into 96-well CulturPlates (PerkinElmer) and grown overnight. The cells were equilibrated in Hank's balanced salt solution at 37 °C before starting the experiment. The cells were stimulated with the agonists for the indicated timeframes when the BRET readings were captured. Coelenterazine (Promega) was added at a final concentration of 5 μM at least 3 min prior to measurement. The signals were detected at 445-505 and 505-565 nm using a PHERAstar FS instrument (BMG LabTech, Offenburg, Germany). Net BRET was determined by subtraction of the vehicle control from the agonist induced response.

Data analysis: GraphPad Prism 6.0b (San Diego, CA) was used for all statistical analysis, nonlinear regression, and simulations.

Analysis of radioligand binding experiments:

Competition-binding curves between [^{3}H]spiperone and dopamine in the absence or presence of **3** were initially fitted to a one-site binding equation and two-site binding equation followed by F-test analysis for best fit.[26] Subsequently, data of experiments using membranes of WT D$_2$R FlpIn CHO cells was fitted to the following allosteric ternary complex model:[49]

$$Y = \frac{[A]Frac_{Hi}}{[A]+\left(\frac{K_A K_B}{\alpha[B]+K_B}\right)\left(1+\frac{[I]}{K_{Hi}}+\frac{[B]}{K_B}+\frac{\alpha'[I][B]}{K_{Hi}K_B}\right)} + \frac{[A](1-Frac_{Hi})}{[A]+\left(\frac{K_A K_B}{\alpha[B]+K_B}\right)\left(1+\frac{[I]}{K_{Lo}}+\frac{[B]}{K_B}+\frac{\alpha'[I][B]}{K_{Lo}K_B}\right)} \quad (1)$$

Where Y is percentage (vehicle control) binding, [A], [B], and [I] are the concentrations of [^{3}H]spiperone, **3**, and dopamine, respectively, K_A and K_B are the equilibrium dissociation constants of [^{3}H]spiperone and **1**, respectively, K_{Hi} and K_{Lo} are the equilibrium dissociation constants of dopamine for the high- and low-affinity receptor state, respectively, Frac$_{Hi}$ is the proportion of receptors in the high-affinity receptor state, and α and α' are the cooperativities between **1** and [^{3}H]spiperone or dopamine, respectively. Values of α (or α') > 1 denote positive cooperativity; values < 1 (but > 0) denote negative cooperativity, and values = 1 denote neutral cooperativity.

Competition-binding curves between [^{3}H]spiperone and **1** or **3** could be fit to the allosteric ternary complex model using the following equation:[50]

$$Y = \frac{\frac{[A]}{K_A}}{\frac{[A]}{K_A}+\left(\frac{1+\frac{[B]}{K_B}}{1+\alpha\frac{[B]}{K_B}}\right)} \quad (2)$$

Where Y is percentage (vehicle control) binding; [A] and [B] are the concentrations of [^{3}H]spiperone

and **1** or **3**, respectively; K_A and K_B are the equilibrium dissociation constants of [^{3}H]spiperone and **1** or

3, respectively; α is the cooperativity between **1** or **3** and [^{3}H]spiperone. Values of $\alpha > 1$ denote

positive cooperativity; values < 1 (but > 0) denote negative cooperativity, and values $= 1$ denote

neutral cooperativity.

Analysis of functional data: All concentration response (C/R) data were fitted to the following modified

four-parameter Hill equation to derive potency estimates:[26]

$$E = Basal + \frac{(E_{max} - Basal).[A]^{nH}}{[A]^{nH} + EC_{50}^{nH}}$$

$$(3)$$

Where E is the effect of the system, nH is the Hillslope, and EC_{50} is the concentration of agonist [A]

that gives the midpoint response between basal and maximal effect of dopamine or other agonists

(E_{max}), which are the lower and upper asymptotes of the response, respectively.

Functional data describing the interaction between 2 and dopamine in [^{35}S]GTPγS or cAMP assays

were globally analyzed according to the allosteric ternary complex model.

$$E = \frac{E_m.[A]^{nH}}{[A]^{nH} + [EC_{50}]^{nH}\left(\dfrac{1 + \dfrac{[B]}{K_B}}{1 + \dfrac{\alpha\beta[B]}{K_B}}\right)}$$

$$(4)$$

Where E_m is the maximum possible cellular response, [A] and [B] are the concentrations of orthosteric

and allosteric ligands, respectively, and K_B is the equilibrium dissociation constant of the allosteric

ligand, $\alpha\beta$ is a composite cooperativity parameter between the orthosteric and allosteric ligand that includes effects upon orthosteric ligand affinity and efficacy and nH is the Hill slope of the orthosteric agonist concentration-response curve. Values of α and/or β greater than 1 denote allosteric potentiation, whereas values less than 1 (but greater than 0) denote allosteric inhibition.

Functional data describing the interaction between **3**, **11a** or derivatives and dopamine at the D_2R in a pERK1/2 assay were analyzed using a complete operational model of allosterism and agonism according to equation 5:[51]

$$E = \frac{E_m(\tau_A[A](K_B + \alpha\beta[B]) + \tau_B[B]K_A)^{nH}}{([A]K_B + K_AK_B + K_A[B] + \alpha[A][B])^{nH} + (\tau_A[A](K_B + \alpha\beta[B]) + \tau_B[B]K_A)^{nH}}$$

(5)

Where E_m is the maximum possible cellular response, [A] and [B] are the concentrations of orthosteric and allosteric ligands, respectively, K_A and K_B are the equilibrium dissociation constant of the orthosteric and allosteric ligands, respectively, and τ_B (constrained to -100) are operational measures of orthosteric and allosteric ligand efficacy (which incorporate both signal efficiency and receptor density), respectively, α is the binding cooperativity parameter between the orthosteric and allosteric ligand, and β (constrained to -100 to represent high negative cooperativity with dopamine efficacy) denotes the magnitude of the allosteric effect of the modulator on the efficacy of the orthosteric agonist. K_A constrained to 11 nM, 188 nM and 191 nM for the WT, V91A and E95A receptors respectively and represents a value of functional affinity determined by an operational model of partial agonism to dose-response data of dopamine (a partial agonist) and apomorphine (a full agonist) in an pERK1/2 assay). $Log\tau_A$ was determined as 0.74 ± 0.07, 0.65 ± 0.19, 0.71 ± 0.24 at the WT, V91A and E95A D_2R expressing cell lines respectively. For compounds that caused a limited rightward shift of the dopamine dose-response curve but no decrease in E_{max} data were fit using an operational model of

allosterism where Logβ was constrained to 0 to represent neutral cooperativity with dopamine efficacy.

For compounds that produced an unlimited rightward shift of a dopamine dose-response curve within

the concentration range of test compound used data were fit using an operational model of allosterism

where both Logα and Logβ were constrained to -100 and 0 respectively to allow estimation of

compound affinity.

A logistic equation of competitive agonist-antagonist interaction was globally fitted to data from

functional experiments measuring the interaction between dopamine and test compounds which caused

an unlimited rightward displacement of a dopamine dose-response curve and no decrease in E_{max} within

the range of concentrations used[26]:

$$Response = Bottom + \frac{(E_{max} - Bottom)}{1 + \left(\frac{10^{-pEC_{50}\left[1 + \left(\frac{[B]}{10^{-K_B}}\right)\right]^s}}{[A]}\right)^{nH}} \tag{6}$$

Where s represents the Schild slope for the test compound and K_B is the equilibrium dissociation

constant of the test compound, nH is the Hillslope, and EC_{50} is the concentration of agonist [A] that

gives the midpoint response between basal and maximal effect of dopamine or other agonists (E_{max}),

which are the lower and upper asymptotes of the response, respectively.

Statistical Analysis: All data points and values shown in the figures and tables are the means ± SEM of

at least 3 separate experiments performed in duplicate unless otherwise stated. Statistically significant

differences (taken at $p < 0.05$) between pK_B, Logα or Logβ values were determined by one-way

ANOVA with a Bonferroni post-test or an unpaired Student's t-test as appropriate.

Supporting Information. Supplementary Table 1: Allosteric ternary complex model binding parameters for the interaction between **3**, dopamine and [^{3}H]spiperone at the $D_{2L}R$ expressed in Flp-In CHO cells.

AUTHOR INFORMATION

Corresponding Author

*For P.J.S.: Phone: +61 (0)3 9903 9542; E-mail: Peter.Scammells@monash.edu. For J.R.L.: Phone +61 (0)3 9903 9095; E-mail: Rob.Lane@monash.edu

Author Contributions

The manuscript was written through contributions of all authors. All authors have given approval to the final version of the manuscript.

Current addresses: ^School of Pharmacy, Centre for Biomolecular Sciences, University of Nottingham, University Park, Nottingham NG7 2RD, United Kingdom, #Department of Chemistry and Pharmacy, Emil Fischer Center, Friedrich Alexander University, Schuhstraße 19, 91052 Erlangen, Germany

Notes

The authors declare no competing financial interest.

ABBREVIATIONS

BOP, (benzotriazol-1-yloxy)tris(dimethylamino)phosphonium hexafluorophosphate; DIPEA,

diisopropylethylamine; DMF-DMA, *N,N*-dimethylformamide, dimethylacetal; ECL, extracellular loop;

FCC, flash column chromatography; HCTU, *O*-(1*H*-6-chlorobenzotriazole-1-yl)-1,1,3,3-

tetramethyluronium hexafluorophosphate; PE, petroleum spirits 40-60; TEA, triethylamine; TFA, 2,2,2

– trifluoroacetic acid.

REFERENCES

(1)   Lagerstrom, M. C.; Schiöth, H. B. Structural Diversity of G Protein-Coupled Receptors and

Significance for Drug Discovery. *Nat. Rev. Drug Discovery* **2008**, *7*, 339–357.

(2)   Christopoulos, A.; Changeux, J.-P.; Catterall, W. A.; Fabbro, D.; Burris, T. P.; Cidlowski, J.

A.; Olsen, R. W.; Peters, J. A.; Neubig, R. R.; Pin, J.-P.; Sexton, P. M.; Kenakin, T. P.; Ehlert, F. J.;

Spedding, M.; Langmead, C. J. International Union of Basic and Clinical Pharmacology. XC. Multisite

Pharmacology: Recommendations for the Nomenclature of Receptor Allosterism and Allosteric

Ligands. *Pharmacol. Rev.* **2014**, *66*, 918–947.

(3)   Lane, J. R.; Sexton, P. M.; Christopoulos, A. Bridging the Gap: Bitopic Ligands of G-Protein-

Coupled Receptors. *Trends Pharmacol. Sci.* **2013**, *34*, 59–66.

(4)   Mohr, K.; Schmitz, J.; Schrage, R.; Traenkle, C.; Holzgrabe, U. Molecular Alliance - From

Orthosteric and Allosteric Ligands to Dualsteric/Bitopic Agonists at G Protein Coupled Receptors.

Angew. Chem. Int. Ed. Engl. **2013**, *52*, 508–516.

(5)   Valant, C.; Lane, J. R.; Sexton, P. M.; Christopoulos, A. The Best of Both Worlds? Bitopic

Orthosteric/Allosteric Ligands of G Protein-Coupled Receptors. *Annu. Rev. Pharmacol. Toxicol.* **2012**,

52, 153–178.

(6)   Steinfeld, T.; Mammen, M.; Smith, J. A. M.; Wilson, R. D.; Jasper, J. R. A Novel Multivalent

Ligand That Bridges the Allosteric and Orthosteric Binding Sites of the M_2 Muscarinic Receptor. *Mol.

Pharmacol.* **2007**, *72*, 291–302.

(7)   Antony, J.; Kellershohn, K.; Mohr-Andrae, M.; Kebig, A.; Prilla, S.; Muth, M.; Heller, E.;

Disingrini, T.; Dallanoce, C.; Bertoni, S.; Schrobang, J.; Traenkle, C.; Kostenis, E.; Christopoulos, A.;

Hoeltje, H.-D.; Barocelli, E.; De Amici, M.; Holzgrabe, U.; Mohr, K. Dualsteric GPCR Targeting: a

Novel Route to Binding and Signaling Pathway Selectivity. *FASEB J.* **2009**, *23*, 442–450.

(8)   Bock, A.; Merten, N.; Schrage, R.; Dallanoce, C.; Baetz, J.; Kloeckner, J.; Schmitz, J.; Matera,

C.; Simon, K.; Kebig, A.; Peters, L.; Mueller, A.; Schrobang-Ley, J.; Traenkle, C.; Hoffmann, C.; De

Amici, M.; Holzgrabe, U.; Kostenis, E.; Mohr, K. The Allosteric Vestibule of a Seven Transmembrane

Helical Receptor Controls G-Protein Coupling. *Nat. Commun.* **2012**, *3*, 1044

(9)   Narlawar, R.; Lane, J. R.; Doddareddy, M.; Lin, J.; Brussee, J.; IJzerman, A. P. Hybrid

Ortho/Allosteric Ligands for the Adenosine A_1 Receptor. *J. Med. Chem.* **2010**, *53*, 3028–3037.

(10) Keov, P.; Valant, C.; Devine, S. M.; Lane, J. R.; Scammells, P. J.; Sexton, P. M.;

Christopoulos, A. Reverse Engineering of the Selective Agonist TBPB Unveils Both Orthosteric and

Allosteric Modes of Action at the M_1 Muscarinic Acetylcholine Receptor. *Mol. Pharmacol.* **2013**, *84*,

425–437.

(11) Valant, C.; Gregory, K. J.; Hall, N. E.; Scammells, P. J.; Lew, M. J.; Sexton, P. M.; Christopoulos, A. A Novel Mechanism of G Protein-Coupled Receptor Functional Selectivity: Muscarinic Partial Agonist McN-a-343 as a Bitopic Orthosteric/Allosteric Ligand. *J. Biol. Chem.* **2008**, *283*, 29312–29321.

(12) Beaulieu, J.-M.; Gainetdinov, R. R. The Physiology, Signaling, and Pharmacology of Dopamine Receptors. *Mol. Cell. Biol.* **2014**, *34*, 182–217.

(13) Lane, J. R.; Donthamsetti, P.; Shonberg, J.; Shonberg, J.; Draper-Joyce, C. J.; Draper-Joyce, C. J.; Dentry, S.; Dentry, S.; Michino, M.; Shi, L.; López, L.; Scammells, P. J.; Capuano, B.; Sexton, P. M.; Javitch, J. A.; Christopoulos, A. A New Mechanism of Allostery in a G Protein-Coupled Receptor Dimer. *Nat. Chem. Biol.* **2014**, *10*, 745–752.

(14) Michino, M.; Donthamsetti, P.; Beuming, T.; Banala, A.; Duan, L.; Roux, T.; Han, Y.; Trinquet, E.; Newman, A. H.; Javitch, J. A.; Shi, L. A Single Glycine in Extracellular Loop 1 Is the Critical Determinant for Pharmacological Specificity of Dopamine D_2 And D_3 Receptors. *Mol. Pharmacol.* **2013**, *84*, 854–864.

(15) Chien, E. Y. T.; Liu, W.; Zhao, Q.; Katritch, V.; Won Han, G.; Newman, A. H.; Javitch, J. A. Structure of the Human Dopamine D_3 Receptor in Complex with a D_2/D_3 Selective Antagonist. *Science* **2010**, *330*, 1091–1095.

(16) Newman, A. H.; Beuming, T.; Banala, A. K.; Donthamsetti, P.; Pongetti, K.; LaBounty, A.; Levy, B.; Cao, J.; Michino, M.; Luedtke, R. R.; Javitch, J. A. Molecular Determinants of Selectivity and Efficacy at the Dopamine D_3 Receptor. *J. Med. Chem.* **2012**, *55*, 6689–6699.

(17) Ma, L.; Seager, M. A.; Wittmann, M.; Jacobson, M.; Bickel, D.; Burno, M.; Jones, K.; Graufelds, V. K.; Xu, G.; Pearson, M.; McCampbell, A.; Gaspar, R.; Shughrue, P.; Danziger, A.;

Regan, C.; Flick, R.; Pascarella, D.; Garson, S.; Doran, S.; Kreatsoulas, C.; Veng, L.; Lindsley, C. W.; Shipe, W. D.; Kuduk, S. D.; Sur, C.; Kinney, G.; Seabrook, G. R.; Ray, W. J. Selective Activation of the M_1 Muscarinic Acetylcholine Receptor Achieved by Allosteric Potentiation. *Proc. Natl. Acad. Sci. U. S. A.* **2009**, *106*, 15950–15955.

(18) Yang, F. V.; Shipe, W. D.; Bunda, J. L.; Nolt, M. B.; Wisnoski, D. D.; Zhao, Z.; Barrow, J. C.; Ray, W. J.; Ma, L.; Wittmann, M.; Seager, M. A.; Koeplinger, K. A.; Hartman, G. D.; Lindsley, C. W. Parallel Synthesis of N-Biaryl Quinolone Carboxylic Acids as Selective M_1 Positive Allosteric Modulators. *Bioorg. Med. Chem. Lett.* **2010**, *20*, 531–536.

(19) Maruyama, M.; Kinomura, N.; Nojima, S.; Takamura, M.; Kakiguchi, K.; Tatamitani, H. N-Acyl Cyclic Amine Derivative or Pharmaceutically Acceptable Salt Thereof. WO 2011/111875, September 15, 2011.

(20) Shonberg, J.; Draper-Joyce, C.; Mistry, S. N.; Christopoulos, A.; Scammells, P. J.; Lane, J. R.; Capuano, B. Structure-Activity Study of N-((Trans)-4-(2-(7-Cyano-3,4-Dihydroisoquinolin-2(1H)-Yl)Ethyl)Cyclohexyl)-1H-Indole-2-Carboxamide (SB269652), a Bitopic Ligand That Acts as a Negative Allosteric Modulator of the Dopamine D2 Receptor. *J. Med. Chem.* **2015**, *58*, 5287–5307.

(21) Kenakin, T. Allosteric Modulators: the New Generation of Receptor Antagonist. *Mol. Interventions* **2004**, *4*, 222–229.

(22) Stemp, G.; Ashmeade, T.; Branch, C. L.; Hadley, M. S.; Hunter, A. J.; Johnson, C. N.; Nash, D. J.; Thewlis, K. M.; Vong, A. K. K.; Austin, N. E.; Jeffrey, P.; Avenell, K. Y.; Boyfield, I.; Hagan, J. J.; Middlemiss, D. N.; Reavill, C.; Riley, G. J.; Routledge, C.; Wood, M. Design and Synthesis of *trans-* N-[4-[2-(6-Cyano-1,2,3,4-tetrahydroisoquinolin-2- yl)ethyl]cyclohexyl]-4-quinolinecarboxamide (SB-277011): a Potent and Selective Dopamine D_3 Receptor Antagonist with High Oral Bioavailability

and CNS Penetration in the Rat. *J. Med. Chem.* **2000**, *43*, 1878–1885.

(23) Silvano, E.; Millan, M. J.; Mannoury la Cour, C.; Han, Y.; Duan, L.; Griffin, S. A.; Luedtke, R. R.; Aloisi, G.; Rossi, M.; Zazzeroni, F.; Javitch, J. A.; Maggio, R. The Tetrahydroisoquinoline Derivative SB269,652 Is an Allosteric Antagonist at Dopamine D_3 And D_2 Receptors. *Mol. Pharmacol.* **2010**, *78*, 925–934.

(24) Lane, J. R.; Powney, B.; Wise, A.; Rees, S.; Milligan, G. G Protein Coupling and Ligand Selectivity of the D_{2l} And D_3 Dopamine Receptors. *J. Pharmacol. Exp. Ther.* **2008**, *325*, 319–330.

(25) Saulière, A.; Bellot, M.; Paris, H.; Denis, C.; Finana, F.; Hansen, J. T.; Altié, M.-F.; Seguelas, M.-H.; Pathak, A.; Hansen, J. L.; Sénard, J.-M.; Galés, C. Deciphering Biased-Agonism Complexity Reveals a New Active AT_1 Receptor Entity. *Nat. Chem. Biol.* **2012**, *8*, 622–630.

(26) Motulsky, H.; Christopoulos, A. *Fitting Models to Biological Data Using Linear and Nonlinear Regression*; GraphPad Software Inc.: San Diego, 2003.

(27) Bordwell, F. G.; Drucker, G. E.; Fried, H. E. Acidities of Carbon and Nitrogen Acids: the Aromaticity of the Cyclopentadienyl Anion. *J. Org. Chem.* **1981**, *46*, 632–635.

(28) Bordwell, F. G. Equilibrium Acidities in Dimethyl Sulfoxide Solution. *Acc. Chem. Res.* **1988**, *21*, 456–463.

(29) Kruse, A. C.; Ring, A. M.; Manglik, A.; Hu, J.; Hu, K.; Eitel, K.; Hübner, H.; Pardon, E.; Valant, C.; Sexton, P. M.; Christopoulos, A.; Felder, C. C.; Gmeiner, P.; Steyaert, J.; Weis, W. I.; Garcia, K. C.; Wess, J.; Kobilka, B. K. Activation and Allosteric Modulation of a Muscarinic Acetylcholine Receptor. *Nature* **2013**, *504*, 101–106.

(30) Alvarez, G. L.; Correa, M. E.; Cruces, V. M. A.; Elorriaga, R. C.; Fernandez-Alvarez, E.;

Nieto, L. O. Preparation of Acetylenic and Allenic Derivatives of 2-Indolylmethylamines and

Preliminary Results of Their Study as Selective Inhibitors for the Monoamine Oxidases a and B. *An.*

Quim., Ser. C **1986**, *82*, 129–134.

(31) Pigulla, J.; Röder, E. Darstellung Von Indol-2-Carboxamiden Und Estern Von (Indol-2-

Ylcarbonylamino)Carbonsäuren Nach Der Imidazolidmethode. *Arch. Pharm. (Weinheim)* **1979**, *312*,

12–18.

(32) Sharma, S. K.; Mandadapu, A. K.; Kumar, B. Synthesis of Iodo-indoloazepinones in an Iodine-

Mediated Three-Component Domino Reaction via a Regioselective 7-*endo-dig* Iodo-cyclization

Pathway. *J. Org. Chem.* **2011**, *76*, 6798–6805.

(33) Chacun-Lefevre, L.; Beneteau, V.; Joseph, B.; Merour, J. Y. Ring Closure Metathesis of Indole

2-Carboxylic Acid Allylamide Derivatives. *Tetrahedron* **2002**, *58*, 10181–10188.

(34) Vlasova, M. I.; Kogan, N. A.; Lesiovskaya, E. E.; Pastushenkov, L. V. Synthesis and

Biological Activity of 1-Aryl-2-oxa-5-aza-5*R*-6-oxocyclooctano[6,7-*b*]indoles. *Pharm. Chem. J.* **1992**,

26, 492–496.

(35) Font, M.; Monge, A.; Cuartero, A.; Elorriaga, A. Indoles and Pyridazino[4, 5-*b*]indoles as

Nonnucleoside Analog Inhibitors of HIV-1 Reverse Transcriptase. *Eur. J. Med. Chem.* **1995**, *30*, 963–

971.

(36) Shida, Y.; Maejima, T.; Takada, T.; Akiba, M. Mass Spectra of Indole-2-carboxylic Acid

Derivatives. *J. Mass Spectrom. Soc. Jpn.* **1989**, *37*, 61–67.

(37) Brehm, W. J. Derivatives of Indole-2-carboxylic Acid. *J. Am. Chem. Soc.* **1949**, *71*, 3541–

3542.

(38) Saxena, M. P.; Ahmed, S. R. Synthesis of 3-Hydroxy- and 3-Methoxyindole-2-carboxamides and Esters. *J. Med. Chem.* **1969**, *12*, 1120–1121.

(39) Caramella, P.; Corsico, A. C.; Corsaro, A.; Del Monte, D. Selectivity in Cycloadditions-IX: Cycloadditions of Nitrile Oxides to Indoles. Reactivity and Regiochemistry. *Tetrahedron* **1982**, *38*, 173–182.

(40) Shi, Z.; Cui, Y.; Jiao, N. Synthesis of *B*- And *Γ*-Carbolinones via Pd-Catalyzed Direct Dehydrogenative Annulation (DDA) of Indole-carboxamides with Alkynes Using Air as the Oxidant. *Org. Lett.* **2010**, *12*, 2908–2911.

(41) Du, J.; Yin, J.; Xia, S.; Jiang, Y. Synthesis and Bioactivity of Benzimidazole-2-Acyl Compounds. *J. China Pharm. Univ. (Zhongguo Yaoke Daxue Xuebao)* **1998**, *29*, 243–246.

(42) Dickore, K.; Sasse, K.; Bode, K. D. Conversions From Benzoxazole Into Benzoxazine Series and Vice-Versa .2. Benzoxazole-2-carboxylic acid Derivatives From 2,3-Dioxo-1,4-benzoxazines. *Justus Liebigs Ann. Chem.* **1970**, *733*, 70–87.
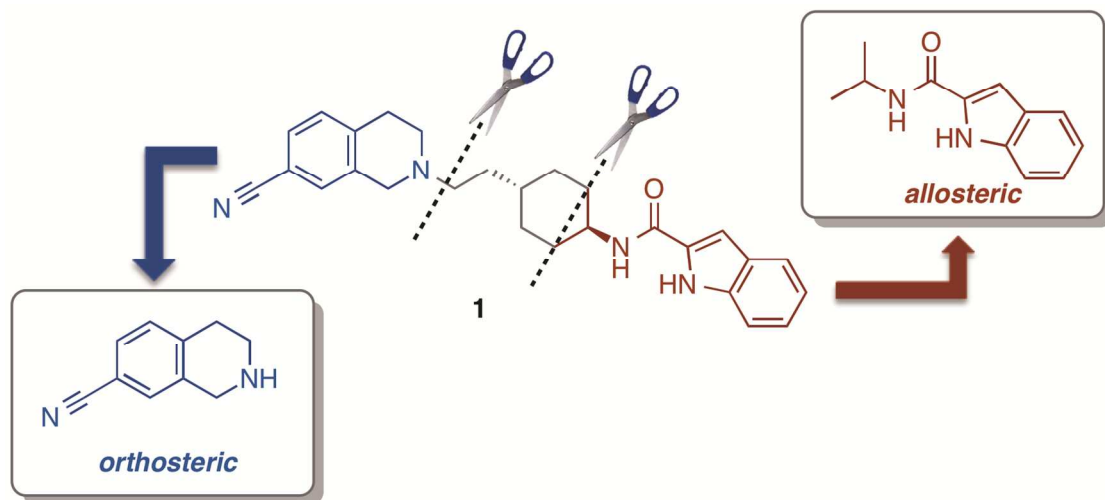
(43) Mndzhoyan, A.; Kaldrikyan, M. A.; Melik-Ogandzhanyan, R. G.; Aroyan, A. A. Benzofuran Derivatives. XII. Synthesis of Some *N*-Benzofurfuryl-*N*-alkylamines and *N*-Benzofurfuryl-*N*-alkyl- and *N*-2,3-Dihydrobenzofurfuryl-*N*-alkyl-*N'*,*N'*-Dialkylpolymethylenediamines. *Arm. Khim. Zh.* **1969**, *22*, 239–244.
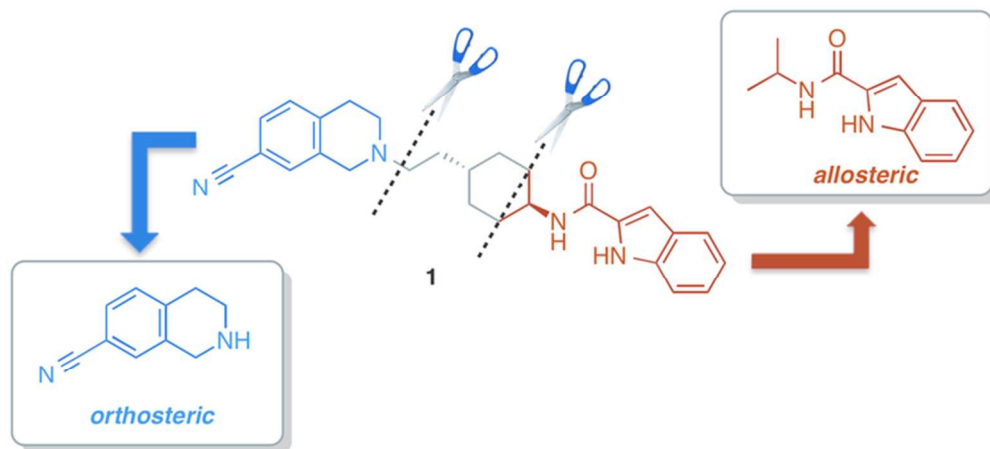
(44) Antonow, D.; Marrafa, T.; Dawood, I.; Ahmed, T.; Haque, M. R.; Thurston, D. E.; Zinzalla, G. Facile Oxidation of Electron-Poor Benzo[*b*]thiophenes to the Corresponding Sulfones with an Aqueous Solution of H_2O_2 And P_2O_5. *Chem. Commun.* **2010**, *46*, 2289.

(45) Thotapally, R.; Kachi, O. G.; Rodge, A. H.; Pathak, A. K.; Kardile, B. S.; Sindkhedkar, M. D.; Palle, V. P.; Kamboj, R. K. Bicyclic Gpr119 Modulators. WO 2012/069917, May 31, 2012.

(46) Shonberg, J.; Herenbrink, C. K.; López, L.; Christopoulos, A.; Scammells, P. J.; Capuano, B.; Lane, J. R. A Structure-Activity Analysis of Biased Agonism at the Dopamine D_2 Receptor. *J. Med. Chem.* **2013**, *56*, 9199–9221.

(47) Canals, M.; Lane, J. R.; Wen, A.; Scammells, P. J.; Sexton, P. M.; Christopoulos, A. A Monod-Wyman-Changeux Mechanism Can Explain G Protein-Coupled Receptor (GPCR) Allosteric Modulation. *J. Biol. Chem.* **2012**, *287*, 650–659.

(48) Yeatman, H. R.; Lane, J. R.; Choy, K. H. C.; Lambert, N. A.; Sexton, P. M.; Christopoulos, A.; Canals, M. Allosteric Modulation of M_1 Muscarinic Acetylcholine Receptor Internalization and Subcellular Trafficking. *J. Biol. Chem.* **2014**, *289*, 15856–15866.

(49) Leach, K.; Loiacono, R. E.; Felder, C. C.; McKinzie, D. L.; Mogg, A.; Shaw, D. B.; Sexton, P. M.; Christopoulos, A. Molecular Mechanisms of Action and in Vivo Validation of an M_4 Muscarinic Acetylcholine Receptor Allosteric Modulator with Potential Antipsychotic Properties. *Neuropsychopharmacology* **2010**, *35*, 855–869.

(50) Christopoulos, A.; Kenakin, T. G Protein-Coupled Receptor Allosterism and Complexing. *Pharmacol. Rev.* **2002**, *54*, 323–374.

(51) Leach, K.; Christopoulos, A.; Sexton, P. M. Allosteric GPCR Modulators: Taking Advantage of Permissive Receptor Pharmacology. *Trends Pharmacol. Sci.* **2007**, *28*, 382–389.

TOC Graphic

66x30mm (300 x 300 DPI)